Numerical simulation of ground-water flow in basin-fill material in Salt Lake Valley, Utah

Prepared by the U.S. Geological Survey

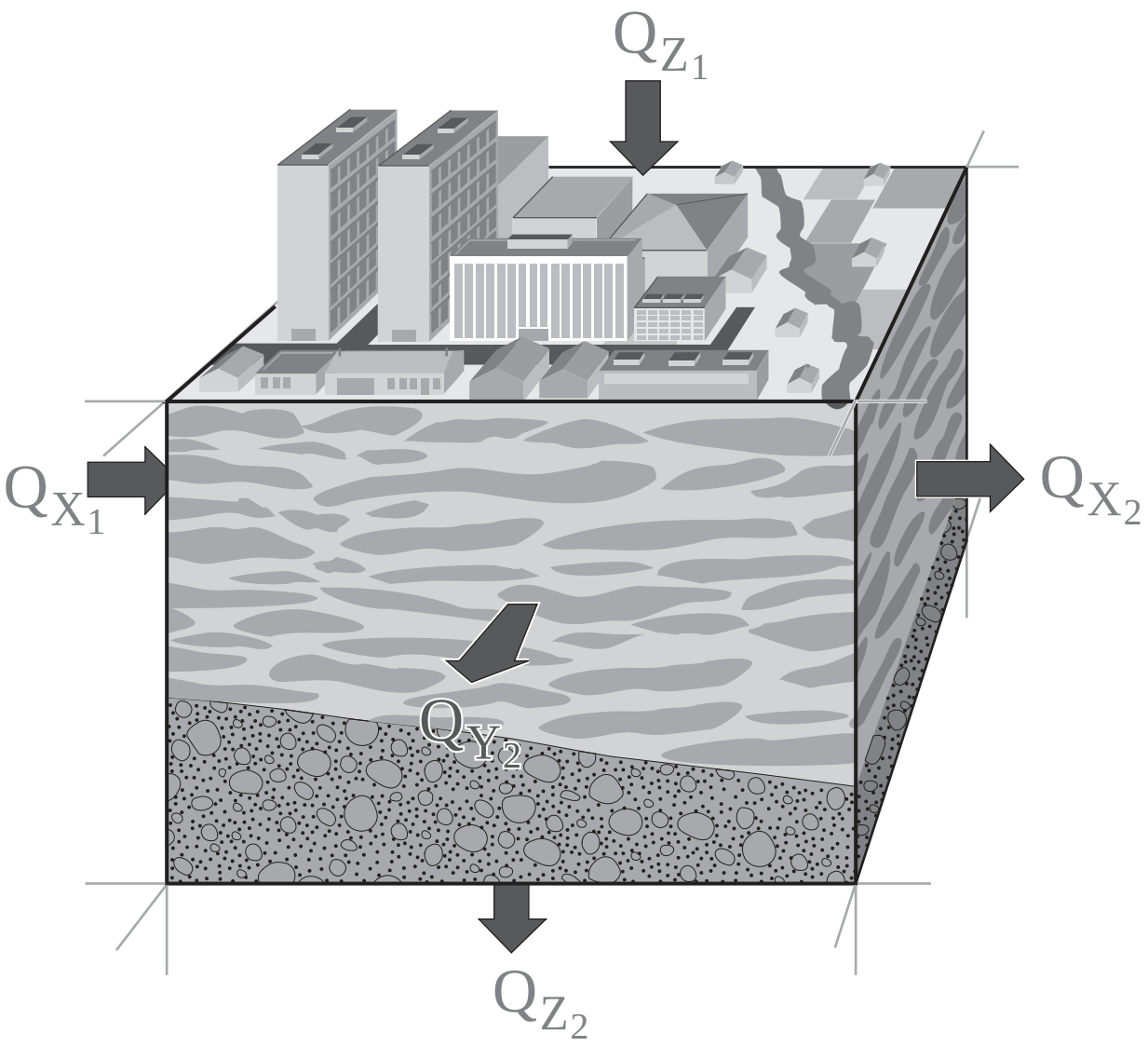

Technical Publication No. 110-B
State of Utah
DEPARTMENT OF NATURAL RESOURCES
1995

This report was prepared as a part of the Statewide cooperative water-resource investigation program administered jointly by the Utah Department of Natural Resources, Division of Water Rights and the U.S. Geological Survey. The program is conducted to meet the water administration and water-resource data needs of the State as well as the water information needs of many units of government and the general public

Ted Stewart
Executive Director
Department of Natural Resources

Robert L. Morgan
State Engineer
Division of Water Rights

Copies available at
Utah Department of Natural Resources
Division of Water Rights
1636 West North Temple, Room 220
Salt Lake City, Utah 84116

STATE OF UTAH
DEPARTMENT OF NATURAL RESOURCES

Technical Publication No. 110-B

NUMERICAL SIMULATION OF GROUND-WATER FLOW IN BASIN-FILL MATERIAL IN SALT LAKE VALLEY, UTAH

By P.M. Lambert
U.S. Geological Survey

Prepared by the
United States Geological Survey
in cooperation with the
Utah Department of Natural Resources,
Division of Water Rights, and
the Utah Department of Environmental Quality,
Division of Water Quality
1995

CONTENTS

FIGURES

FIGURES—Continued

TABLES

CONVERSION FACTORS AND VERTICAL DATUM

Multiply	By	To obtain
acre	0.4047	hectare
	4,047	square meter
acre-foot (acre-ft)	0.001233	cubic hectometer
	1,233	cubic meter
acre-foot per year (acre-ft/yr)	0.001233	cubic hectometer per year
	1,233	cubic meter per year
foot (ft)	0.3048	meter
foot per day (ft/d)	0.3048	meter per day
foot squared per day[1] (ft^2/d)	0.0929	meter squared per day
gallon per day (gal/d)	0.003785	cubic meter per day
inch (in.)	25.4	millimeter
mile (mi)	1.609	kilometer

In this report, units for equation variables are expressed using the generic units length (L) and time (t).

Sea level: In this report, "sea level" refers to the National Geodetic Vertical Datum of 1929—a geodetic datum derived from a general adjustment of the first-order level nets of the United States and Canada, formerly called Sea Level Datum of 1929.

[1]Expresses transmissivity. An alternative way of expressing transmissivity is cubic foot per day per square foot, times foot of aquifer thickness [ft^3/d/ft^2]ft.

Numerical Simulation of Ground-Water Flow in Basin-Fill Material in Salt Lake Valley, Utah

By P.M. Lambert
U.S. Geological Survey

ABSTRACT

A three-dimensional, finite-difference, numerical model was developed to simulate ground-water flow in the basin-fill material in Salt Lake Valley, Utah. The model was calibrated to steady-state and transient-state conditions. The steady-state simulation was developed and calibrated using hydrologic data defining average conditions for 1968. The transient-state simulation was developed and calibrated using hydrologic data from 1969-91.

Areally the model grid is 94 rows by 62 columns, with each cell 0.35 mile on a side. Vertically, the aquifer system is divided into seven layers. The model simulates recharge to the basin-fill ground-water flow system from (1) consolidated rock, (2) streams and canals, (3) precipitation on the valley floor, (4) irrigated land, (5) reservoirs and evaporation ponds in the southwestern part of the valley, and (6) underflow at Jordan Narrows. Estimated discharge to wells, canals, and springs is incorporated in the model. During simulation, the model computes (1) ground-water flow to and seepage from the Jordan River and the lower reaches of its principal tributaries, (2) recharge from consolidated rock at the northern end of the Oquirrh Mountains, (3) discharge to drains, and (4) discharge by evapotranspiration.

During steady-state calibration, calibration variables were adjusted within probable ranges to minimize differences between model-computed and measured water levels, model-computed and estimated ground-water discharge to the Jordan River, and simulated and measured vertical hydraulic gradients. The transient-state simulation was calibrated to measured water-level changes and estimated annual gains in the Jordan River.

INTRODUCTION

Salt Lake Valley is the main population and industrial center in the State of Utah (fig. 1). Maintenance of an adequate supply of water suitable for domestic use is one of the most important factors in sustaining the current population and industrial activity and in allowing for continued economic growth. State officials are in need of detailed information concerning the occurrence and potential movement of poor-quality ground water with high dissolved-solids concentrations to anticipate and prevent migration of this water to points of withdrawal and thus to better manage development of the ground-water system. In July 1990, the U.S. Geological Survey, in cooperation with the Utah Department of Natural Resources, Division of Water Rights, and the Utah Department of Environmental Quality, Division of Water Quality, began a study of ground-water flow and solute transport in Salt Lake Valley. Local municipalities and water users also participated in the study, including the Salt Lake City Corporation, the Salt Lake County Water Conservancy District, Murray City, the Granger-Hunter Improvement District, the Taylorsville-Bennion Improvement District, the City of South Salt Lake, and the Kearns Improvement District.

The objectives of this study were (1) to better define the chemical quality of water in shallow sediments and underlying confining units; (2) to determine the hydrologic properties of shallow sediments and underlying confining units; (3) to better define the entire ground-water/hydrochemical flow system, including three-dimensional variation of hydrologic properties and ground-water quality in the ground-water flow system; and (4) to evaluate the movement of poor-quality water and the effects of changes in water use on ground-water quality. The approach to the third and fourth objectives included the development of ground-water and solute-movement computer simulations to enable planners to better understand the direction and rate at which ground water and chemical solutes move into, out of, and within this system under different stress conditions created by ground-water pumping. One of the first steps toward achieving these objectives included the development of a three-dimensional ground-water flow model of Salt Lake Valley.

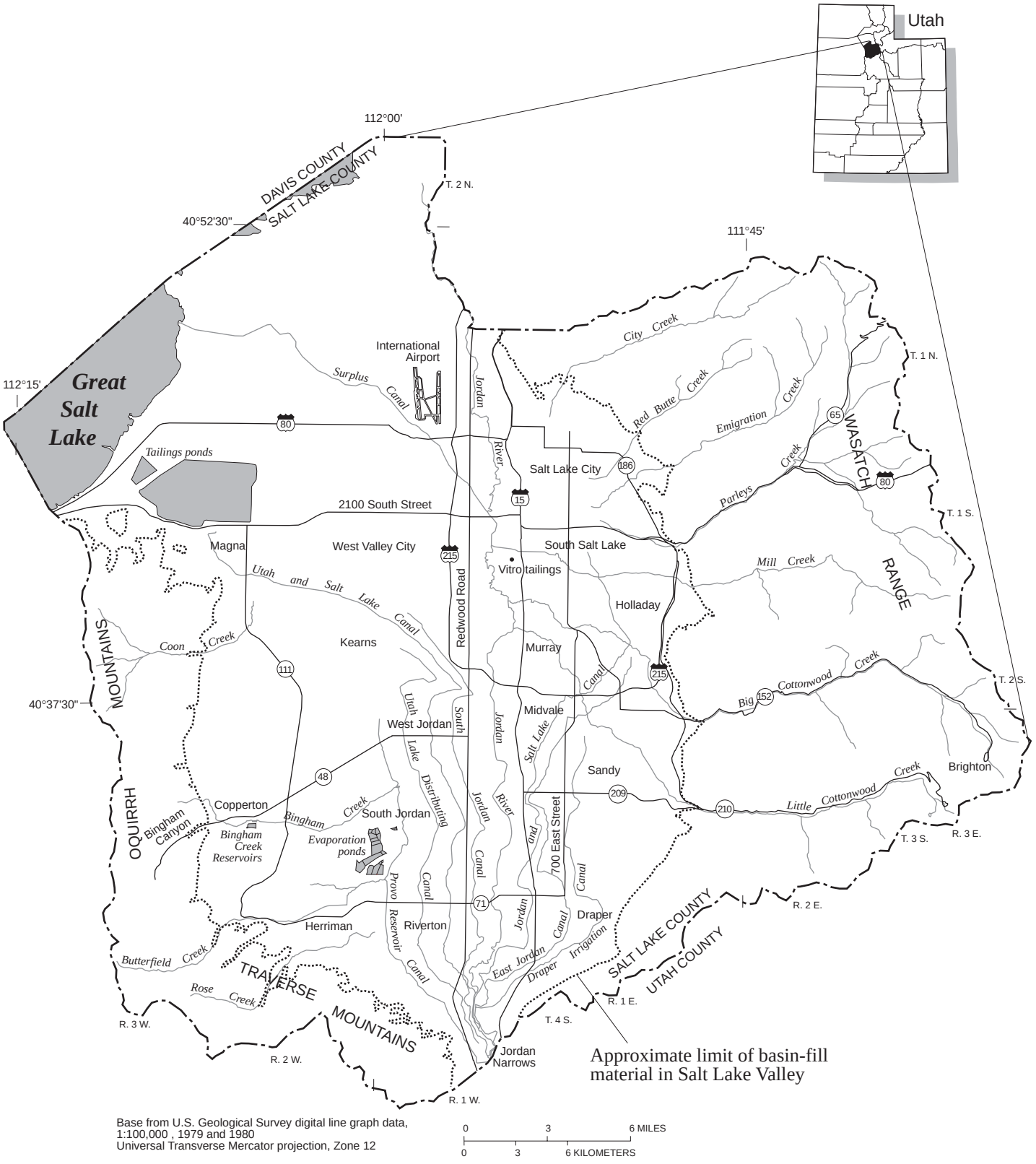

Figure 1. Location of Salt Lake Valley study area, Utah.

Purpose and Scope

The purpose of this report is to document the development and calibration of a three-dimensional, finite-difference, numerical model to simulate the ground-water flow system in basin-fill material in Salt Lake Valley, Utah (fig. 1). The model described in this report can be used to evaluate the movement of ground water and can be used in combination with other computer models and post-processing packages to evaluate the movement of solutes in ground water and the effects of water use on ground-water quality in Salt Lake Valley. This report describes the approach used in modeling the flow system and the data on which the model is based and includes discussions of the ability of the model to accurately reproduce measured hydrologic conditions. The report also includes a discussion of the limitations of the model as an accurate representation of the ground-water flow system.

This is the third in a series of reports on Salt Lake Valley. The first report presented hydrologic data collected in Salt Lake Valley during this study from 1990-92 (Thiros, 1992). The second report presented interpretations of those data and describes selected chemical properties of water and hydrologic properties of the basin-fill aquifer in Salt Lake Valley referenced in this report (Thiros, 1995).

Previous Work

Several previous studies were used in combination with data collected during this study as the foundation for the development of the numerical model documented in this report. Marine and Price (1964) described the geology and ground-water conditions in Salt Lake Valley, dividing the valley into ground-water districts on the basis of observed geomorphic features of the surface and subsurface geology. Mattick (1970) determined the thickness of unconsolidated and semiconsolidated sediments of Tertiary and Quaternary age in Salt Lake Valley using previously published geologic and geophysical data, including gravity and aeromagnetic surveys, seismic-refraction profiles, and data from geologic and drillers' logs of wells. Arnow and others (1970) determined the altitude of the base of the Quaternary sediments in Salt Lake Valley on the basis of drillers' logs of water wells and other geological and geophysical data. This work was updated with additional information in 1981 (Salt Lake County Division of Water Quality and Water Pollution Control, 1981). Hely and others (1971) presented a comprehensive description of surface-water conditions and the ground-water flow system in Salt Lake Valley on the basis of data mainly for 1964-68. Seiler and Waddell (1984) did a reconnaissance of the shallow unconfined aquifer in Salt Lake Valley and described the occurrence, water-surface altitude, and quality of ground water in the aquifer. Herbert and others (1985) presented the results of a seepage study of six major canals in Salt Lake County. Waddell and others (1987) presented estimates of annual recharge to and discharge from the ground-water flow system for 1969-82. Waddell and others (1987) developed a numerical flow model to evaluate the response of increased withdrawals on the ground-water flow system. The Waddell and others (1987) model simulated the ground-water flow system in Salt Lake Valley with two model layers, dividing the modeled area horizontally into 1,064 model cells of varying size. The model was calibrated using hydrologic data from 1968-83. This model was used by water-resource managers to estimate the limitations on the quantity of ground water that could be developed in Salt Lake Valley. The Waddell and others (1987) model was not, however, designed to define ground-water flow velocities or solute transport within and between water-yielding zones in the aquifers of the ground-water flow system.

Kennecott Utah Copper and entities associated with that company have collected and analyzed geologic and hydrologic data in the southwestern and northwestern parts of the valley. These data and analyses are presented in many volumes and appendixes of data reports and interpretive reports, some of which are referenced individually in this report.

Hydrogeology

The hydrogeology of the study area has been previously described in detail by Marine and Price (1964), Hely and others (1971), and Waddell and others (1987). The following discussion is based mainly on information from those reports.

Salt Lake Valley is a structural graben filled with semiconsolidated and unconsolidated basin-fill material. The valley is surrounded by the Oquirrh Mountains on the west, the Traverse Mountains on the south, the Wasatch Range on the east and northeast, and Great Salt Lake on the northwest (fig. 1). The surrounding mountains are composed of consolidated rock with negligible primary porosity but with substantial sec-

ondary porosity in the form of fractures and solution openings (Hely and others, 1971, p. 10). Geophysical data indicate that the consolidated-rock base of the valley is an irregular surface formed by the tops of fault blocks (Cook and Berg, 1961, p. 81), with inner-valley grabens containing, in some places, more than 4,000 ft of unconsolidated and semiconsolidated basin fill (Mattick, 1970, fig. 6). The general thickness of basin fill in Salt Lake Valley is shown in figure 2.

The basin-fill material consists mostly of sediments of Tertiary and Quaternary age and is made up of clay, silt, sand, gravel, tuff, and lava. The history and sequence of deposition of these sediments was described by Marine and Price (1964) as "extremely complex" as a result of the different mechanisms of deposition and erosion working in the valley and in the adjacent mountains throughout time. The valley received lake deposits in areas that were inundated by a series of ancient lakes, the most extensive of which was Lake Bonneville. As lakes dried, lake sediments were subjected to stream erosion, and previously inundated areas received stream-channel and flood-plain deposits. Alluvial fans formed along the mountain fronts at canyon mouths; glacial and mud-rock flow deposits also were laid down at the margins of the valley. As lakes reappeared and filled the valley, lacustrine deposition again predominated. The changes in depositional environments in the valley as lakes formed, dried up, and reappeared has resulted in the interlayered lacustrine, alluvial, and glacial sediments that make up most of the basin fill today, with coarse-grained sediments common near the mountains, and finer-grained sediments in the low-lying areas of the central and northern parts of the valley.

The basin-fill ground-water flow system in Salt Lake Valley (fig. 3) has been described by Hely and others (1971, p. 107) as consisting of (1) a confined (artesian) aquifer, (2) a deep unconfined aquifer between the confined aquifer and the mountains, (3) a shallow unconfined aquifer overlying the confined aquifer, and (4) local unconfined perched aquifers. The confined aquifer is in the central and northern parts of the valley and consists of deposits of clay, silt, sand, and gravel. In the confined aquifer, beds and lenses of fine-grained material of slight to moderate permeability tend to confine water in beds of sand and gravel. In the northern part of the valley, fine-grained sediments may make up most of the confined aquifer. In other areas of the confined aquifer, the beds and lenses are relatively thin and discontinuous; therefore, there is appreciable movement of water between more permeable beds of sand and gravel. Overlying the confined aquifer are sediments of relatively low permeability that consist of interfingering and overlapping layers and lenses of clay, silt, and fine-grained sand of Quaternary age. Although the continuity of these sediments varies, in many areas they act as a single bed, the top of which generally lies within 100 ft of land surface. For the purpose of discussion, this bed of fine-grained sediments is referred to in this report as the shallow confining layer. Near the margins of the valley where confining sediments are absent, ground water is unconfined. The confined zone beneath the shallow confining layer and the unconfined zones near the margins of the valley make up the principal aquifer of the ground-water flow system, which is the main source of most of the ground water withdrawn from wells in the valley (Hely and others, 1971, p. 109; Waddell and others, 1987, p. 5).

The thickness of basin-fill material of Quaternary age that makes up most of the principal aquifer ranges from 0 to 2,000 ft. This thickness was evaluated on the basis of information presented by Arnow and others (1970) describing the altitude of the pre-Quaternary surface in the valley and is shown in figure 4. Quaternary-age basin fill of the principal aquifer generally overlies relatively impermeable, semiconsolidated sediments of Tertiary and pre-Tertiary age (Arnow and others, 1970, p. D257). In some areas of the valley, however, more permeable Tertiary-age basin fill containing sand and gravel yields water to wells. Tertiary-age basin fill is known to yield water to wells in the vicinity of Kearns and to the west, near Murray, and near Herriman and Riverton (Hely and other, 1971, p. 107). Water-yielding zones in Tertiary-age basin fill are included with the principal aquifer in the discussions that follow.

A shallow unconfined aquifer overlies the shallow confining layer. The aquifer is composed mainly of fine-grained sediments and in some areas of the valley cannot be differentiated from the underlying confining layer. The aquifer is the source of water for local irrigation but is seldom used to supply water for domestic or industrial purposes because it yields water slowly and generally contains water of poor quality (Seiler and Waddell, 1984, p. 2). Ground water is perched in areas where the water level in the principal aquifer is below the bottom of the shallow confining layer; thus, an unsaturated zone exists between the water table in the principal aquifer and the body of perched water above it. Areas of perched water occur east of Midvale and between Herriman and Riverton.

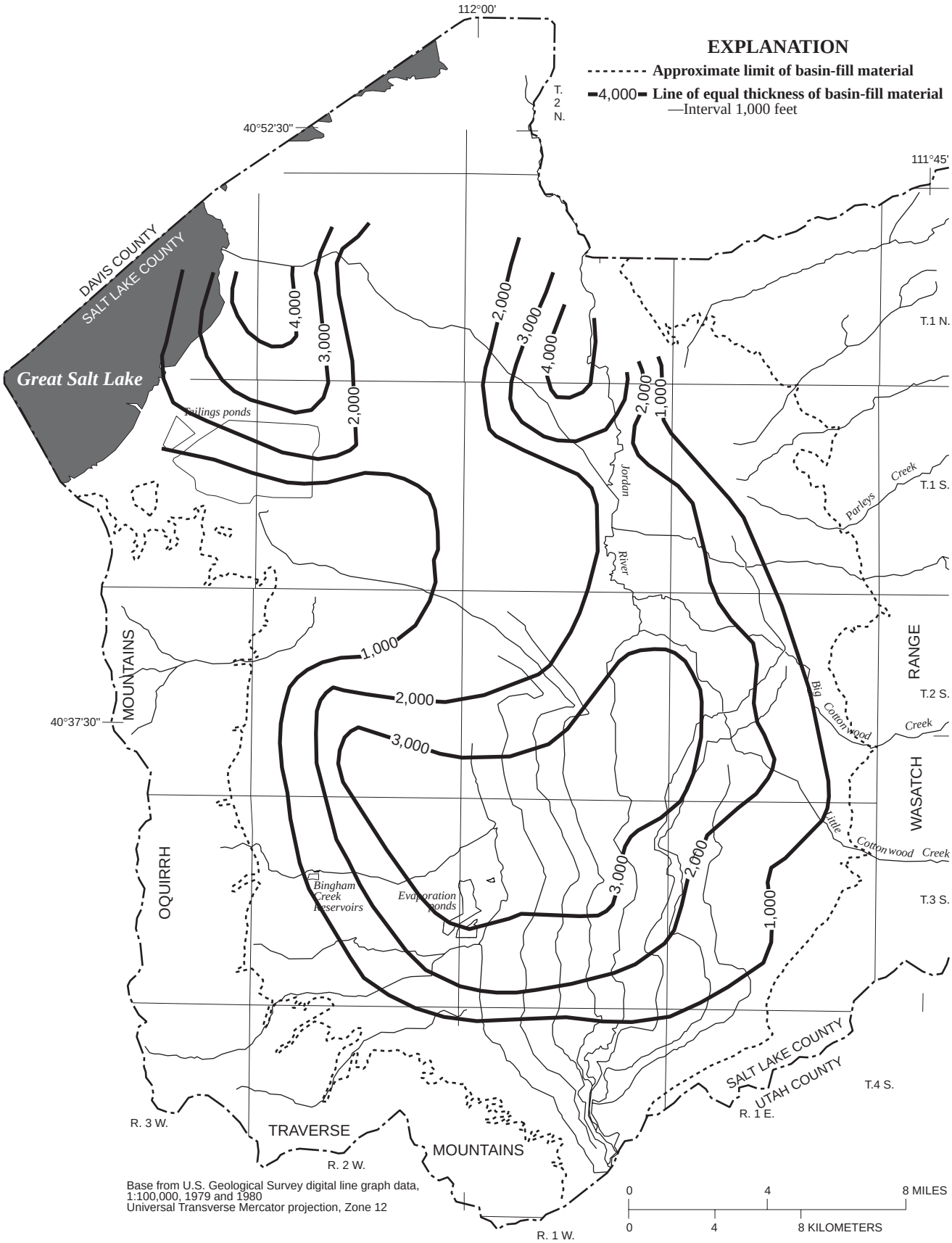

Figure 2. Thickness of the basin-fill material in Salt Lake Valley, Utah. Modified from Mattick (1970).

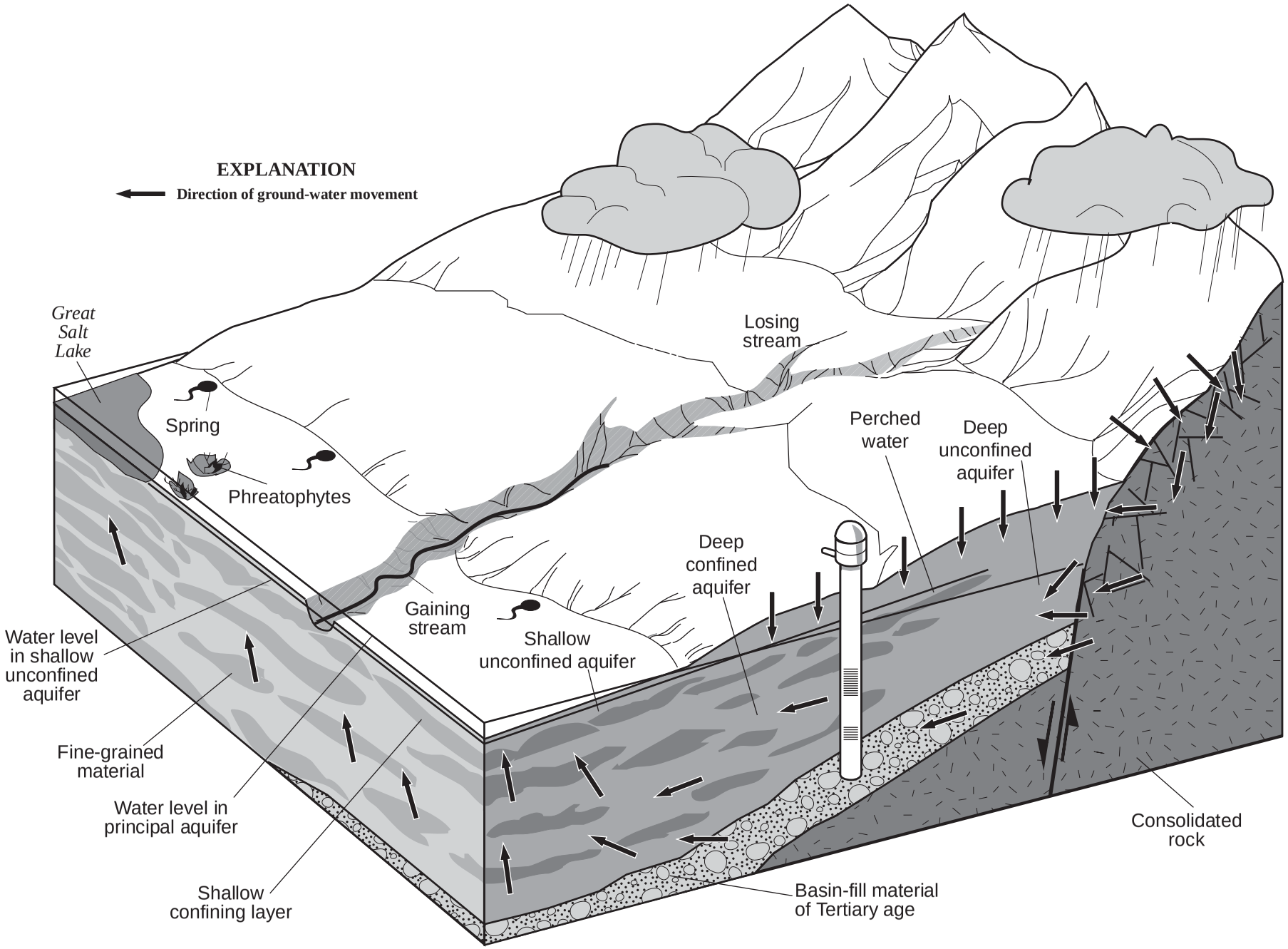

Figure 3. Generalized block diagram showing the basin-fill ground-water flow system in Salt Lake Valley, Utah. Modified from Hely and others, (1971).

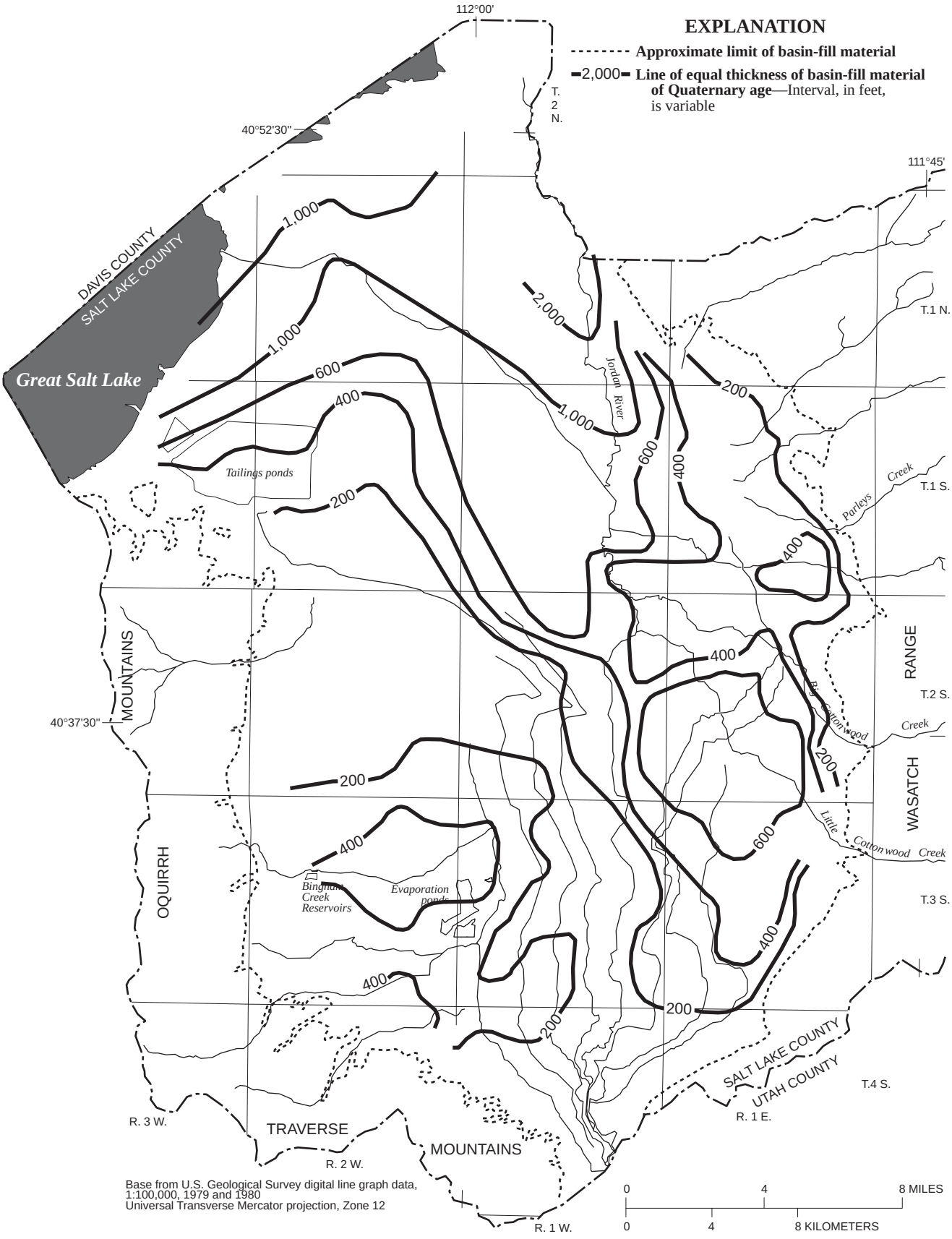

Figure 4. Thickness of basin-fill material of Quaternary age in Salt Lake Valley, Utah.

Recharge to the basin-fill ground-water flow system primarily is from inflow from consolidated rock at the margins of the valley, seepage from streams and canals with a water-surface altitude higher than that of the water table, infiltration of precipitation on the valley floor, and infiltration of unconsumed irrigation water from fields, lawns, and gardens. Ground water moves from primary recharge areas near the margins of the valley to the center and northern parts of the valley (fig. 3). As ground water moves laterally from the deep unconfined aquifer beneath recharge areas into the confined aquifer, an upward vertical gradient is established. From the axial part of the valley, ground water moves upward in the confined aquifer, into and through the overlying confining layer, and into the shallow unconfined aquifer, where it is discharged mainly into the Jordan River or to drains, is used by riparian vegetation, or evaporates at land surface. Most of the discharge from the basin-fill ground-water flow system, other than discharge from wells, is via the shallow unconfined aquifer.

Present-day hydrology in Salt Lake Valley is greatly affected by municipal and industrial use of ground water. A summary of annual ground-water withdrawal from wells during 1931-68 (Hely and others, 1971, fig. 66) indicates a range from 38,000 acre-ft in 1931 to 118,000 acre-ft in 1966. The rate of withdrawals began to level off about 1964 and averaged 107,000 acre-ft per year during 1964-68 (Hely and others, 1971, p. 140). Increases in ground-water withdrawals during 1987 to 1991 combined with less-than-average recharge to the ground-water flow system have resulted in water-level declines in the southeastern part of the valley of up to 26 ft for that period (Batty and others, 1993, fig. 11).

MODELING APPROACH

The modular, three-dimensional, finite-difference, ground-water flow model of the U.S. Geological Survey (McDonald and Harbaugh, 1988) was used to simulate the regional flow system in the basin-fill material in Salt Lake Valley. The model was calibrated to steady-state and transient-state conditions.

Steady-state conditions require the volume of water flowing into the simulated system to equal the volume of water flowing out. The steady-state simulation therefore was developed using available data that were assumed to represent near-equilibrium conditions under which storage of ground water does not change appreciably. Because of relatively constant pumpage and small changes in storage during 1964-68 (Waddell and others, 1987, p. 39), recharge was assumed to be about the same as discharge during 1968 and representative of near-steady-state conditions. During 1968, withdrawals from wells were about 105,000 acre-ft, 2,000 acre-ft less than the average for 1964-68 (Waddell and others, 1987). Changes in storage were less than 2,000 acre-ft in 1968 and averaged about 3,000 acre-ft during 1964-68 (Waddell and others, 1987, p. 39); both quantities represent less than 1 percent of the estimated total ground-water budget for that period (Waddell and others, 1987, tables 1 and 3). Also, the amount of available data for recharge, discharge, and water levels for 1968 was much greater than that of earlier years when the ground-water flow system may have been nearer to a natural steady-state equilibrium. Steady-state calibration involved comparing model-computed and measured water levels, model-computed and estimated ground-water flow to the Jordan River, and simulated and measured vertical hydraulic gradients. The simulated ground-water budget was compared with estimates of the ground-water budget derived during prior studies to help evaluate the fit of the model to measured conditions.

The transient-state simulation was developed using hydrologic data from 1969-91. The results of steady-state calibration were used as initial conditions for the transient-state simulation. The transient-state simulation includes the simulation of annual variations in recharge from surface and subsurface sources and discharge by pumpage with time. During model calibration, model-computed water-level changes were compared with measured water-level changes. Also, simulated flow rates at model boundaries that simulate ground-water discharge to the Jordan River were compared with independently estimated annual seepage rates during model calibration.

In the following subsections, the approach to mathematically simulating ground-water flow in Salt Lake Valley is presented. Where necessary, the requirements of the steady-state and transient-state simulations are distinguished.

Discretization

Areally, the model grid is 94 rows by 62 columns (fig. 5), with each model cell 0.35 mi on a side. Vertically, the aquifer system is divided into seven layers. The shallow unconfined aquifer and the underlying shallow confining layer were represented by one model

Figure 5. Grid and location of active cells in layers 3 to 7 of the ground-water flow model of Salt Lake Valley, Utah.

layer each (model layers 1 and 2, respectively) (fig. 6). The thickness of model layers 1 and 2 is variable and roughly imitates the estimated depth and thickness of the shallow unconfined aquifer and the underlying shallow confining layer. The principal aquifer was divided into five layers (model layers 3 to 7) (fig. 5). Model layers 3 to 5 are each 150 ft thick; the simulated saturated thickness of model layer 3 may vary during problem solution. Model layer 6 is 200 ft thick. Model layer 7 ranges in thickness from 200 ft to more than 1,500 ft. The thickness of each of model layers 4 to 7 was not explicitly incorporated into the model but was implicitly incorporated in model input defining aquifer properties of those model layers. Vertical discretization of the principal aquifer allowed for improved simulation of the geometry of the basin-fill aquifer system and for the incorporation of vertical anisotropy.

The transient-state simulation period, from January 1969 to December 1991, was divided into 23 stress periods of 1 year in length. During a stress period, external stresses on the simulated system, representing average recharge or discharge for a given year, are held constant. Each stress period was divided into three time steps. The length of the first time step of each stress period was 77 days (rounded) and was increased with advancing time by a time-step multiplier of 1.5. Time-step length was reduced during transient-state calibration to ensure that the accuracy of the simulation was not affected by truncation error resulting from an inappropriate initial time-step size. Results of simulations using shorter time steps did not indicate a significant change in model-computed water levels or flow rates.

In this report, an "i, j, k" indexing convention is used when discussing model cells and their location in the model grid. As indicated in figure 5, i is the row index, and j is the column index. The index k refers to model layers; layer 1 (k = 1) is the top model layer and layer 7 (k = 7) is the bottom model layer. The term "vertical column," as used in this report, is the set of model cells with the same row (i) and column (j) index.

Boundary Conditions

The ground-water flow model requires specific types of mathematical boundaries to be assigned to the ground-water system to simulate flow at surface boundaries and internal sources and sinks. The flow boundary may simulate no-flow conditions, recharge to the ground-water flow system, or discharge from the ground-water flow system.

A no-flow boundary at the base of the modeled area corresponds to the contact between consolidated rock of pre-Tertiary age and basin-fill material, or to a depth within the basin fill below which sediments were assumed not to contribute substantially to the basin-fill ground-water flow system. On the west and east sides of the modeled area, no-flow boundaries correspond to the contact between the consolidated rock of the mountains and the basin fill. The northern border of the modeled area approximates a flow line and was treated also as a no-flow boundary. The shore of Great Salt Lake in the northwestern part of the modeled area was treated as a constant-head boundary representing the altitude of the lake surface.

Specified-flux boundaries were used to simulate recharge entering the ground-water flow system as (1) inflow from consolidated rock in areas at the margins of the valley, (2) seepage from streams and major canals, (3) infiltration of precipitation on the valley floor, (4) infiltration of unconsumed irrigation water from fields, lawns, and gardens, (5) seepage from reservoirs at the mouth of Bingham Canyon and evaporation ponds in the southwestern part of the valley, and (6) underflow at Jordan Narrows. Specified-flux boundaries also were used to simulate discharge from the ground-water flow system to wells, canals, and springs. The specified-flux boundary condition allows the flow rate across a given boundary to be specified as a function of location and time. Flow rates across these boundaries are specified in advance in the steady-state simulation and for each stress period of the transient-state simulation. Flow rates do not deviate at these boundaries during problem solution and are not affected by simulated conditions in the ground-water flow system.

Head-dependent flux boundaries were used to simulate (1) ground-water flow to and seepage from the Jordan River and the lower reaches of its principal tributaries, (2) inflow from consolidated rock at the northern end of the Oquirrh Mountains, (3) discharge from the shallow unconfined aquifer to drains, and (4) discharge by evapotranspiration. A head-dependent flux boundary allows the flow rate across the boundary surface to change in response to changes in water level in the aquifer adjacent to the boundary. Flow rate is therefore a function of the water level in the adjacent aquifer and may vary during problem solution and from one time step to the next in the transient-state simulation.

A head-dependent river boundary (McDonald and Harbaugh, 1988, p. 6-1) was used in the model to

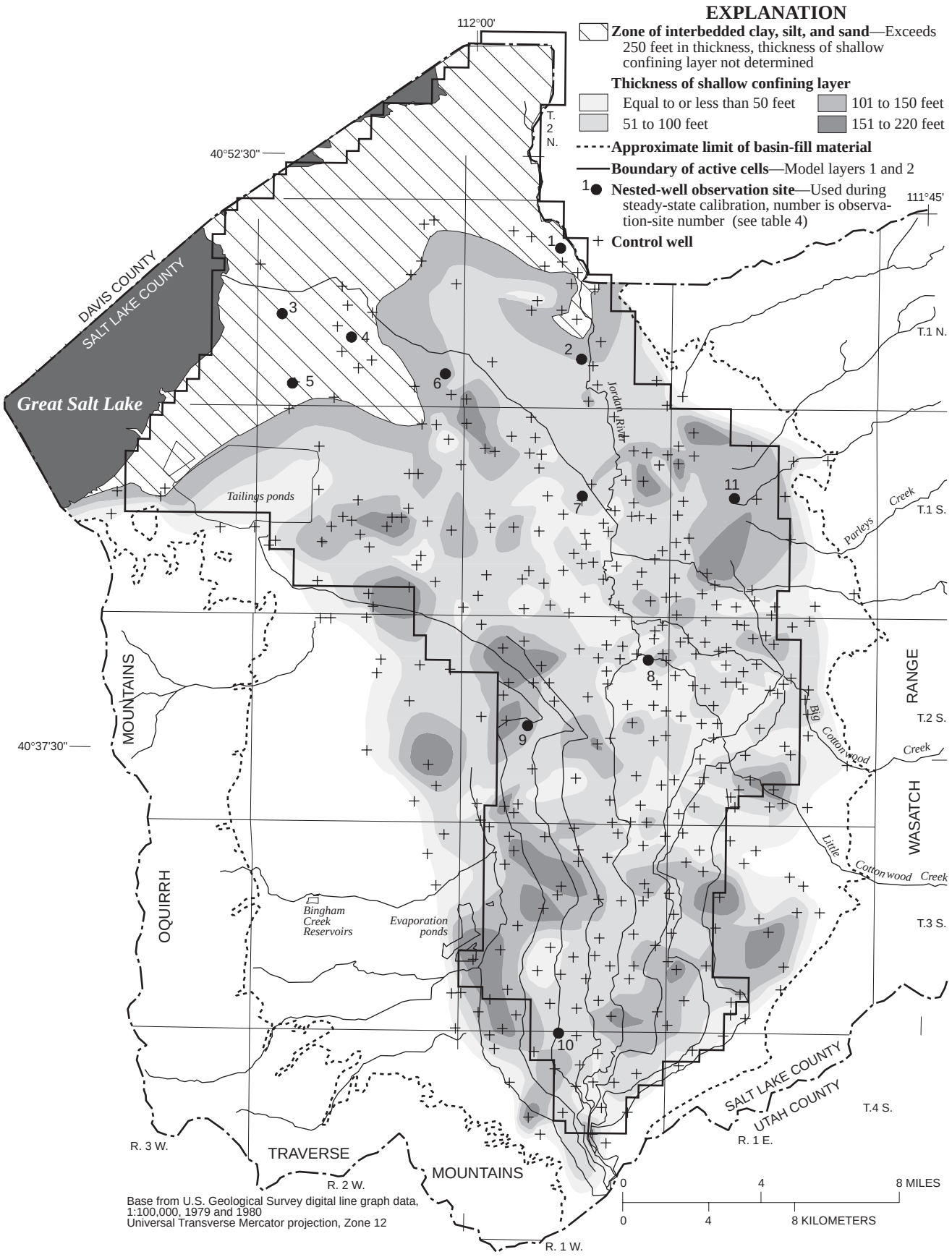

Figure 6. Extent and thickness of the shallow confining layer, and location of active cells in layers 1 and 2 of the groundwater flow model, Salt Lake Valley, Utah.

represent the Jordan River and the lower reaches of its major tributaries and simulates ground-water flow to or seepage from the river depending on the simulated water-level gradient between the river and the adjacent aquifer. Flow between the river and the adjacent aquifer at a given cell containing a river boundary is simulated according to the following equation set (McDonald and Harbaugh, 1988, p. 6-8):

$$QRIV = CRIV\,(HRIV - h), \quad if \quad h > RBOT, \tag{1a}$$

$$QRIV = CRIV(HRIV - RBOT), \quad if \quad h <= RBOT, \tag{1b}$$

where

QRIV = flow to or from the river (positive if flow is from the river to the aquifer)(L^3/t),
HRIV = specified water level in the river (L),
CRIV = the hydraulic conductance of the river-aquifer interconnection (river-bed conductance) (L^2/t),
h = model-computed water level in the cell containing the river boundary (L), and
RBOT = altitude of the river bottom (L).

No flow is simulated at a river boundary when *h* is equal to *HRIV*. For larger values of *h*, ground-water flow to the river is simulated, and for smaller values of *h*, flow from the river to the aquifer is simulated. Flow from the river to the aquifer increases linearly as *h* decreases, until *h* reaches *RBOT*; thereafter, flow remains constant.

A head-dependent drain boundary was used to simulate the influence of surface and buried drains on the ground-water flow system. The head-dependent drain boundary is similar to the river boundary but does not simulate flow from a drain to the aquifer. When the model-computed water level in a given cell containing a drain boundary (*h*) is lower than the specified altitude of the drain in that cell (*D*), no flow to or from the drain is simulated. When the model-computed water level in a cell is higher than the specified altitude of the drain in that cell, flow to the drain (*QD*) is simulated according to the following equation (McDonald and Harbaugh, 1988, p. 9-3):

$$QD = CD(h - D) \text{ for } h > D \tag{2}$$

where *CD* (drain conductance) is equal to the hydraulic conductance of the drain-aquifer interconnection.

A head-dependent boundary termed a general-head boundary by McDonald and Harbaugh (1988, p. 11-1) was used to simulate inflow from consolidated rock at the northern end of the Oquirrh Mountains. The general-head boundary is mathematically similar to the river boundary and the drain boundary because flow into or out of a given boundary cell (*QGHB*) from an external source is a function of the difference between the model-computed water level in the cell (*h*) and the specified water level of the external source (h_b), and the conductance between the external source and the cell (*CGHB*):

$$QGHB = CGHB(h - h_b) \tag{3}$$

In this case, *CGHB* represents the conductance of the consolidated-rock/basin-fill aquifer interconnection, and h_b represents the water level in the consolidated-rock aquifer.

The model incorporates a linear head-dependent function to simulate ground-water discharge by evapotranspiration. In a given cell, the evapotranspiration rate will be equal to a specified maximum rate if the model-computed water level in the cell is higher than a specified altitude (typically land surface). If the simulated water table is at a depth equal to or less than a specified extinction depth, the evapotranspiration rate will be zero. If the simulated water table is between the land surface and the extinction depth, the evapotranspiration rate will decrease linearly from the maximum rate to zero.

Transmissivity, Storage Coefficient, and Vertical Leakance

In model layers 1 to 3, transmissivity varies spatially as a function of the wetted thickness of the layer and the equivalent horizontal hydraulic conductivity of the sediments in the layers. In model layers 4 to 7, which represent deep sediments of the principal aquifer, wetted thickness of model layers was assumed to remain constant and transmissivity was specified in all simulations and does not vary during problem solution.

In model layer 1, and in model layer 3 in areas where the shallow unconfined aquifer is not simulated, unconfined conditions are assumed to always prevail and changes in storage are computed by the model as a function of drainable porosity. In these areas, the storage coefficient used in the model is equivalent to specific yield. In model layer 2, and in model layer 3 in areas where the shallow unconfined aquifer is simulated, the model allows for a storage coefficient that depends on the relation between model-computed water level in a model layer and the top of the model layer. If the model-computed water level is higher than

the top of the layer (confined conditions), then the change in storage caused by water-level changes is a function of the elastic properties of the aquifer. If the model-computed water level is lower than the top of the model layer (unconfined conditions), then changes in storage are a function of drainable porosity, and the storage coefficient used by the model is equivalent to specific yield. The model does not convert from confined-aquifer storage coefficient to specific yield in model layers 4 to 7, where confined conditions are assumed to always prevail.

The model computes vertical conductance from model input termed "vertical leakance" (McDonald and Harbaugh, 1988, p. 5-12). Vertical leakance between model layers varies as a function of equivalent vertical hydraulic conductivity and the thickness of sediments present between the midplanes of adjacent model layers. The vertical leakance between model layers k and k+1 is

$$VL_{k+1} = K'_{v,k+1/2} / b_{k+1/2,} \quad (4)$$

where

$K'_{v,k+1/2}$ = equivalent vertical hydraulic conductivity between the midplanes of model layers k and k+1 (L/t), and

$b_{k+1/2}$ = distance between the midplanes of the two adjacent model layers (L).

Where adjacent model layers are characterized by different vertical hydraulic conductivities ($K_{v,k}$, $K_{v,k+1}$), the equivalent vertical hydraulic conductivity ($K'_{v,k+1/2}$) can be calculated with the following equation (Freeze and Cherry, 1979, p. 34):

(5)

$$K'_{v,\,k+1/2} = \frac{b_{k+1/2}}{(b_k/2)/K_{v,\,k} + (b_{k+1}/2)/K_{v,\,k+1}},$$

where

b_k = thickness of layer *k* (L), and

b_{k+1} = thickness of layer *k+1* (L).

PARAMETER ESTIMATION AND AVAILABLE DATA

Data from previous work in the valley and data collected during this study were used to evaluate model parameters. Estimates defining (1) the geometry of the ground-water flow system, (2) seepage from reservoirs at the mouth of Bingham Canyon and evaporation ponds in the southwestern part of the valley, (3) discharge to wells, and (4) discharge to springs were made independent of the model and were not adjusted during model calibration. All other model parameters were considered to be calibration variables that could be adjusted within prescribed ranges during model calibration. In the following subsections, data used for independently evaluating model parameters are discussed and the values used in the model are presented. Those parameters that were calibration variables also are discussed. Ranges of probable values for calibration variables are defined where possible, and preliminary estimates used in the model are presented. Final estimates of model parameters resulting from model calibration are presented later in subsections of the "Model calibration" section of this report.

System Geometry

The location and dimension of active cells in the model grid (figs. 5 and 6) depict the general geometry of the valley and the physical characteristics of the basin-fill material. Location of no-flow boundaries in each model layer and the specified altitude of the top and bottom of model layers were determined mainly on the basis of an evaluation of the following physical characteristics: (1) the horizontal extent, altitude, and thickness of the shallow confining layer and the shallow unconfined aquifer, (2) the altitude of the contact between basin fill of Quaternary and Tertiary age, and (3) the altitude of the contact between consolidated rock and basin fill.

More than 300 drillers' logs of water wells and test wells were reviewed during this study to determine the horizontal extent, altitude, and thickness of the shallow confining layer and the overlying shallow unconfined aquifer (fig. 6). The description of material encountered during drilling was reviewed on each log, and the depth to the top and bottom (relative to land surface) of the uppermost zone of material that (1) consisted mostly of clay and (or) silt and (2) was more than 20 ft thick were recorded. Well logs used in the analysis were selected on the basis of the completeness of the description of the material encountered during drilling and on the location of the well. The zone of fine-grained sediments defined by this analysis was assumed to represent the shallow confining layer that underlies the shallow unconfined aquifer (fig. 6). The area of active cells in model layers 1 and 2 (fig. 6) corresponds to the area where the shallow confining layer was identified in this analysis and where it was determined, on the basis of measurements at shallow wells, that the

water table was above the top of the shallow confining layer.

The altitude of the base of the shallow unconfined aquifer and the base of the shallow confining layer was interpolated from the data obtained from the analyses of drillers' logs and was explicitly incorporated into the model. The shaded contour patterns shown in figure 6 were defined with the aid of a computer contouring program and reflect, in general, the values incorporated in the model as the thickness of model layer 2. In the northern part of the valley, where thick sequences of fine-grained sediments occur (fig. 6), the shallow unconfined aquifer and the shallow confining layer could not be delineated and the altitudes incorporated in the model for the top and bottom of model layer 2 were arbitrarily chosen as 75 ft below land surface and 150 ft below land surface, respectively. In some areas, information from drillers' logs identified the top of the shallow confining layer to be at or near land surface. In these areas, the altitude of the top of model layer 2 was arbitrarily chosen to be one-half the distance between land-surface altitude and the altitude of the bottom of the shallow confining layer.

Active cells in model layers 3 to 7 represent basin-fill material of Quaternary age in the principal aquifer, and in areas include the upper part of the underlying basin-fill material of Tertiary age. In general, Tertiary-age basin fill in the valley is relatively impermeable and may not be a significant avenue for movement of ground water in most areas. More permeable Tertiary-age basin fill, however, has been identified locally in the valley. For this reason, the upper part (150 to 400 ft) of the Tertiary unit was included in areas as part of the active area of the model.

Active cells in model layers 3 to 7 were defined on the basis of the type of sediments they represented. The thickness of the basin-fill material delineated by age as shown in figures 2 and 4 was evaluated at vertical columns in the model. Cells were defined as active or inactive according to the following guidelines: (1) All cells containing basin fill of Quaternary age were designated as active, (2) Cells below the contact of Tertiary- and Quaternary-age basin fill were designated as active if they were less than 1,000 ft below land surface and directly beneath a cell containing Quaternary-age basin fill, and (3) Cells below the consolidated-rock/basin-fill contact were designated as inactive. In areas where the thickness of Quaternary-age basin fill exceeded 1,000 ft, the bottom of the principal aquifer was assumed to be the base of the Quaternary-age basin fill.

Hydrologic Properties

All model parameters defining the hydrologic properties of the basin-fill material were considered to be calibration variables. Initial estimates and ranges of probable values for these parameters were determined on the basis of information obtained during this study that was reported by Thiros (1992 and 1995) and on the results of previous studies, including the results of the calibration of numerical flow models. Estimates of hydrologic properties determined during the calibration of a two-layer ground-water flow model documented by Waddell and others (1987) were used to generate initial estimates for some model parameters. The modeled area in the Waddell and others (1987) model is about the same as that of the model documented here, and provided a good source of initial estimates, particularly where data from other sources were sparse.

Horizontal Hydraulic Conductivity Of Shallow Sediments

During this study, new data pertaining to the hydrologic properties of the sediments that make up the shallow unconfined aquifer, and of the underlying shallow confining layer were collected from shallow monitoring wells. Hydraulic-conductivity values estimated from the results of 32 slugs tests at wells completed in the shallow unconfined aquifer ranged from 0.003 ft/d to 65.5 ft/d (Thiros, 1995, table 4). The wide range of values typifies the spatial variability of the hydrologic properties of the shallow sediments of the valley. The tests were conducted in small intervals of material, and individual test results were not assumed to represent the equivalent hydraulic conductivity of the shallow unconfined aquifer. Test results were used, however, to define a probable range of values that could be used to place conceptual limits on model input for use during model calibration. Initial values of hydraulic conductivity of the shallow unconfined aquifer used in the model were based on estimates determined during calibration of the Waddell and others (1987, p. 30, fig. 16) model and limited by the range defined above.

The results of four slug tests at wells completed in what was assumed to be the shallow confining layer (S.A. Thiros, U.S. Geological Survey, written commun., 1993) indicate values of hydraulic conductivity ranging from 0.04 ft/d to 2.28 ft/d with a mean of 1.2 ft/d. A preliminary value for hydraulic conductivity of 1 ft/d was used for model layer 2, which represents the shallow confining layer.

Transmissivity of the Principal Aquifer

The transmissivity of the principal aquifer has been estimated in previous studies from specific-capacity data and the results of aquifer tests. Price (1988) and Price and Conroy (1988) combined data reported by Hely and others (1971, fig. 59) with additional data to create a map of transmissivity of the principal aquifer in Salt Lake Valley. The results of four aquifer tests done during this study (Thiros, 1995) were combined with the ranges of transmissivity defined in previous studies and a modified map showing transmissivity was produced (fig. 7). The resulting ranges of transmissivity are assumed to represent the total transmissivity of the principal aquifer.

Total transmissivity of the principal aquifer (T) represented in the model is a summation of the transmissivity of each part of the aquifer, Quaternary and Tertiary, and is implicitly represented in the model in the transmissivities of model layers 3 to 7. Because T is equivalent to the product of the hydraulic conductivity and aquifer thickness, total transmissivity of the principal aquifer represented in vertical columns of the model ($T_{i,j}$) can be represented using the following summation:

$$T_{i,j} = K_{Qu,i,j} b_{Qu,i,j} + K_{T,i,j} b_{T,i,j} \quad (6a)$$

where

$K_{Qu,i,j}$ = hydraulic conductivity of Quaternary-age basin fill at vertical column *i,j* (L/t),

$b_{Qu,i,j}$ = thickness of Quaternary-age basin fill at vertical column *i,j* (L),

$K_{T,i,j}$ = hydraulic conductivity of Tertiary-age basin fill at vertical column *i,j* (L/t), and

$b_{T,i,j}$ = thickness of Tertiary-age basin fill at vertical column *i,j* (L).

To derive initial estimates for transmissivity of the individual model layers 3 to 7, estimates of the horizontal hydraulic conductivity of basin-fill material within vertical columns of the model grid were made. The hydraulic conductivity of Tertiary-age basin fill (K_T) was initially estimated to be 1 ft/d throughout the valley. This estimate was based on values reported by Dames and Moore (1988, table 8) for semiconsolidated basin fill in the southwestern part of the valley. The hydraulic conductivity of Quaternary-age basin fill (K_{Qu}) was then determined at vertical columns by rearranging equation 6a and solving for $K_{Qu,i,j}$,

$$K_{Qu,i,j} = \frac{T_{i,j} - K_{T,i,j} b_{T,i,j}}{b_{Qu,i,j}}, \quad (6b)$$

using estimates of $T_{i,j}$ obtained by interpolation from the data presented in figure 7.

A conceptual limit of 230 ft/d was assumed for the hydraulic conductivity of the unconsolidated basin-fill material on the basis of the results of a synthesis of hydrologic properties of rocks of the Basin and Range Province by Bedinger and others (1986). At vertical columns where the hydraulic-conductivity value of Quaternary-age basin fill calculated using equation 6b exceeded 230 ft/d, the hydraulic-conductivity value of Tertiary-age basin fill was assumed to be greater than 1 ft/d. At these vertical columns, K_{Qu} was set equal to 230 ft/d and a new estimate of K_T was computed using equation 6b. Given estimates of K_{Qu} and K_T at each vertical column, the equivalent hydraulic conductivity of sediments represented in model cells could be calculated, and the transmissivity of each cell could be calculated as a function of the equivalent hydraulic conductivity and cell thickness.

Total transmissivity of the principal aquifer was used as a calibration variable. Estimates were adjusted from initial values indicated in figure 7 during model calibration, and new individual transmissivity values for model layers 3 to 7 were calculated using the procedure described in the previous paragraphs. The method of incorporating total transmissivity of the principal aquifer in the model described in this section defines a simplifying construct resulting in a distribution of transmissivity that reflects, in general, the lithologic variations within the principal aquifer, including the assumption that the hydraulic conductivity of Quaternary-age basin fill is generally greater than that of Tertiary-age basin fill.

To facilitate calibration of the model, transmissivity of model layer 3 was specified initially in the model and was simulated as being constant during problem solution. At the end of steady-state calibration, the simulation properties of model layer 3 were changed such that the equivalent hydraulic conductivity of sediments represented in the layer was input to the model, and transmissivity of the layer was computed by the model as a product of hydraulic conductivity and model-computed saturated thickness as described in the "Model approach" section of this report. This was done to more accurately simulate the changes in transmissivity of model layer 3 resulting from fluctuations in the water-table surface simulated during transient-state simulations.

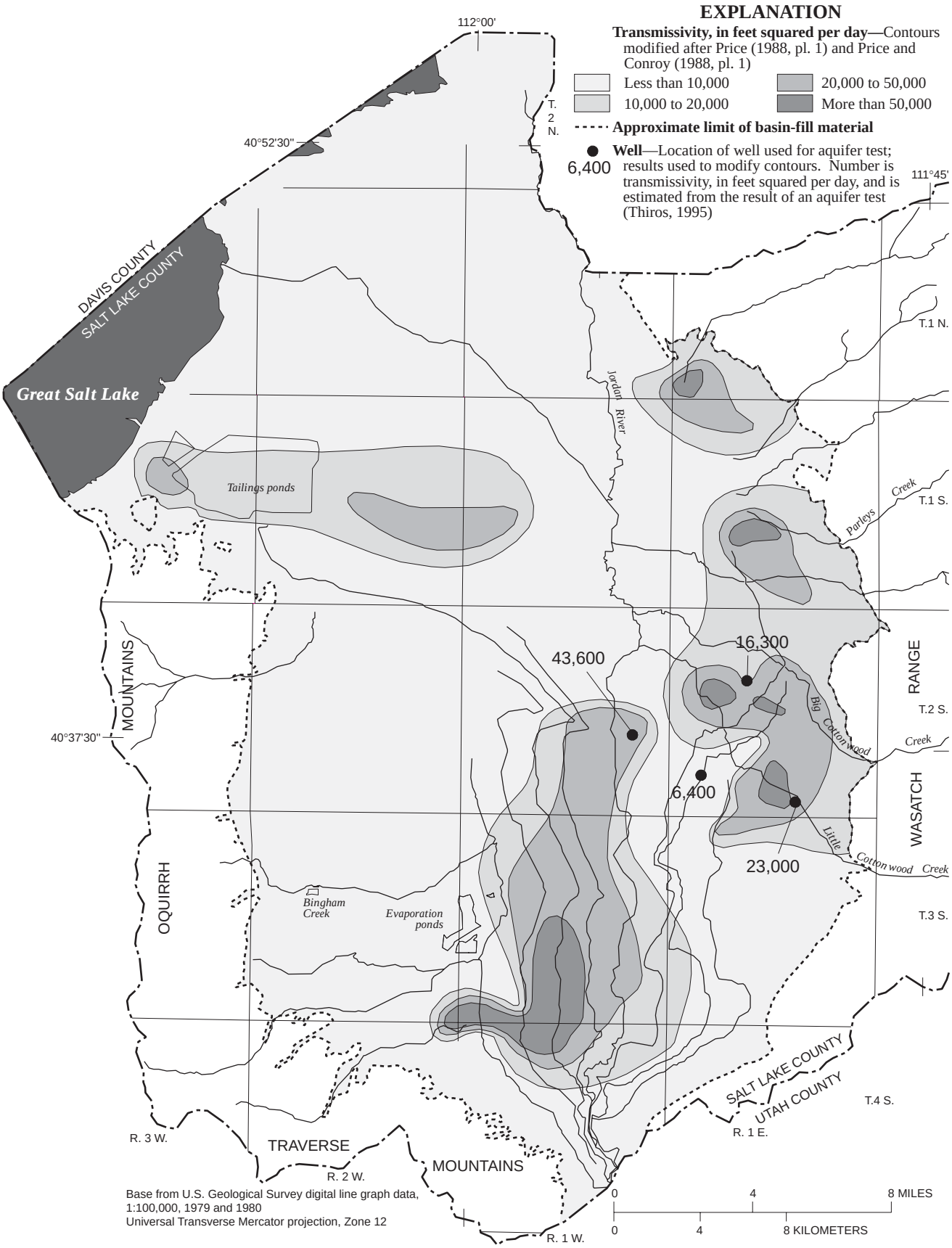

Figure 7. Transmissivity of the principal aquifer in Salt Lake Valley, Utah.

Vertical Hydraulic Conductivity and Vertical Leakance

The vertical hydraulic conductivity of basin-fill material was not explicitly incorporated in the model but was implicitly incorporated in vertical leakance (VL) between model layers (equation 4). Independent estimates of vertical hydraulic conductivity (K_v) of the basin fill were evaluated and used to define conceptual limits for vertical leakance.

Estimates of vertical hydraulic conductivity (K_v) for the shallow confining layer were made by Hely and others (1971, p. 118) for two areas of the valley. A value of 0.016 ft/d was estimated for an area near Great Salt Lake, and a value of 0.049 ft/d was estimated for an area between Holladay and Murray (fig. 1). These estimates were developed on the basis of the hydraulic gradient and ground-water discharge through an area of the shallow confining layer. A K_v of 0.12 ft/d was estimated for shallow sediments near the Vitro Tailings area (fig. 1) by Waddell and others (1987, p. 30) from the results of an aquifer test. A range of K_v for the upper confining layer of 0.01 ft/d to 1.0 ft/d was estimated from the results of three multiple-well aquifer tests done during this study at well sites in the vicinity of Sandy and Midvale (Thiros, 1995, p. 33-38). Thiros (1992, table 12) also reported a range in magnitude for K_v for shallow sediments of 5.1×10^{-5} ft/d to 0.02 ft/d determined from laboratory tests of 35 core samples. The cored material typically consisted of silt and clay and was assumed to represent sediments of the shallow confining layer or the shallow unconfined aquifer.

Initial estimates of vertical leakance between model layers 1 and 2 (VL_2) and between model layers 2 and 3 (VL_3) were based mainly on estimates of vertical leakance derived during calibration of the model documented by Waddell and others (1987). Conceptual limits for leakance values used during model calibration were defined on the basis of a probable order-of-magnitude range of values for vertical hydraulic conductivity (K_v) for model layers 1 and 2 of 1.0×10^{-5} ft/d to 1 ft/d. In many areas of the valley, the sedimentary characteristics of the shallow unconfined aquifer resemble those of the shallow confining layer; therefore, the same probable range of values for K_v was assumed for both layers.

There are no reported vertical hydraulic-conductivity (K_v) data for the sediments of the principal aquifer. Several estimates, however, have been made during previous studies on the basis of the results of the development and calibration of numerical flow models. In a three-dimensional flow model of the ground-water flow system in the southwestern part of the valley, Dames and Moore (1988, table 8) estimated K_v of unconsolidated basin-fill material to be 0.5 ft/d. Holdsworth (1985, table 2), in a two-dimensional flow model in the same area, estimated K_v for unconsolidated basin fill to range from 1 ft/d to 30 ft/d.

Initial estimates for vertical leakance (VL) between model layers that represent the principal aquifer were made by dividing the aquifer into four zones that represent areas of different sedimentary characteristics (fig. 8), and estimating vertical hydraulic conductivity (K_v) for each zone. Definition of lithologic zones was based on information collected from drillers' logs during this study and on an evaluation of sedimentary characteristics of the principal aquifer made by Marine and Price (1964, fig. 12). Zone 1 represents an area of the aquifer that consists primarily of lake-bottom clays interbedded with thin sand lenses. Because of the predominance of bedded clays, a K_v of 0.01 ft/d was initially assumed. Zone 2 represents the area of transition in the principal aquifer from thick sequences of interbedded clay, silt, and fine-grained sand to coarser-grained material. A K_v of 0.1 ft/d was used as an initial estimate in zone 2. Zone 3 represents the remainder of the principal aquifer overlain by the shallow unconfined aquifer. Observations at well sites indicate that sediments in this area typically consist of 25- to more than 50-percent gravel-bearing sediments (Marine and Price, 1964, fig. 12). A K_v of 5 ft/d was initially used in this zone. A K_v of 10 ft/d was initially assumed in zone 4, which represents the unconfined area of the principal aquifer near the margins of the valley. The shallow confining layer is absent in this area, and coarse-grained sediments generally predominate. During calibration, it was assumed that K_v values used to calculate vertical leakance between model layers of the principal aquifer for zones 1 and 2 could range from 1.0×10^{-5} ft/d to 1 ft/d. For zones 3 and 4, it was assumed that K_v could range from 1 ft/d to 30 ft/d.

Storage Coefficient and Specific Yield

Data evaluated by Hely and others (1971, fig. 60) including specific-capacity values and the results of aquifer tests indicate a range of storage-coefficient values in confined zones of the principal aquifer of 1×10^{-3} to less than 1×10^{-4}. The results of three multiple-well aquifer tests done during this study (Thiros, 1995, p. 33-38) indicated a storage-coefficient value of about 1×10^{-4} for the principal aquifer. Initial estimates of stor-

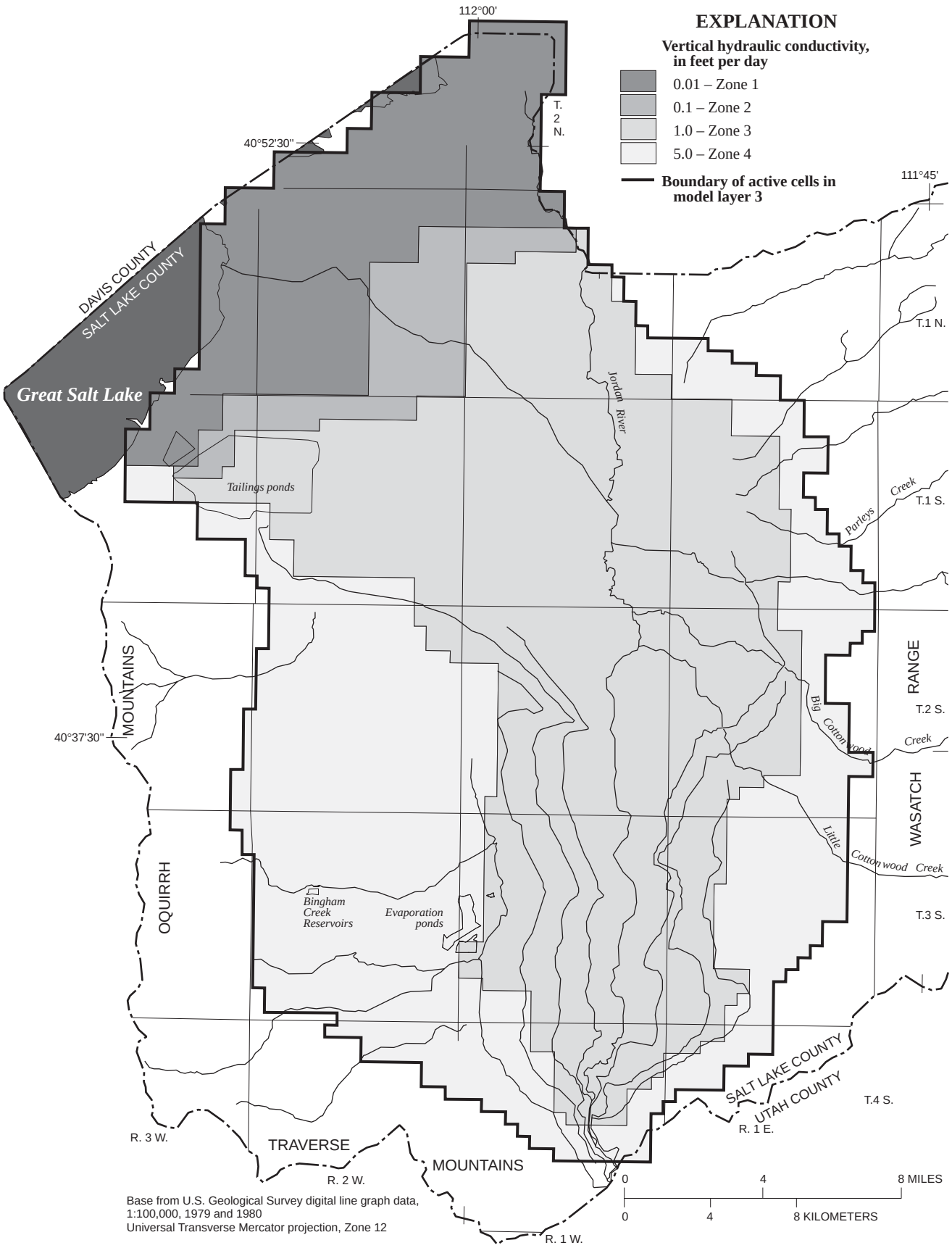

Figure 8. Zones and final values of vertical hydraulic conductivity of the principal aquifer incorporated in the groundwater flow model of Salt Lake Valley, Utah.

age-coefficient values for vertical columns ($S_{i,j}$) were based on data presented by Hely and others (1971, fig. 60). Initial estimates of storage coefficient for individual model cells ($S_{i,j,k}$) were calculated to represent a percentage of $S_{i,j}$ on the basis of the ratio of cell thickness to total thickness of the principal aquifer using the equation

$$S_{i,j,k} = S_{i,j} d_{i,j,k} / d_{i,j}, \quad (7)$$

where

$d_{i,j,k}$ = thickness of the cell i,j,k (L), and

$d_{i,j}$ = thickness of the principal aquifer at the vertical column (i,j) containing the cell (i,j,k) (L).

The range of probable values of storage coefficient for confined zones of the principal aquifer ($1x10^{-3}$ to $1x10^{-4}$) was assumed also to apply to the storage-coefficient value of the shallow confining layer represented by model layer 2; an initial estimate of $5x10^{-4}$ was used in model layer 2.

On the basis of lithologic characteristics of the sediments, Hely and others (1971, p. 116) estimated specific yield of the shallow unconfined aquifer to range from 0.10 to 0.20. Specific yield of the shallow unconfined aquifer was estimated to be 0.15 during calibration of the Waddell and others (1987) model; thus, an initial estimate for specific yield of 0.15 was used in model layer 1. An initial estimate of 0.15 also was used for the specific yield of the unconfined zones of the principal aquifer represented in model layer 3. Hely and others (1971, p. 112) reported the upper limit of the range of specific yield for unconfined zones of the principal aquifer to be 0.3. This value was assumed to be the maximum possible value that could be used in the model during calibration.

Recharge Simulated at Specified-Flux Boundaries

In the following subsections, estimates of recharge simulated in the model at specified-flux boundaries are discussed. In the transient-state simulation, specified recharge simulating inflow from consolidated rock, infiltration of unconsumed irrigation water from fields, lawns, and gardens, infiltration of precipitation on the valley floor, and seepage from streams was varied with time using the results of the steady-state calibration as an initial condition. The methods used to estimate specified recharge rates for yearly stress periods of the transient-state simulation are presented.

Inflow from Consolidated Rock

Inflow from consolidated rock has been estimated to be the largest component of recharge to the ground-water flow system (Hely and others, 1971, table 21; and Waddell and others, 1987, table 1). Recharge to the basin-fill ground-water flow system from consolidated rock was estimated by Hely and others (1971, p. 119) to be 135,000 acre-ft/yr for 1964-68. The estimate was developed on the basis of an evaluation of the disposal of mountain precipitation and on an evaluation of the hydraulic gradient near the mountain front. Waddell and others (1987, table 1) estimated steady-state recharge from consolidated rock to be 154,000 acre-ft/yr on the basis of results of calibration of their flow model.

Recharge from consolidated rock in areas other than the northern end of the Oquirrh Mountains was simulated by placing specified-flux cells in model layers 3 and 4 along the mountain front inside the no-flow boundary (fig. 9). Recharge from consolidated rock at the northern end of the Oquirrh Mountains was simulated using a head-dependent boundary and is discussed in the subsequent "Head-dependent and constant-head boundaries" section of this report. The distribution of specified-flux cells used to simulate recharge from consolidated rock and the initial recharge rates at those cells were based on the results of the calibration of the Waddell and others (1987) model, with total simulated recharge at specified-flux cells initially equaling 118,000 acre-ft/yr in the steady-state simulation. Steady-state recharge from consolidated rock at the northern end of the Oquirrh Mountains was estimated to be 36,000 acre-ft/yr in the Waddell and others (1987) model.

Hely and others (1971, p. 10, pl. 1) evaluated the rock types of the mountains bounding the valley and grouped them into hydrologic units on the basis of their inferred relative ability to transmit water in the subsurface. They defined consolidated rock along the east side of the valley near Mill Creek as having the highest relative permeability. Consolidated rock on the east side of the valley south of Mill Creek and at the south end of the valley in the Traverse Mountains was reported to have the lowest relative permeability. During steady-state calibration, the relative permeability of the consolidated rock was considered when adjusting the distribution of recharge from initial estimates.

Specified recharge from consolidated rock was varied with time in the transient-state simulation on the basis of the assumption that annual recharge from con-

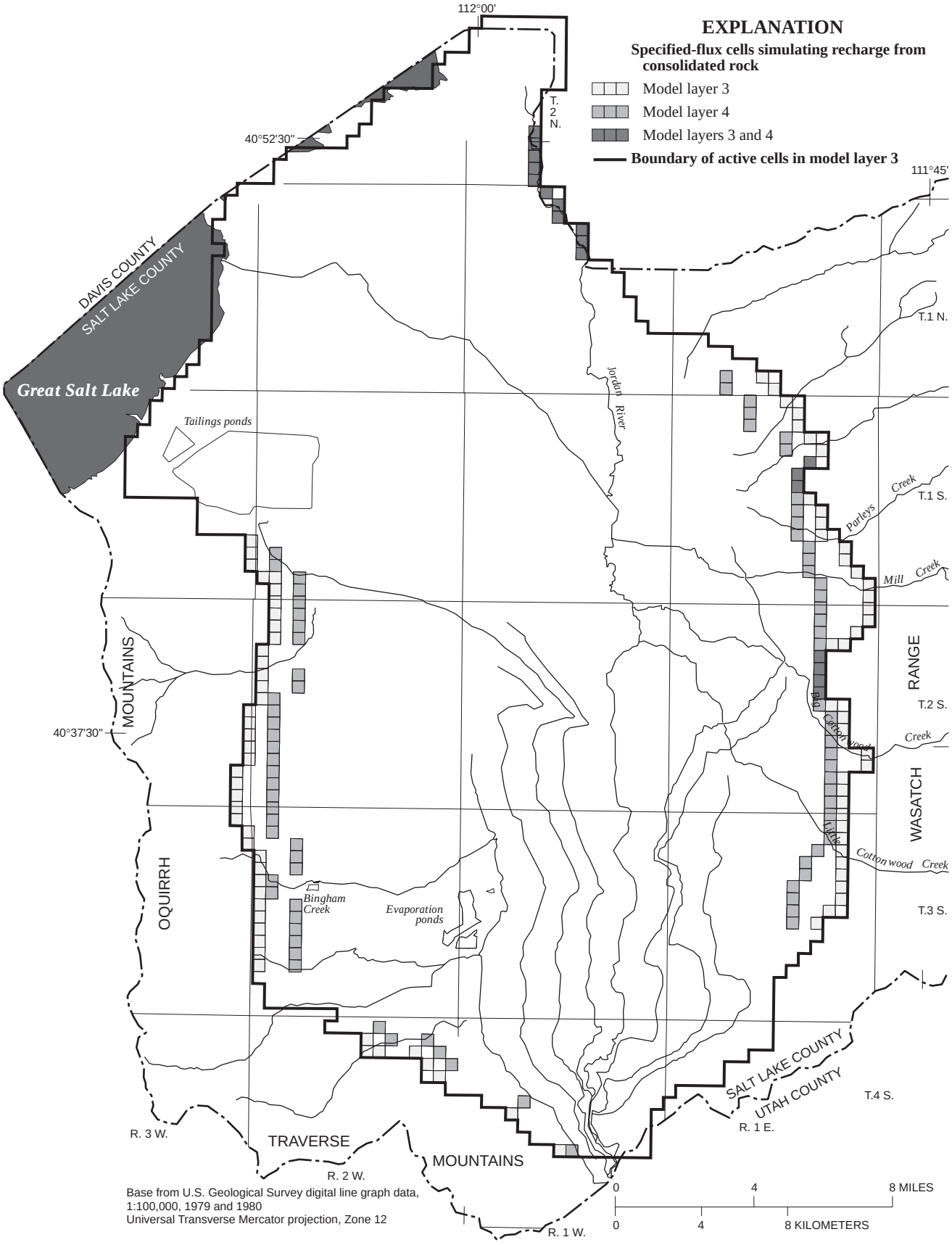

Figure 9. Location of specified-flux cells used to simulate recharge from consolidated rock in the ground-water flow model of Salt Lake Valley, Utah.

solidated rock at the mountain front varies with changes in annual precipitation in the surrounding mountains. Estimates of recharge from consolidated rock for yearly stress periods in the transient-state simulation ($QCON_{yr}$) were made by assuming that the recharge determined during steady-state calibration ($QCON_{ss}$) varied as a function of the ratio of annual precipitation at Silver Lake at Brighton ($MPRE_{yr}$) (fig. 10) to average annual precipitation at Silver Lake at Brighton ($MPRE_{ave}$) (fig. 10):

$$QCON_{yr} = QCON_{ss}[(((MPRE_{yr}/MPRE_{ave}) - 1) \times C) + 1] \qquad (8)$$

The coefficient C in this equation was used during transient-state calibration as a variable to adjust the simulated effect of fluctuations in the amount of precipitation in the mountains on recharge from consolidated rock. For example, if C is set equal to zero, then $QCON_{yr}$ is equal to $QCON_{ss}$ for all stress periods simulating no effect from annual fluctuation in precipitation; if C is set equal to 1, then recharge as inflow from consolidated rock is simulated as varying proportionately with $MPRE_{yr}/MPRE_{ave}$; if C is set equal to 2, then the magnitude of the simulated effect of deviations from the average amount of precipitation in the mountains on recharge from consolidated rock is magnified relative to a proportional relation.

Infiltration of Unconsumed Irrigation Water from Fields, Lawns, and Gardens

Hely and others (1971, p. 126) estimated recharge to the ground-water flow system by infiltration of unconsumed irrigation water from fields to be about 30 percent of the water applied to those fields, or about 81,000 acre-ft/yr for 1964-68. Waddell and others (1987) noted that the simulation of the recharge rate estimated by Hely and others (1971) resulted in water levels computed by their model that were much higher than observed water levels. The rate of seepage from irrigated fields used in the Waddell and others (1987) model was 48,000 acre-ft/yr.

Hely and others (1971, p. 126) estimated deliveries to lawns and gardens to be substantially less than those to fields with commercial crops. On the basis of an estimate that deep infiltration from lawns and gardens is about 30 percent of the water applied, Hely and others (1971) estimated recharge as infiltration of unconsumed irrigation water from lawns and gardens to be 17,000 acre-ft/yr for 1964-68. Waddell and others (1987, table 1) estimated average recharge from lawns and gardens for 1969-82 in their model to be 28,000 acre-ft/yr.

Land-use data presented by Hely and others (1971, fig. 79) were used to identify irrigated areas and to assign specified-flux cells to simulate recharge from irrigated fields, or from lawns and gardens (fig. 11). Recharge was simulated at the upper most active cells of vertical columns in these defined areas. Initially, a total recharge of 48,000 acre-ft/yr was simulated for recharge from irrigated fields and 28,000 acre-ft/yr was simulated for recharge from lawns and gardens. Recharge was distributed to all cells indicated in figure 11 on the basis of the percentage of cell area that represented irrigated fields or the percentage that represented residential or commercial land.

Decrease in recharge from irrigated fields throughout time as a result of urbanization of agricultural land was represented in the transient-state simulation. Changes in irrigated acreage were evaluated using land-use data for 1964-68 presented by Hely and others (1971, fig. 79) and land-use data for 1988-91 from the Utah Department of Natural Resources, Division of Water Resources (written commun., 1993). The evaluation indicates a decrease in irrigated commercial crops of about 40,000 acres from 1968 to 1988. Most of this acreage has been converted for use as residential or commercial land. At model cells where irrigated lands have been urbanized (fig. 11), simulated recharge for yearly stress periods was estimated by assuming a linear decrease for 1968-88 from the calibrated steady-state recharge rate per unit area for irrigated fields to the calibrated steady-state recharge rate per unit area for lawns and gardens. In some areas of the valley, land classified as undeveloped or as dry farms during 1968 has since been converted to residential or commercial land. At model cells in these areas (fig. 11), estimated recharge for yearly time steps was derived assuming a linear increase for 1969-88 from a steady-state initial condition of no simulated recharge, to the recharge rate per unit area estimated in the steady-state simulation for lawns and gardens. Specified recharge from irrigated fields, lawns, and gardens was held constant for stress periods representing 1988-91.

Infiltration of Precipitation on the Valley Floor

Hely and others (1971, table 21) estimated recharge from infiltration of precipitation on the valley floor to be 60,000 acre-ft/yr for 1964-68. The estimate was derived by calculating the difference between precipitation available for evapotranspiration and ground-

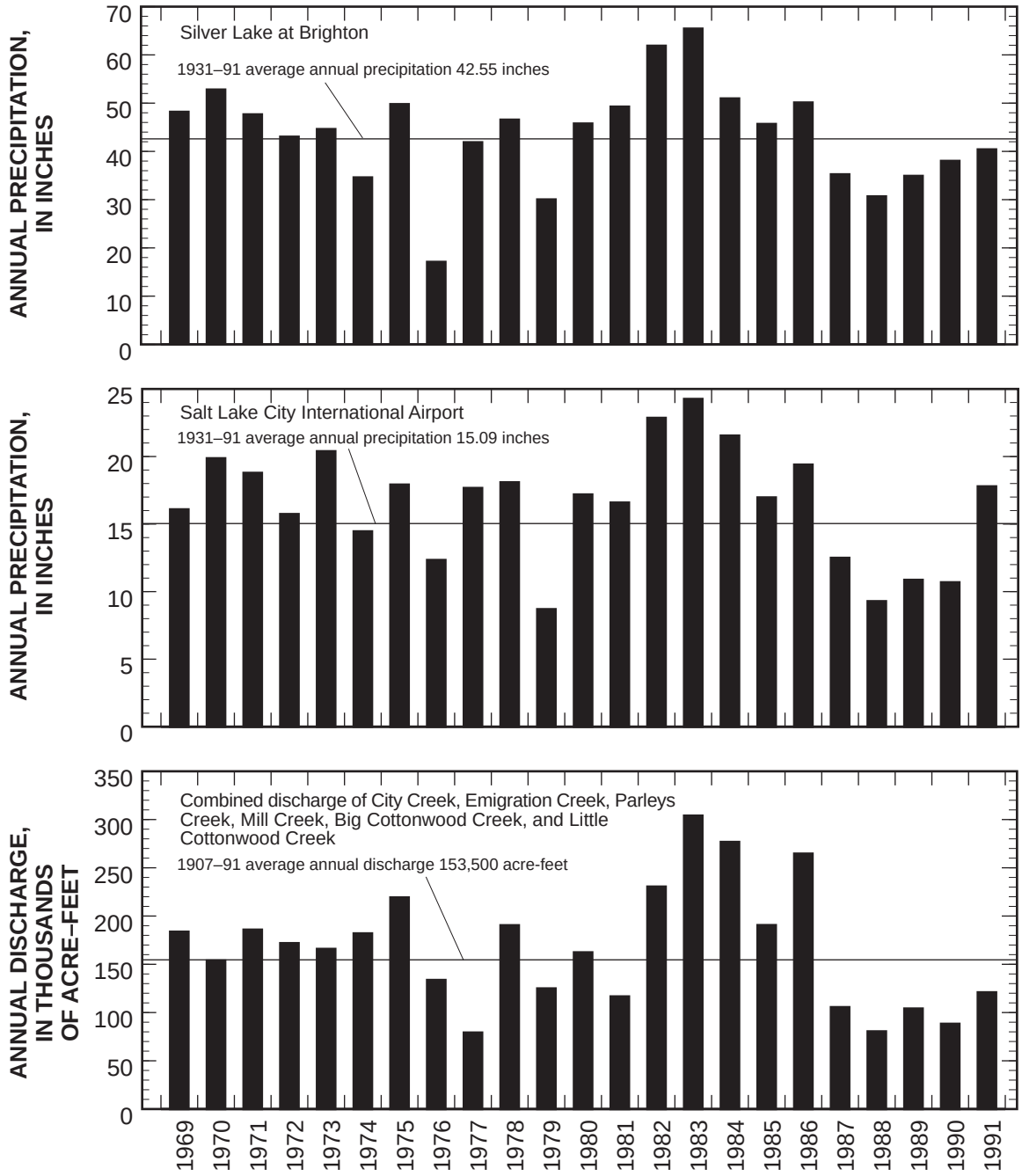

Figure 10. Annual precipitation at Silver Lake at Brighton, annual precipitation at Salt Lake City International Airport, and combined annual discharge from the mouths of six streams along the Wasatch Front, Salt Lake Valley, Utah.

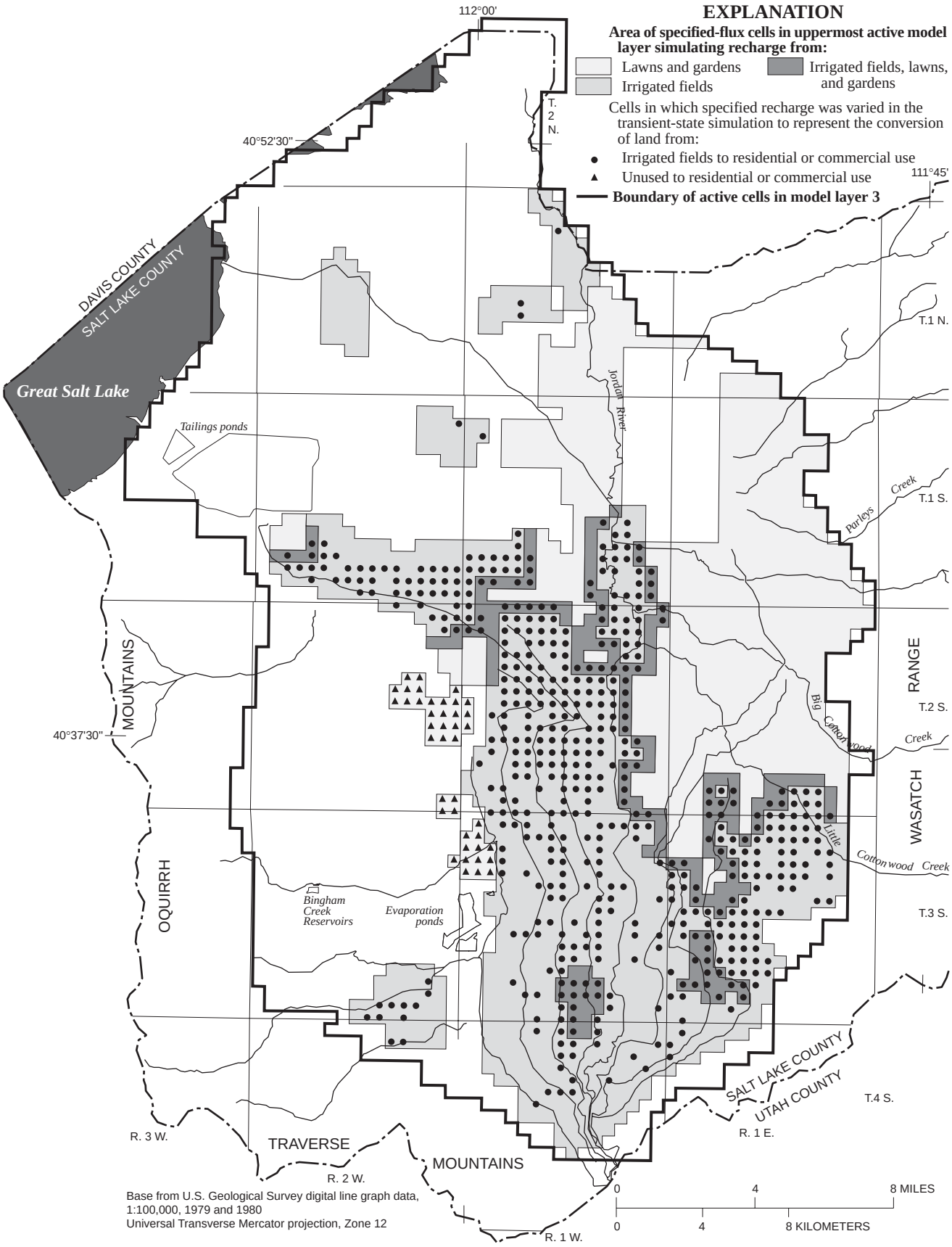

Figure 11. Location of specified-flux cells used to simulate recharge from irrigated fields, lawns, and gardens in the groundwater flow model of Salt Lake Valley, Utah.

water recharge and the evapotranspiration of precipitation in the valley. Waddell and others (1987, table 1) estimated recharge from precipitation on the valley floor to be 70,000 acre-ft/yr during calibration of their ground-water flow model.

Recharge from precipitation on the valley floor was simulated at the uppermost active cells of vertical columns, except in commercial and dense residential areas in Salt Lake City, where precipitation was assumed to be collected as runoff in drain systems. Recharge was distributed areally on the basis of the distribution of annual average precipitation in the valley as defined by Hely and others (1971, fig. 5). Estimates of recharge from precipitation on the valley floor for yearly stress periods in the transient-state simulation ($QPRE_{yr}$) were made by assuming that the recharge determined during steady-state calibration ($QPRE_{ss}$) varied as a function of the ratio of annual precipitation at the Salt Lake City International Airport (PRE_{yr}) (fig. 10) to average annual precipitation at the Salt Lake City International Airport (PRE_{ave}) (fig. 10):

$$QPRE_{yr} = QPRE_{SS}[(((PRE_{yr}/PRE_{ave}) - 1) \times C) + 1] \qquad (9)$$

The coefficient C in equation 9 was varied during transient-state calibration to adjust the simulated effect of fluctuations in precipitation on the valley floor on recharge from precipitation to the basin-fill ground-water flow system.

Seepage from Major Canals

Hely and others (1971, table 21) estimated seepage losses from major canals in the valley to be about 48,000 acre-ft/yr. Their estimate was based on measured losses from one canal, and losses were extrapolated to other major canals. During 1982-83, Herbert and others (1985) estimated seepage from major canals to be about 28,000 acre-ft/yr on the basis of measurements from selected reaches of six major canals in the valley.

Initial distribution of recharge at specified-flux cells that simulate seepage from canals (fig. 12) was determined on the basis of the results of calibration of the Waddell and others (1987) model. Recharge was simulated at the uppermost active cells of vertical columns as indicated in figure 12. Total simulated recharge from canals initially equaled 24,000 acre-ft/yr. Estimates of seepage at individual reaches of canals presented by Herbert and others (1985) were used for comparison during model calibration.

Seepage from Streams and Underflow in Channel Fill

Stream channels in the valley lose water mainly as mountain streamflow leaves the canyons and crosses coarse-grained basin-fill material where the ground-water level is below the streambed. Hely and others (1971, p. 123 and table 5) estimated annual channel water losses from six Wasatch streams for 1964-68 to be 14,730 acre-ft/yr and losses from smaller ungaged streams to be about 3,000 acre-ft/yr. Recharge from underflow in channel fill where the streamflow leaves the canyons and at Jordan Narrows was estimated by Hely and others (1971, p. 121-122) to be about 3,500 acre-ft/yr. Total recharge from seepage from streams and underflow in channel fill, including underflow at Jordan Narrows, was estimated in the Waddell and others (1987) model to be about 20,000 acre-ft/yr.

Specified-flux cells were located along six Wasatch streams near canyon mouths to simulate recharge from streams and from underflow in channel fill, including underflow at Jordan Narrows (fig. 12). Recharge from these sources is simulated at the uppermost active cells of vertical columns. Initial recharge rates at individual cells were determined on the basis of estimates made during the calibration of the Waddell and others (1987) model. Estimates made by Hely and others (1971, table 5) for individual streams were used for comparison during model calibration. Seepage from smaller ungaged streams and underflow at the mouths of small canyons was assumed to be accounted for by specified-flux boundaries at the mountain front that simulate recharge from consolidated rock.

Simulated recharge from streams and underflow in channel fill was varied as a function of time in the transient-state simulation on the basis of the assumption that annual recharge from these sources varies with changes in annual flow in streams at canyon mouths. Hely and others (1971, p. 56) evaluated the relation of channel loss in Wasatch streams to runoff at canyon mouths. They noted that the magnitude of losses changed with fluctuations in runoff and generally ranged from 8 to 16 percent of runoff and averaged about 15 percent for periods of low or moderate runoff. Estimates of recharge from streams and underflow in channel fill for yearly stress periods in the transient-state simulation ($QSTRM_{yr}$) were made by assuming that the recharge determined during steady-state calibration ($STRM_{ss}$) varies as a function of the ratio of total annual runoff at the six Wasatch streams at canyon mouths ($STFL_{yr}$) (fig. 10) to average annual runoff

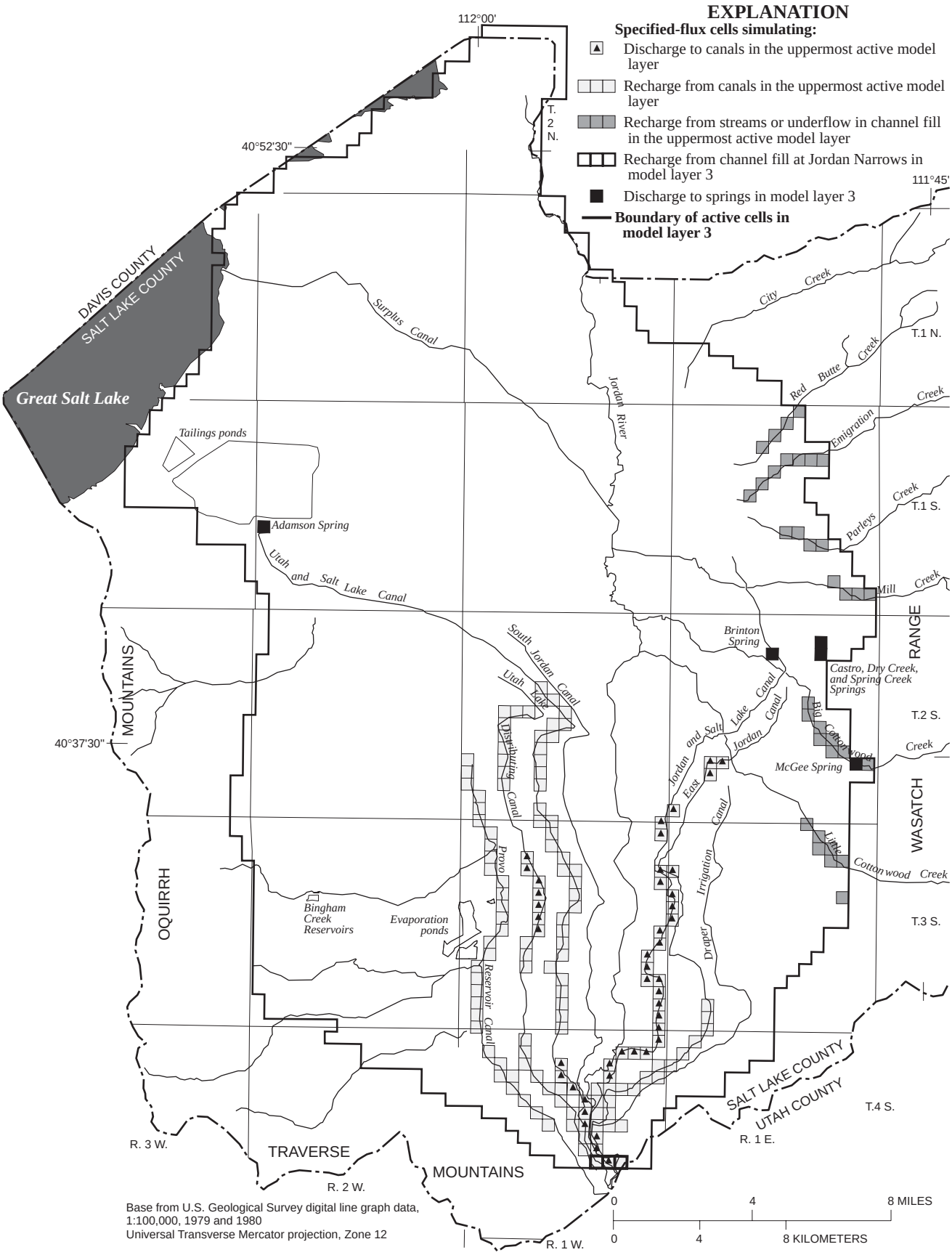

Figure 12. Location of specified-flux cells used to simulate discharge to or recharge from canals, recharge from streams or underflow in channel fill, and discharge to springs, in the ground-water flow model of Salt Lake Valley, Utah.

at the six Wasatch streams at canyon mouths ($STFL_{ave}$) (fig. 10):

$$QSTRM_{yr} = QSTRM_{ss}[(((STFL_{yr}/STFL_{ave})\text{-}1)\ x\ C)+1] \quad (10)$$

The coefficient *C* in equation 10 was varied during transient-state calibration to adjust the simulated effect of fluctuations in runoff in streams on recharge from streams to the basin-fill ground-water flow system.

Seepage from Reservoirs and Evaporation Ponds

Two reservoirs near the mouth of Bingham Canyon (the large Bingham Creek Reservoir and the small Bingham Creek Reservoir) (fig. 1) were constructed in the early- to mid-1960s to contain mine drainage and wastewater from ore-leaching facilities. A smaller pond (the cemetery pond) was built near the reservoirs in 1984 to lime-treat water associated with mining operations (Dames and Moore, 1988, p. 4). Seepage losses from the large Bingham Creek Reservoir have been estimated to be in the range of 1 to 7 million gal/d (about 1,000 to 8,000 acre-ft/yr) (Dames and Moore, 1988, p. 60). Recharge rates assigned to specified-flux cells that simulate seepage from these reservoirs in the steady-state and transient-state simulations (fig. 13) were estimated on the basis of seepage estimates reported by Dames and Moore (1989, table 4). Recharge was simulated at the uppermost active cells of vertical columns containing the reservoirs. The Dames and Moore (1989) estimates were determined mainly from water-balance evaluations, calculations of underflow beneath the ponds, and theoretical calculations of vertical seepage using estimates of hydrologic properties of pond bottoms and underlying sediments (Dames and Moore, 1988, p. 5). In 1990 and 1991, the small Bingham Creek Reservoir was reconstructed with liners and leak-detection systems to improve water management and to eliminate seepage of water from the reservoir to the principal aquifer (Kennecott Utah Copper, 1992a, p. 48 and 51, and David Cline, oral commun., 1994). Similar work was begun on large Bingham Creek Reservoir in 1992 (David Cline, oral commun., 1994). As of 1992, the cemetery pond was no longer in use (Kennecott Utah Copper, 1992a, p. 36).

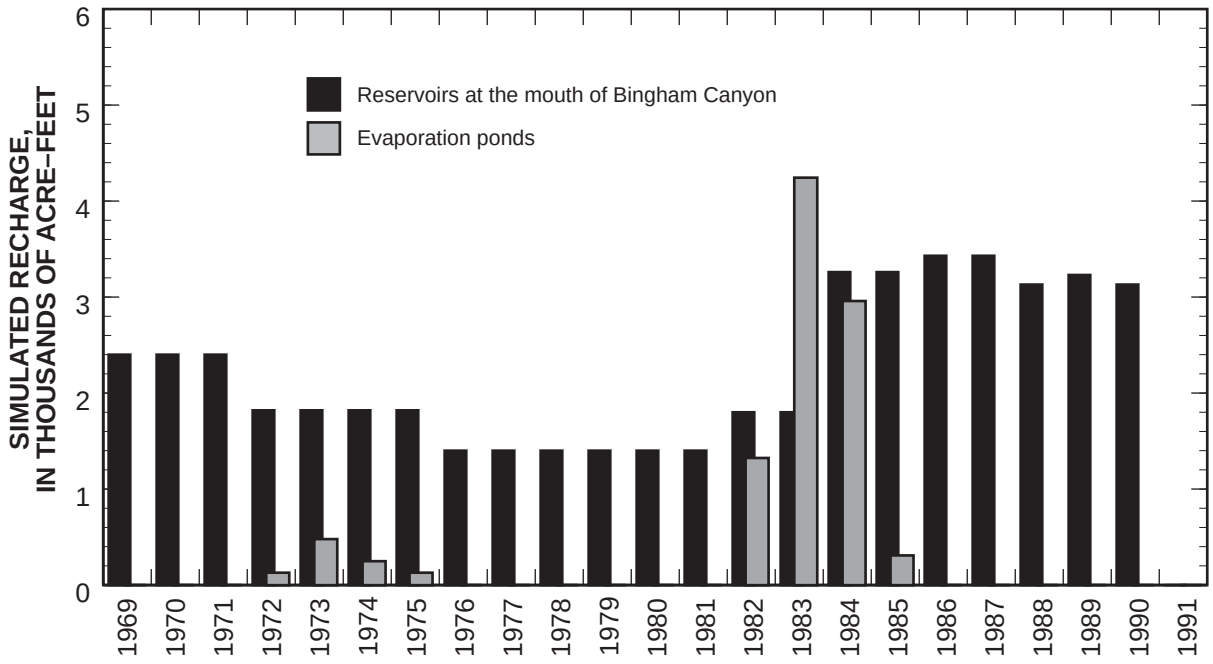

Figure 13. Simulated recharge at specified-flux cells that represents seepage from reservoirs at the mouth of Bingham Canyon and from evaporation ponds in the southwestern part of Salt Lake Valley, Utah, 1969–91.

Several evaporation ponds about 5 mi east of the Bingham Creek Reservoirs (fig. 1) were used to store and evaporate Bingham Canyon watershed waters, waste-rock leach-process waters, and sediment from storm runoff in Bingham Canyon (Dames and Moore, 1988, p. 4). The ponds were used continuously from 1936 until 1965 and periodically from 1972 to 1985. No surface water has been diverted to the ponds since 1986 (Kennecott Utah Copper, 1992a, table 1). Estimates of surface-water flow to these ponds reported by Kennecott Utah Copper (1992a, table 1) and estimates of seepage from the ponds reported by Dames and Moore (1989, table 4) were used to assign recharge rates to specified-flux cells that represent the evaporation ponds in the steady-state and transient-state simulations (fig. 12). Recharge was simulated at the uppermost active cells in vertical columns containing the ponds.

Discharge Simulated at Specified-Flux Boundaries

Withdrawal from Wells

Specified-flux cells were placed in model layers 3 to 7 to simulate withdrawal from wells in the principal aquifer. Specified discharge at cells that simulate ground-water withdrawal from public-supply, irrigation, and industrial wells (fig. 14) was based on annual-withdrawal data reported by water users and on unpublished records of the U.S. Geological Survey (unpub. data, 1964-91). Discharge from these wells was distributed vertically on the basis of available well-construction data, including depth of the well and the depths of well-casing perforations. If no construction data were available for a well, discharge was assumed to occur at all active cells of model layers 3 to 7 in the vertical column containing that well.

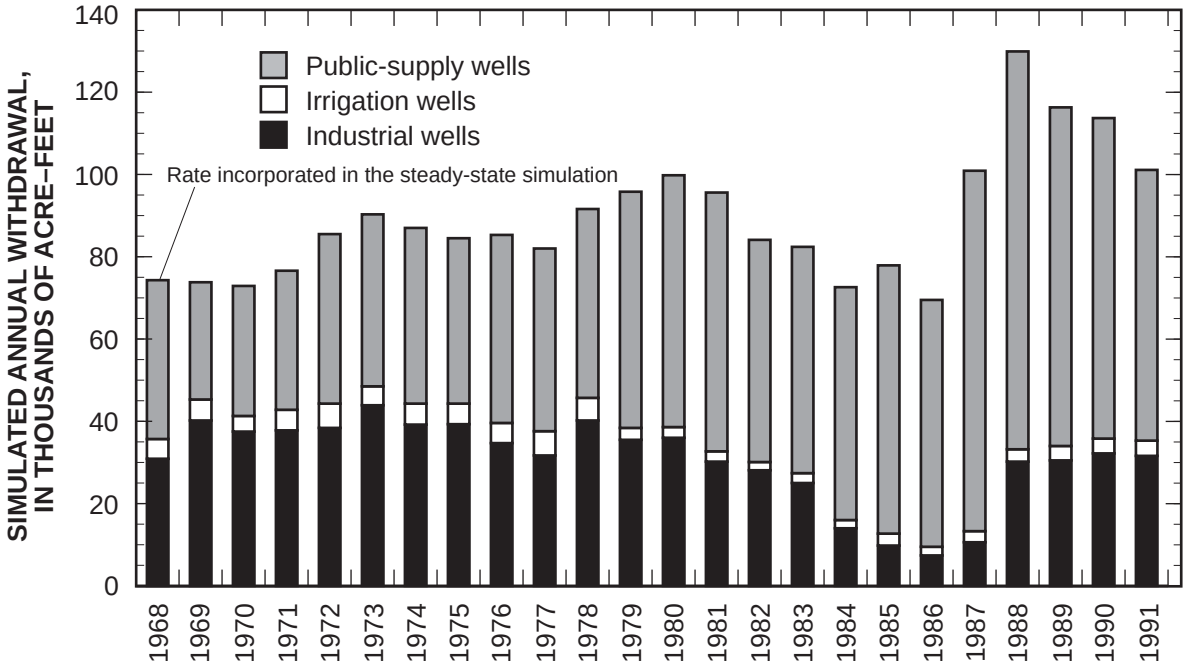

Figure 14. Annual withdrawal of ground water by public-supply, irrigation, and industrial wells simulated in the ground-water flow model of Salt Lake Valley, Utah, 1968–91.

Discharge from wells classified as stock or domestic wells also was simulated by the model. Hely and others (1971, p. 140) estimated annual withdrawal from stock and domestic wells to be about 30,000 acre-ft for 1964-68. Waddell and others (1987, p. 22) estimated a decrease in withdrawal from domestic and stock wells during 1969-82 of less than 10 percent. No new measurements or estimates of discharge from stock and domestic wells were made during this study; therefore, a rate of 30,000 acre-ft/yr was incorporated in the model and was not adjusted during calibration. Areal distribution of discharge from stock and domestic wells was determined on the basis of locations recorded by the Utah Department of Natural Resources, Division of Water Rights (written commun., 1992). Discharge from stock and domestic wells was simulated in model layer 3. Information on the classification and depth of wells reported by Waddell and others (1987, table 4) indicates that about 70 percent of wells constructed before 1982 are less than 300 ft deep, a range that generally corresponds to the simulated depth of model layer 3. A specified recharge rate at a given model cell in layer 3 was determined as a function of the ratio of the number of stock and domestic wells in the cell to the total number of existing stock and domestic wells.

Seepage to Major Canals and Discharge to Springs

Waddell and others (1987, p. 27) estimated seepage gains in major canals for 1983 to be about 13,000 acre-ft on the basis of measurements by Herbert and others (1985). Waddell and others (1987, p. 27) assumed that the 1983 estimate represented greater-than-average discharge to canals because 1983 was a wet year and because during calibration of their model, average recharge was evaluated and estimated to be about 10,000 acre-ft/yr. Discharge rates were assigned in the model to specified-flux cells that simulate ground-water seepage to Utah Lake Distributing Canal, Utah and Salt Lake Canal, East Jordan Canal, and Jordan and Salt Lake City Canals (fig. 12) on the basis of the results of calibration of the Waddell and others (1987, table 3) model and initially totaled 10,000 acre-ft/yr. Discharge to these canals is simulated from the uppermost active cells in vertical columns as indicated in figure 12. Estimates of seepage at individual gaining reaches of these canals made by Herbert and others (1985) were used for comparison during model calibration.

Discharge to springs from basin-fill material was estimated by Hely and others (1971, p. 135-136) to be about 19,000 acre-ft/yr for 1964-68. No new data were collected during this study, and no adjustment from this estimate was made during model calibration. Discharge to springs is simulated from model layer 3. Discharge from thermal springs in the valley is not assumed to originate in the basin-fill aquifer system (Taylor and Leggette, 1949, p. 35) and was not incorporated in the model.

Head-Dependent and Constant-Head Boundaries

Incorporation of a head-dependent river boundary in model layer 1 to simulate seepage to or from the Jordan River and the lower reaches of its principal tributaries (fig. 15) requires specification of the water level in the river, river-bed altitude, and river-bed conductance (equations 1a and 1b). River-bed altitudes were estimated using topographic maps of the valley. Stage of the river was specified at river cells on the basis of estimates made during the calibration of the Waddell and others (1987) model. Neither of these values was adjusted during model calibration. River-bed conductance (*CRIV*) was derived using the following equation:

$$CRIV = (K_{riv}L_{riv})\left(\frac{W}{M}\right) \qquad (11)$$

where

K_{riv} = hydraulic conductivity of the river bed (L/t),

L_{riv} = length of the river reach in the model cell (L), and

W/M = ratio of the width of the river bed to the thickness of the river bed (L/L).

The length of river reaches in model cells containing river boundaries (L_{riv}) was determined using geographic information from 1:24,000-scale topographic maps. River-bed width and thickness were not measured in the field. The ratio of the width of the stream to the river-bed thickness (*W/M*) was assumed to be 10 in all river cells. During model calibration, *CRIV* specified in the model was adjusted by varying estimates of K_{riv}. A probable range of K_{riv} values for use during model calibration was assumed to be defined by the range of measured or estimated values of vertical hydraulic conductivity (K_v) for basin-fill material, 5.1×10^{-5} ft/d to 30 ft/d, discussed previously in this report. Initial *CRIV* conductance values used in the model were computed using a K_{riv} value of 1 ft/d.

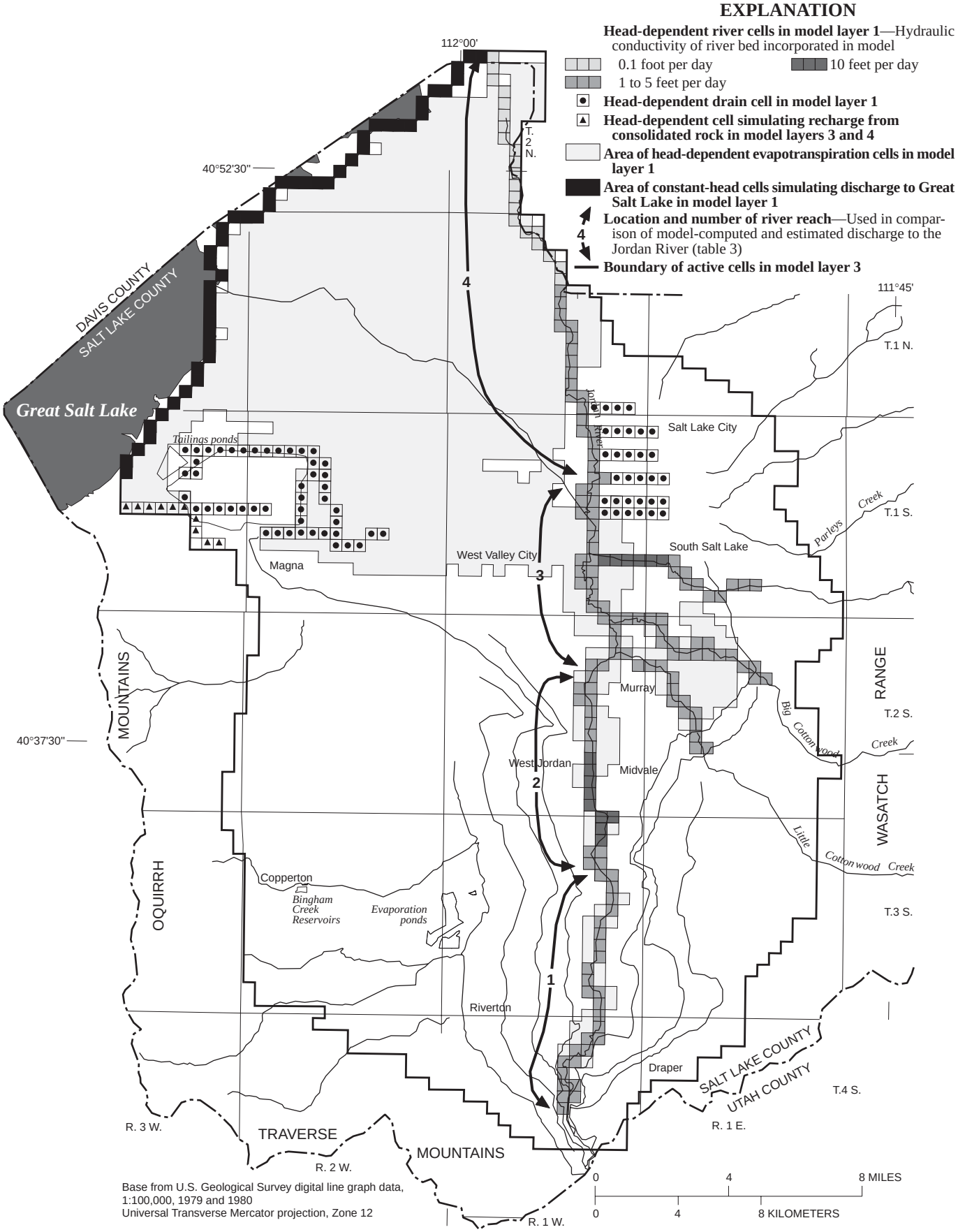

Figure 15. Location of head-dependent river cells, and hydraulic conductivity of river bed; and location of head-dependent drain cells, head-dependent cells that simulate recharge from consolidated rock, head-dependent evapotranspiration cells, and constant-head cells that simulate discharge to Great Salt Lake; in the ground-water flow model of Salt Lake Valley, Utah.

Head-dependent drain cells were located in model layer 1 (fig. 15) to simulate ground-water discharge from the shallow unconfined aquifer to surface drains north of Magna and to buried storm drains in Salt Lake City. Discharge to drains north of Magna was estimated by Hely and others (1971, p. 136) to be about 5,000 acre-ft/yr. Discharge of shallow ground water to buried drains in the Salt Lake City area has not been measured. A steady base flow, however, has been observed by the employees of the Salt Lake City Department of Public Utilities (Charles H. Call, Jr., oral commun., 1992) and is assumed by them to be seepage from shallow ground water. Drain altitudes were specified to be 10 ft less than land-surface altitude. Drain conductance was not measured, and initial values used in the model were arbitrarily selected.

Assignment of evapotranspiration cells in model layer 1 (fig. 15) was based on the delineation of areas of ground-water discharge by evapotranspiration for 1968 made by Hely and others (1971, pl. 5). Hely and others (1971) divided the entire area of evapotranspiration of ground water into five major land categories: bare ground, cultivated land, urbanized land, waterfowl-management land, and areas of phreatophytes. The phreatophyte area was further subdivided by plant group (Hely and others, 1971, pl. 5). Initial maximum evapotranspiration rates for non-phreatophyte areas used in the model (table 1) were based on estimates made by Hely and others (1971, p. 179-187). Initial estimates of maximum rates of consumptive use or evapotranspiration for plants types (table 1) were made using a formula derived by Blaney and Criddle (1962) for consumptive use during an entire growing season:

$$U = kF$$

where

U = consumptive use or evapotranspiration, in inches,
k = consumptive-use coefficient, and
F = consumptive-use factor.

The consumptive-use factor (F) is a function of temperature and percentage of daylight hours. Criddle and others (1962, p. 11) determined F for the Salt Lake City International Airport to be 39.22. Consumptive-use coefficients (k) for water-table depths of less than 12 in. were obtained from evaluations of k for phreatophytes by Rantz (1968) and by the U.S. Department of Agriculture (1969, figs. 6a and 6b). The extinction depth at which evapotranspiration is assumed to be zero was set at 15 ft. The extinction-depth value was selected on the basis of information on the depth of ground water in areas of phreatophytes presented by Robinson (1958) and summarized by Hely and others (1971, p. 182). The information indicated that ground-water levels in areas of phreatophytes that are common in Salt Lake Valley generally do not exceed 15 ft below land surface.

Maximum evapotranspiration rates listed in table 1 were determined assuming 100-percent foliage density. Although 100-percent foliage density does not occur in much of the evapotranspiration area, initial incorporation of these values in the model allowed for the simulation of relative differences in evapotranspiration rates between land-use categories and plant types. During calibration, the evapotranspiration rates were decreased uniformly from initial values shown in table 1.

Head-dependent flux cells were located in the model at the northern end of the Oquirrh Mountains (fig. 15) to simulate recharge from consolidated rock. In this area, the Oquirrh Mountains are extensively fractured, and these fractures are hydrologically interconnected and allow ground water to move from the consolidated-rock aquifer into the basin-fill aquifer (Kennecott Utah Copper, 1992b, p. 2). The altitude of the potentiometric surface in the consolidated-rock aquifer has been measured at about 4,250 ft in an area west of Magna (Engineering Technologies Associates, Inc., 1992, p. VII-7). Discharge from springs near the contact between consolidated rock and the basin-fill material keeps the potentiometric surface of the consolidated-rock aquifer at a near-constant level near the

Table 1. Maximum evapotranspiration rate for five major land-use categories in Salt Lake Valley, Utah, used during development and calibration of the ground-water flow model

Land-use category	Maximum evaporation rate (feet per year)
Bare ground	0.76
Cultivated	.38
Urbanized	.38
Waterfowl management	.76
Phreatophytes	
Greasewood	2.66
Picklewood	2.47
Saltgrass	2.28
Saltcedar	5.88

springs (Kennecott Utah Copper, 1992b, p. 42). Specified heads in these cells were set at 4,250 ft. The conductance of the boundary between the consolidated rock and the basin fill was not measured, and initial values used in the model were arbitrarily selected.

Constant-head cells are located in model layer 1 along the northwestern border of the modeled area, which represents the shore of Great Salt Lake (fig. 15). Specified water-level altitudes in these cells were set at 4,200 ft, the approximate average historic water level of Great Salt Lake (Arnow and Stephens, 1990, p. 1). The density of ground water and water in Great Salt Lake varies spatially in this area. The density of salt water in the southern end of Great Salt Lake, which may be up to 5 ft deep in the area of constant-head cells, is typically about 1.10 g/cm^3 for lake-level altitudes near 4,200 ft (ReMillard and others, 1993, p. 181 and ReMillard and others, 1994, p. 179). Less-saline ground water, of lower density, occurs beneath the edge of the lake and to the east of the lake. Density variations in a flow system may create pressure gradients within the system that are not indicated from measured water-level altitudes. Mechanisms used to normalize water-level measurements near the lake shore relative to a constant density, however, resulted in an adjustment of less than 1 ft in the lake altitude at the edge of the lake. Therefore, the average value of 4,200 ft was assumed to be a reasonable specified water-level altitude for constant-head cells located at the lake shore.

MODEL CALIBRATION

Model calibration incorporated steady-state and transient-state simulations. During the calibration process, model parameters defined as calibration variables were adjusted within probable ranges until a reasonable match between model-computed and measured water levels, and model-computed and estimated recharge and discharge, was achieved. One calibration variable, the transmissivity of the principal aquifer, was adjusted during calibration to both steady-state and transient-state conditions. Following adjustments to this parameter during transient-state calibration, the steady-state and transient-state simulations were rerun. Results of steady-state calibration presented in subsequent sections of this report reflect adjustments made during transient-state calibration.

Steady-State Calibration

Method

Three measures of the state of the ground-water flow system were used during calibration to steady-state conditions: (1) Measured water levels in the principal and shallow unconfined aquifer, (2) estimated discharge to the Jordan River and its tributaries, and (3) measured vertical hydraulic gradients between the principal aquifer and the shallow unconfined aquifer. A comparison of the simulated ground-water budget and the ground-water budget derived during previous studies also was used to help evaluate the fit of the model to measured conditions.

Water levels computed during steady-state simulations were compared with water levels measured primarily during February 1969 in 102 wells completed in the principal aquifer. In areas where water-level data were insufficient or were not available, 1968 data were used. Computed water levels for model layer 1 were compared with water levels measured in 112 wells completed in the shallow unconfined aquifer. Water-level data for the shallow unconfined aquifer are sparse previous to 1983, and most of the water-level measurements used for comparison during calibration were made from 1983 to 1991. For each individual model run, three statistics for differences between model-computed water levels and measured water levels (residuals) were calculated and analyzed to determine the accuracy of the simulation: (1) the mean of the residuals, which indicates the bias in the distribution of positive and negative values, (2) the standard error, which is the mean of the absolute values of residuals, and (3) the standard deviation of the residuals. Residuals at observation sites in the shallow unconfined aquifer and in the principal aquifer were evaluated separately. In addition, the match between model-computed and measured water levels was evaluated at individual observation sites. An observation site was considered to be calibrated if the model-computed water level in the cell containing the site was within a predetermined range of the measured water level. The criteria for the range was determined on the basis of the estimated accuracy of the water level and the observed horizontal hydraulic gradient across the model cell that contained the observation site; therefore, near the margins of the valley where the gradient is steep, the acceptable range was large, as much as 75 ft or greater. For most sites in the shallow unconfined aquifer where

the horizontal hydraulic gradient is much smaller, a limit of 15 ft was chosen.

Flow rates at cells that contain river boundaries computed during steady-state simulations were compared with estimates of ground-water discharge to the Jordan River for water years 1966-68 made by Hely and others (1971, table 11). Hely and others (1971, table 22) estimated average net gain from ground-water inflow to the Jordan River to be about 170,000 acre-ft/yr for 1964-68. The estimate includes some discharge of shallow ground water that reaches the river quickly after irrigation of fields (Hely and others, 1971, p. 82), possibly in shallow perched zones above the shallow unconfined aquifer. Hely and others (1971, table 11) estimated the stable part (unaffected by seasonal changes) of the estimated gain in the Jordan River for three subreaches from Jordan Narrows to 2100 South Street (fig. 1) to total about 147,000 acre-ft/yr. This estimate was made, in part, on the basis of measurements of river gains during winter months, which were assumed least likely to be affected by local runoff, evapotranspiration, or return flow. The model does not simulate rapid return flow to the river from runoff or from ground water discharging from shallow perched zones above the shallow unconfined aquifer; thus, the smaller quantity of 147,000 acre-ft/yr estimated as ground-water discharge to the river between Jordan Narrows and 2100 South Street was the value used for comparison during calibration. Estimates of seepage to the Jordan River for 1932 by Taylor and Leggette (1949, p. 42) and for 1966-68 by Hely and others (1971, p. 86-88) indicate no appreciable gain in flow downstream from 2100 South Street. Hely and others (1971, p. 88 and 136) note, however, that water-level data indicate a hydraulic gradient toward the river in the area, which indicates that some ground water might discharge to the river. Hely and others (1971, p. 88) suggest that the indication of no appreciable gain in the river could be, in part, the result of the balance between gains from ground water and the numerous small diversions from the river downstream from 2100 South Street. During model calibration, therefore, flow at river cells was simulated downstream 2100 South Street and river-bed conductance was adjusted to match water levels in the adjacent aquifer.

The accuracy with which the model reproduces measured vertical hydraulic gradients between the principal aquifer and the shallow unconfined aquifer was evaluated during calibration. Simulated vertical hydraulic gradients between the principal aquifer and the shallow unconfined aquifer were compared with gradients measured at 11 nested-well observation sites (fig. 6). During this study, water-level data were gathered at nested-well observation sites, which consist of a well used for monitoring the shallow unconfined aquifer and a well completed in the principal aquifer. At pre-existing sites, historic water-level data were used to calculate vertical hydraulic gradients. Vertical hydraulic gradients were calculated by dividing the measured difference in water levels in the two nested wells by the distance between the midpoint of the screened intervals of the wells. If more than one set of water-level measurements for the wells was available, an average gradient was computed. These values were compared with vertical hydraulic gradients simulated by the model. Simulated gradients at vertical columns containing nested-well observation sites were determined by dividing the difference in model-computed water levels between model layers at observation sites by the distance between the midpoints of the model layers. Few water-level data were available at nested-well observation sites previous to 1983, and most water-level measurements used to calculate vertical hydraulic gradients were made from 1983 to 1991.

Results of Calibration

Final statistics for sets of residuals (table 2) indicate that steady-state calibration resulted in a reasonable match between model-computed and measured

Table 2. Statistics of differences between model-computed and measured water levels in the steady-state simulation of the ground-water flow model of Salt Lake Valley, Utah

[Values calculated as model-computed minus measured water level; difference is in feet]

	Observation sites in the principal aquifer	Observation sites in the shallow unconfined aquifer
Number of comparisons	102	112
Mean	1.0	1.1
Standard error (mean of absolute values of differences)	9.5	6.4
Standard deviation	13.1	8.2
Maximum difference lower than measured	-36.5	-16.6
Maximum difference higher than measured	32.6	24.4

water levels. The model-computed potentiometric surface in model layer 3, which represents the upper zone of the principal aquifer, and residuals for observation wells in the principal aquifer are shown in figure 16. The model-computed water-table surface in model layer 1, which represents the shallow unconfined aquifer, and residuals at observation wells are shown in figure 17. The distribution of residuals for individual observation sites shown in figures 16 and 17 generally does not indicate a bias in the distribution of positive and negative values. All residuals for the principal aquifer met the criteria set for calibration. Residuals at four observation sites in the shallow unconfined aquifer (fig. 17) exceed their prescribed calibration criteria (15 ft). These sites, however, are in near proximity to other observation sites where the match between model-computed and measured water levels is satisfactory; therefore, the level of calibration in the region was assumed to be acceptable.

Model-computed ground-water discharge to the Jordan River is compared with estimated values in table 3. River reaches used in the comparison are shown in figure 15. Total model-computed net discharge to the Jordan River in the calibrated steady-state simulation was about 136,000 acre-ft/yr. Although the match between model-computed and estimated total net gain in the river is reasonably good, the comparison of model-computed and estimated gains in subreaches of the river indicate substantial differences. Efforts to improve the match between model-computed and estimated gains at subreaches of the river by altering the distribution of recharge from nearby sources or the hydrologic properties of the aquifer in the vicinity of the river resulted in an unsatisfactory match between model-computed and measured water levels. The possible inaccuracy in estimates of stream gain made by Hely and others (1971) at subreaches was not evaluated by them. The comparison with simulation results indicates that the model may be better able to simulate observed gains in the Jordan River for long reaches of the river than for short subreaches.

Vertical hydraulic gradients in the steady-state simulation between the principal aquifer and the shallow unconfined aquifer at nested-well observation sites (fig. 6) are compared with vertical hydraulic gradients calculated from measured water levels in table 4. A negative value indicates an upward vertical hydraulic gradient and upward ground-water flow from the principal aquifer through the shallow confining layer to the shallow unconfined aquifer. A positive value indicates the opposite, a downward vertical head gradient and downward ground-water flow through the shallow confining layer. A vertical hydraulic gradient of zero indicates no vertical component of flow. The model simulated, at all but one site, the observed direction of vertical gradient, and a satisfactory match to measured gradients was generally achieved.

Table 3. Model-computed steady-state flow rates at river cells and estimated average annual gains from ground water in the Jordan River, Utah, 1966-68 water years

Estimated gain from ground water: From Hely and others, 1971, table 11 and page 136.

River reach (see fig. 15)	Model-computed net gain, steady-state simulation (acre-feet per year)	Estimated gain from ground water (acre-feet per year)
1	49,900	27,000
2	30,600	64,000
3	40,700	56,000
4	14,700	1,000
Total (rounded)	136,000	148,000

The steady-state ground-water budget (table 5) matches reasonably well with independent estimates of budget components made by Hely and others for 1965-68 (1971, tables 21 and 22) and with estimates resulting from the calibration of a two-layer flow model by Waddell and others (1987, tables 1 and 3). Total flow into and out of the ground-water flow system computed in the steady-state simulation is about 14 percent less than independent estimates by Hely and others (1971) and about 8 percent less than total flow simulated in the Waddell and others model (1987). Most of the decrease in recharge relative to previous estimates was the result of a smaller rate of simulated recharge from lawns and gardens. During calibration, specified recharge from lawns and gardens was adjusted within a range of zero to 28,000 acre-ft/yr. The best match between model-computed and measured water levels was obtained when a rate of 10,000 acre-ft/yr was simulated. Simulated recharge from lawns and gardens was eliminated in the dense industrial and commercial area of Salt Lake City and resulted in improved matches between model-computed and measured water levels in that area. The decrease in simulated recharge from initial estimates was matched mainly by lower model-com-

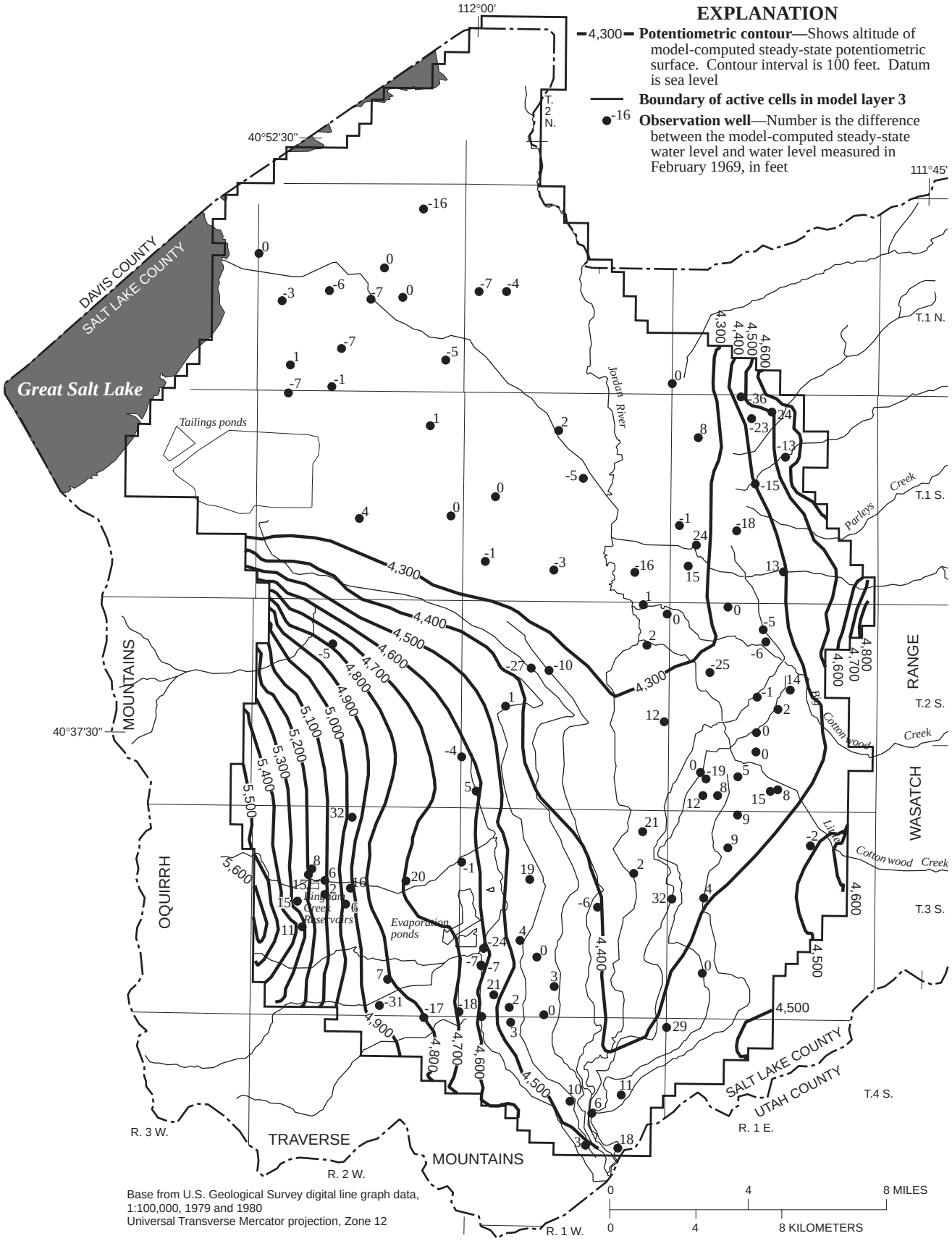

Figure 16. Model-computed steady-state potentiometric surface of model layer 3 and the difference between model-computed steady-state water levels and water levels measured during 1968–69 at observation wells in the principal aquifer, Salt Lake Valley, Utah.

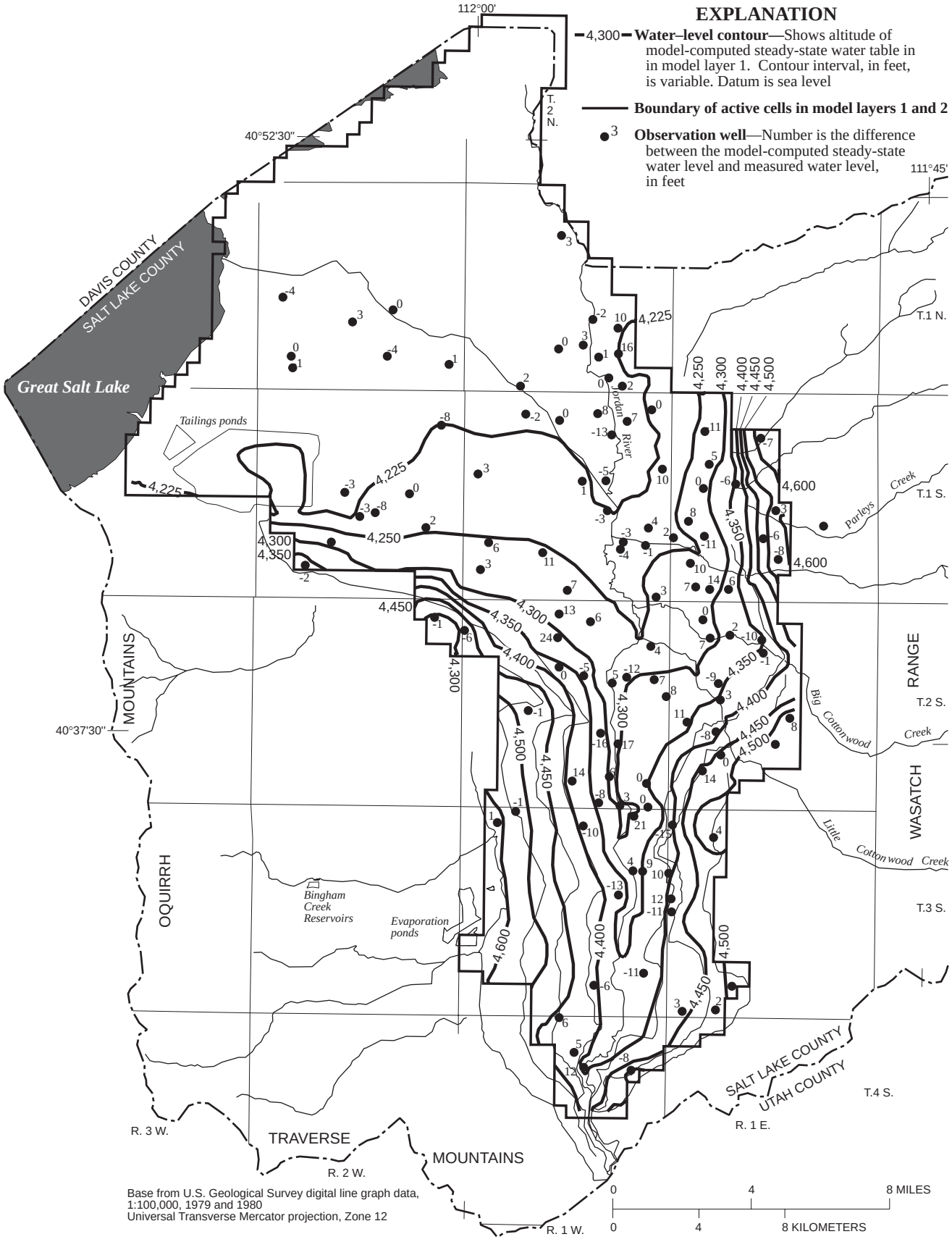

Figure 17. Model-computed steady-state water-table surface of model layer 1 and the difference between model-computed steady-state water levels and measured water levels in the shallow unconfined aquifer, Salt Lake Valley, Utah.

Table 4. Simulated vertical hydraulic gradient in the steady-state simulation and measured vertical hydraulic gradient at nested well sites in Salt Lake Valley, Utah

[See figure 6 for location of observation site; vertical hydraulic-gradient values are unitless; (-) indicates upward vertical hydraulic gradient; (+) indicates downward vertical hydraulic gradient]

Observation-site number	Model layers monitored at nested wells	Simulated vertical hydraulic gradient in the steady-state simulation	Vertical hydraulic gradient calculated from measured water levels
1	1,3	-0.046	-0.057
2	1,4	-.037	-.067
3	1,5	-.037	-.028
4	1,5	-.006	-.028
5	1,3	-.091	-.052
6	1,5	-.028	-.026
7	1,5	-.020	-.028
8	1,3	-.071	-.10
9	1,4	+.272	+.362
10	1,4	+.064	+.005
11	1,3	+.024	-.003

puted discharge to the Jordan River and by evapotranspiration.

During steady-state calibration, values for conductance at head-dependent boundaries that simulate recharge from consolidated rock at the northern end of the Oquirrh Mountains, recharge to or discharge from the Jordan River, and discharge to drains were adjusted to match measured water levels and measured or estimated flow rates. Conductance values for all head-dependent boundaries that simulate inflow from consolidated rock (*CGHB*) were set at 65,000 ft^2/d (rounded), and model-computed recharge from consolidated rock totaled 18,000 acre-ft/yr in the steady-state simulation. River-bed conductance values for river cells (*CRIV*) ranged from 900 ft^2/d to 250,000 ft^2/d (rounded) and were computed using streambed-conductivity (K_{riv}) values ranging from 0.1 ft/d to 10 ft/d (fig. 15). Assigned conductance values for drain cells (*CD*) near Magna in the northwestern part of the valley ranged from 2,000 ft^2/d to 13,000 ft^2/d (rounded). The conductance value at drain cells (*CD*) in Salt Lake City was 4,000 ft^2/d (rounded).

During steady-state calibration, recharge rates at specified-flux cells along the mountain front that simulate recharge from consolidated rock (fig. 9) were adjusted to match measured water levels and estimated flow rates. Final recharge rates at specified-flux cells on the east side of the valley from Mill Creek to the north totaled about 59,000 acre-ft/yr; recharge rates at specified-flux cells on the east side of the valley south of Mill Creek total about 33,000 acre-ft/yr; and recharge rates at specified-flux cells on the west side of the valley totaled about 32,000 acre-ft/yr.

During steady-state calibration, specified maximum rates of evapotranspiration were uniformly adjusted to match water levels in areas of shallow ground water. The best match was achieved when maximum rates listed in table 1 were decreased uniformly by 75 percent. Model-computed steady-state discharge by evapotranspiration was about 40 percent less than the average computed by Hely and others (1971) for 1964-68 and about 30 percent less than the average estimated by using the Waddell and others (1987) model. Attempts to increase discharge by evapotranspiration during calibration by increasing maximum evapotranspiration rates at model cells and increasing specified recharge from precipitation on the valley floor resulted in a poorer match between model-computed and measured water levels in the shallow unconfined aquifer and the principal aquifer, regionally.

Steady-state calibration resulted in refined estimates of model parameters defining the hydrologic properties of the basin-fill aquifer system. The final distribution of hydraulic-conductivity values for model

Table 5. Ground-water budget for Salt Lake Valley, Utah, as reported in previous studies and specified or computed in the steady-state simulation

[Data in acre-feet per year]

	Estimated for 1964-68 (Hely and others, 1971, table 21)	Estimated in Waddell and others (1987, tables 1 and 3) steady-state simulation	Specified or computed in the steady-state simulation
Recharge from			
Consolidated rock	135,000	154,000	142,000
Irrigated fields, lawns, and gardens	98,000	76,000	57,000
Precipitation	60,000	70,000	67,000
Canals	48,000	24,000	30,000
Streams and channel fill	21,500	17,500	16,000
Underflow at Jordan Narrows	2,500	2,500	2,500
Seepage from tailings ponds near Magna	2,400	0	0
Reinjection from air conditioning	2,000	2,000	[2]0
Reservoirs and evaporation ponds	0	0	1,900
Jordan River and tributaries	0	0	1,000
Total (rounded)	369,000	346,000	317,000
Discharge to			
Jordan River and tributaries	170,000	146,000	137,000
Wells	107,000	102,000	105,000
Evapotranspiration	60,000	54,000	36,000
Springs	21,000	21,000	19,000
Drains	5,000	5,000	10,000
Great Salt Lake	4,000	7,200	1,300
Canals	0	10,000	9,200
Total (rounded)	367,000	[1]345,000	317,000

[1]Previously reported in Waddell and others (1987, table 3) as 346,000.
[2]Amounts reinjected were subtracted from amounts pumped for same wells.

layer 1, which represents the shallow unconfined aquifer, is shown in figure 18. A hydraulic-conductivity value of 1 ft/d was used for model layer 2, which represents the shallow confining layer. Ranges for total transmissivity of the principal aquifer (T) incorporated in the model in the transmissivity of individual model layers 3 to 7 is shown in figure 19. The final distribution of vertical hydraulic-conductivity values (K_v) for model layer 1 incorporated in the vertical leakance between model layers 1 and 2 (VL_2) is shown in figure 20. The final distribution of vertical hydraulic-conductivity values for model layer 2 incorporated in the vertical leakance between model layers 1 and 2 (VL_2), and model layers 2 and 3 (VL_3) is shown in figure 21. Final estimates of vertical hydraulic conductivity for zones of the principal aquifer used to compute vertical leakance values between model layers are shown in figure 8.

Transient-State Calibration

Method

The transient-state simulation is calibrated to hydrologic conditions for 1969-91. The results of the steady-state simulation were used as the initial condition. Annual fluctuation in recharge and withdrawals from public-supply, irrigation, and industrial wells was simulated for that period. Estimates of annual recharge from irrigated fields, lawns, and gardens for yearly stress periods were determined on the basis of steady-state estimates and changes in land use with time described previously in this report. Simulated recharge from irrigated fields was decreased each stress period in uniform increments from an initial rate of 47,800 acre-ft/yr (specified in the steady-state simulation) to 31,800

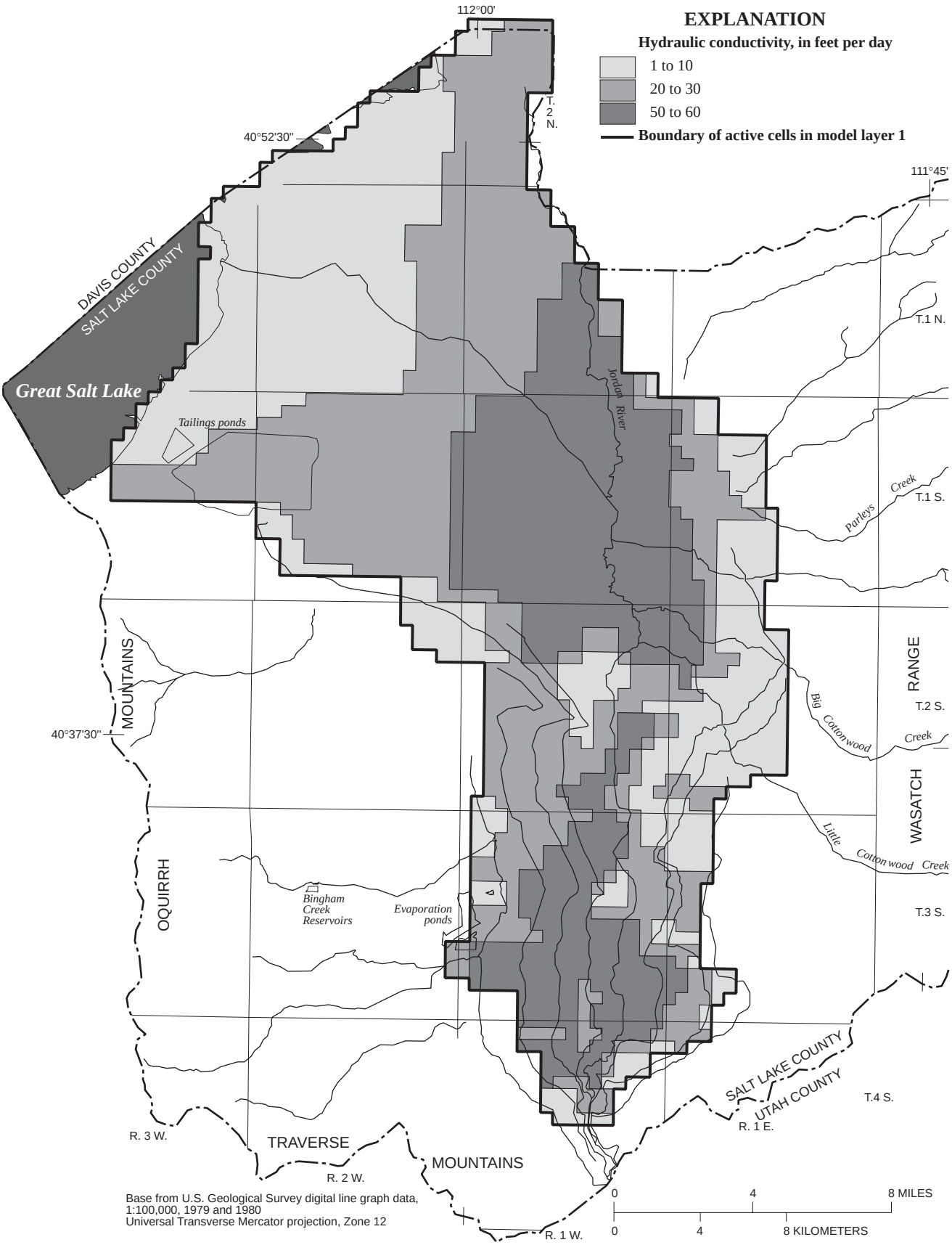

Figure 18. Final distribution of hydraulic-conductivity values for layer 1 of the ground-water flow model of Salt Lake Valley, Utah.

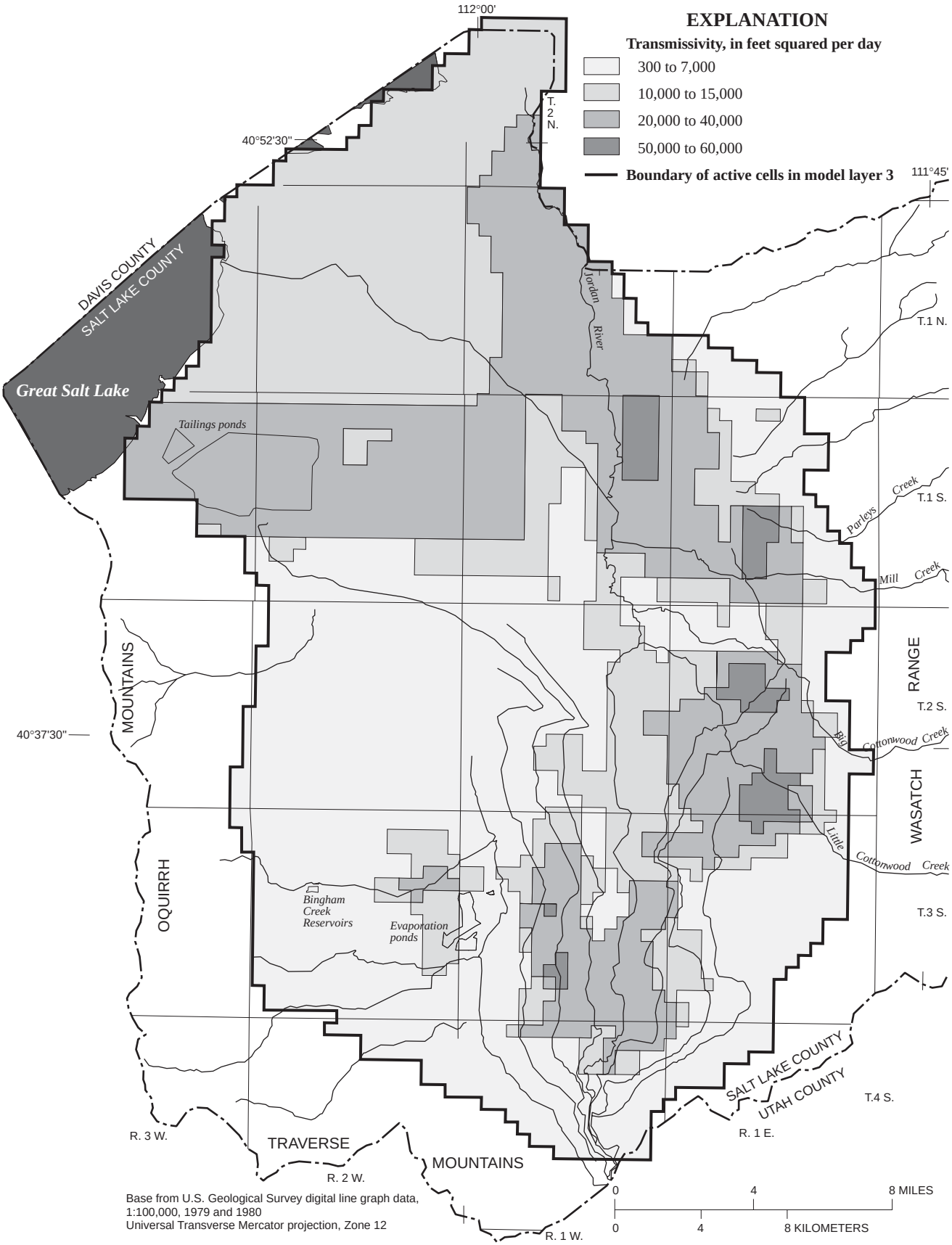

Figure 19. Final distribution of transmissivity values for the principal aquifer simulated in layers 3 to 7 of the ground-water flow model of Salt Lake Valley, Utah.

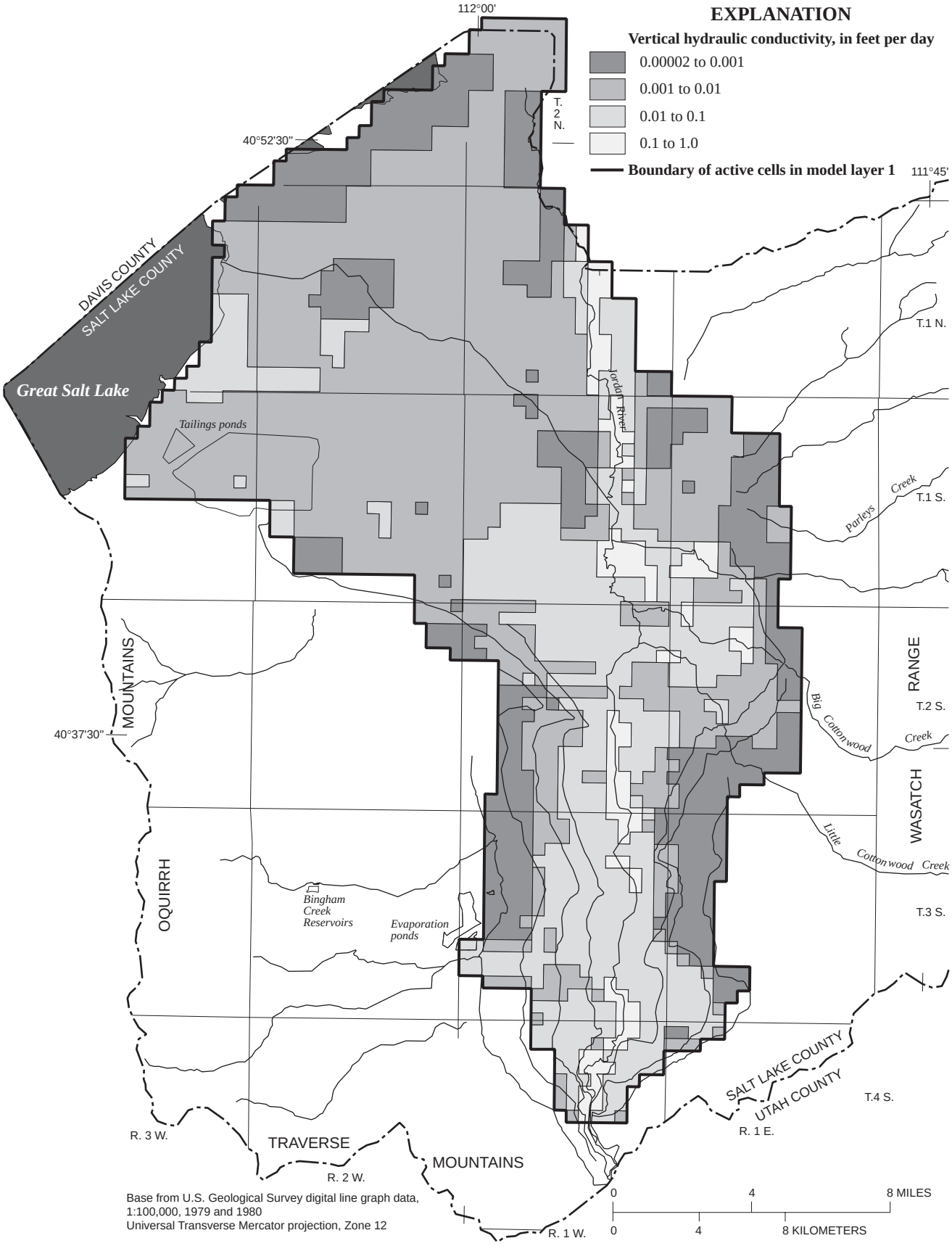

Figure 20. Final distribution of vertical hydraulic-conductivity values for layer 1 incorporated in the vertical leakance between layers 1 and 2 of the ground-water flow model of Salt Lake Valley, Utah.

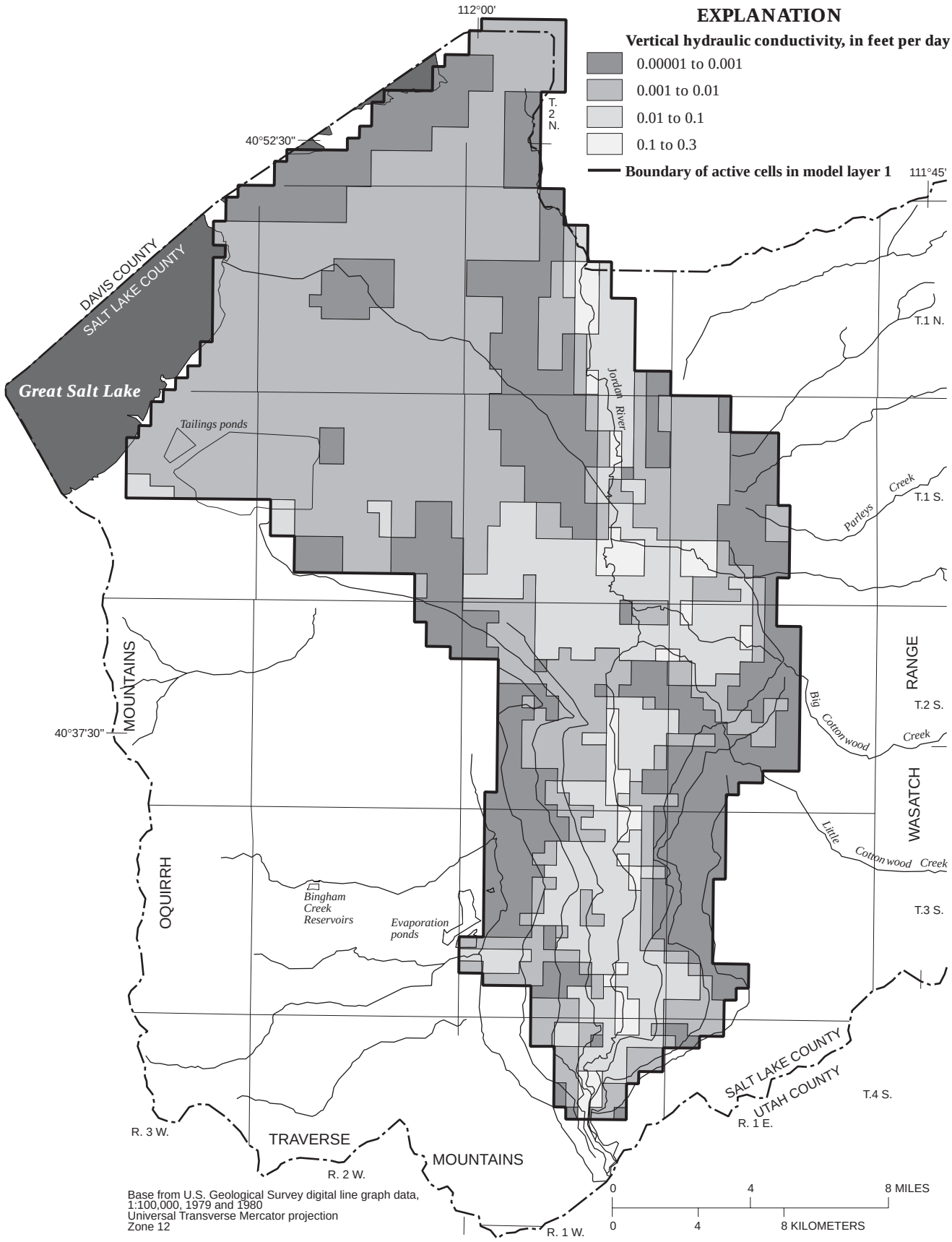

Figure 21. Final distribution of vertical hydraulic-conductivity values for layer 2 incorporated in the vertical leakance between layers 1 and 2 and between layers 2 and 3 of the ground-water flow model of Salt Lake Valley, Utah.

acre-ft/yr in stress period 20, to represent conditions in 1988. Simulated recharge from irrigated fields remained constant for stress periods representing conditions during 1988-91. Simulated recharge from non-irrigated land that was converted to residential or commercial use (fig. 11) was increased each stress period in uniform increments from the initial steady-state condition of zero recharge to 400 acre-ft/yr in stress period 20 and remained constant during subsequent stress periods. Annual recharge rates representing recharge from irrigated fields, lawns, and gardens incorporated in the transient-state simulation are shown in figure 22.

Transient-state calibration involved adjusting calibration variables and comparing model-computed water levels and water-level changes with measured water levels and water-level changes at observation wells in the principal aquifer. Model parameters considered to be calibration variables during transient-state calibration were (1) storage coefficient of confined zones of the aquifer system, (2) specific yield of unconfined zones of the aquifer system, (3) transmissivity of the principal aquifer, and (4) variation from steady-state values of simulated annual recharge to the basin-fill ground-water flow system from consolidated rock, streams, and precipitation on the valley floor. For each individual model run, model-computed water-level changes from one stress period to the next were compared with water-level changes determined from yearly February water-level measurements at observation wells to determine the accuracy of the simulation. Periodically, water levels computed during the final stress period of the transient simulation, which represent conditions at the end of 1991, were compared with water levels of the principal aquifer measured in 1991-92. Also, model-computed ground-water discharge to the Jordan River was compared with estimated annual discharge to the river.

Results of Calibration

Transient-state calibration resulted in a reasonable match between model-computed and measured annual water-level changes for the simulation period in most of the modeled area (fig. 23). A comparison of model-computed and measured water-level changes at selected observation wells in the northwestern part of the valley is shown in figure 23a. Water levels in this area are affected mainly by long-term trends in regional precipitation and withdrawal from industrial wells near

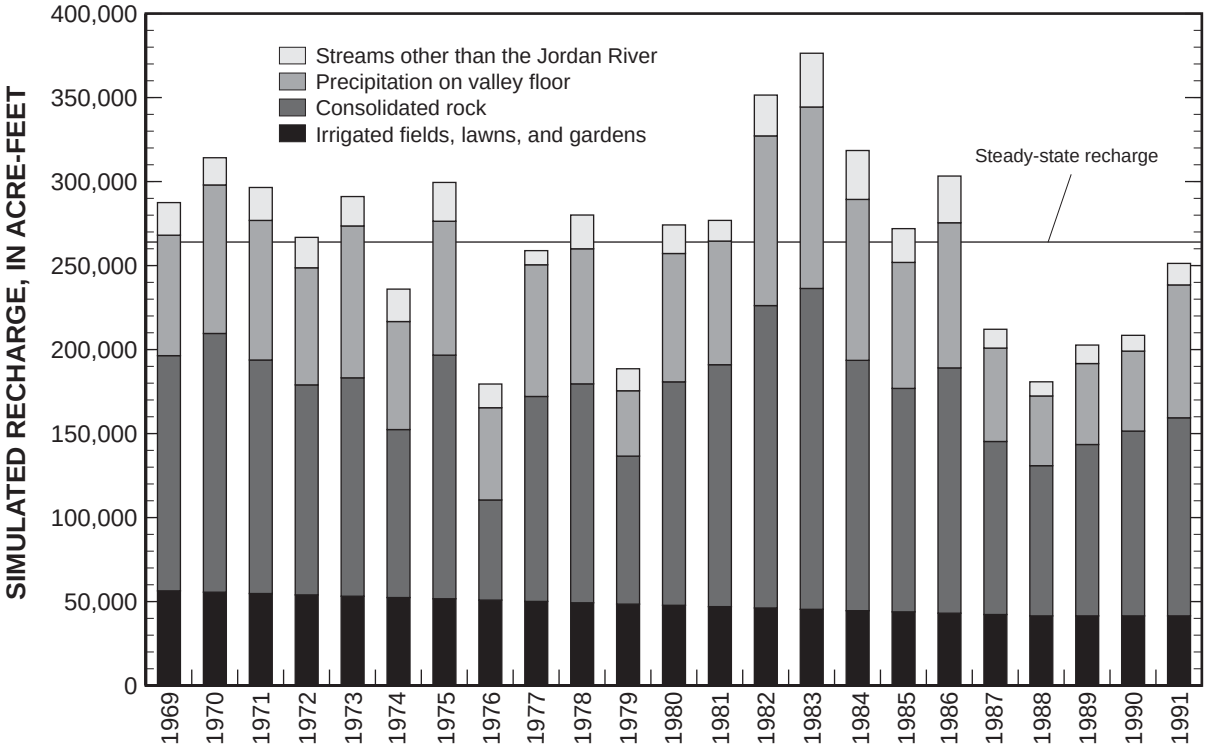

Figure 22. Simulated recharge at selected specified-flux boundaries for the 1969–91 transient-state simulation of the ground-water flow model of Salt Lake Valley, Utah.

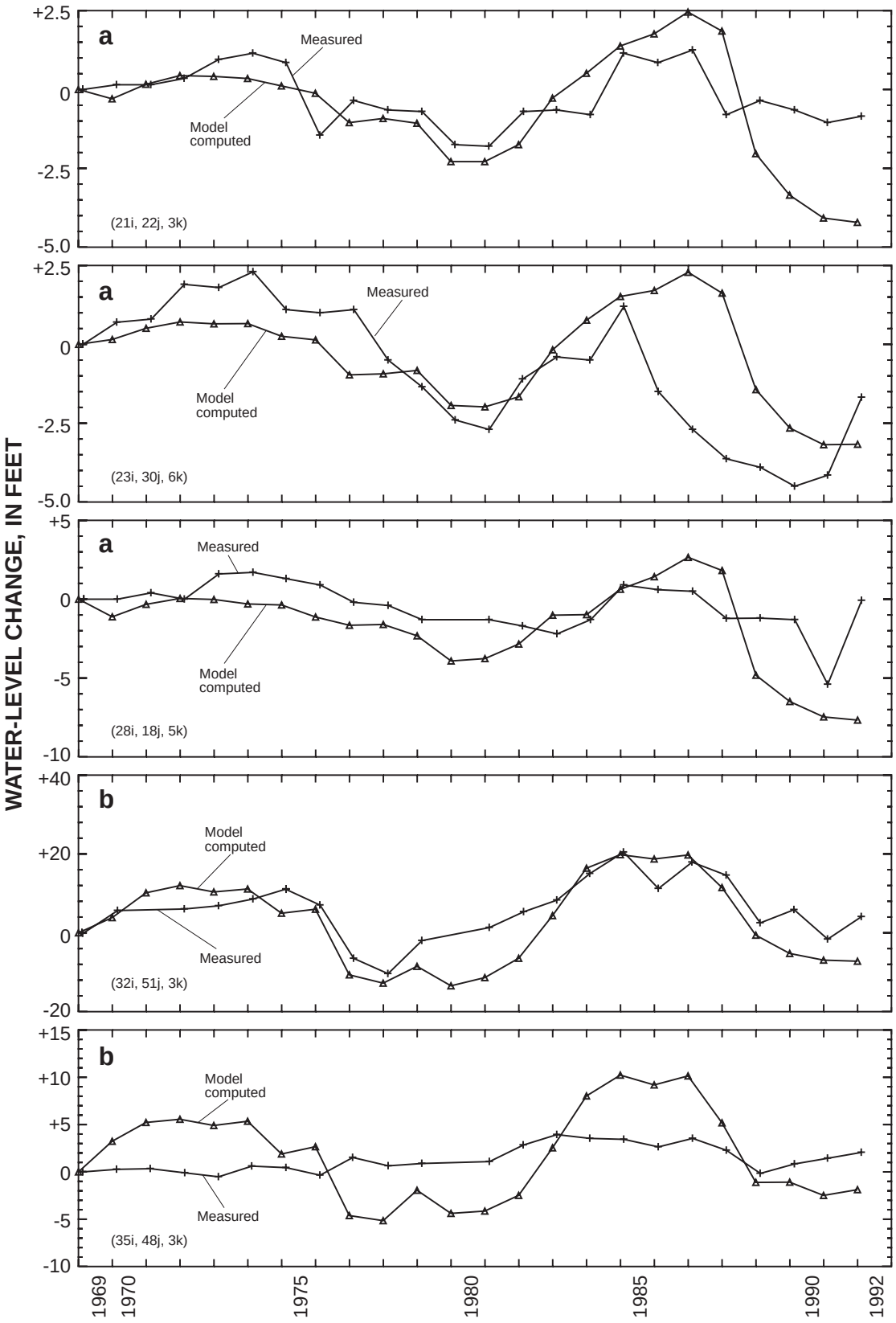

Figure 23. Model-computed and measured water-level changes at selected observation wells in the (a) northwestern, (b) eastern, and (c) western and southwestern parts of Salt Lake Valley, Utah, 1969–92. Numbers in parentheses represent row, column, and layer of model cell.

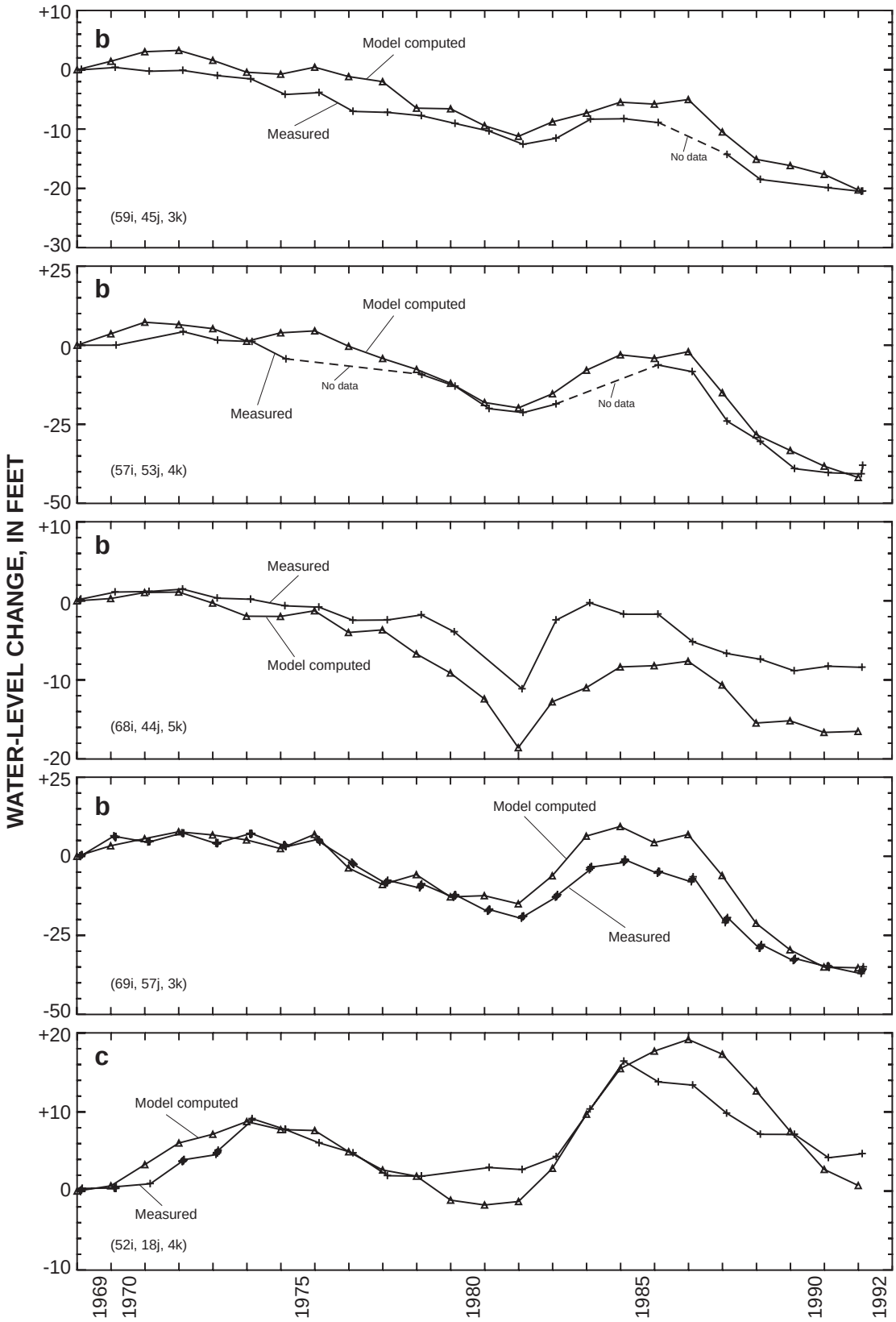

Figure 23. Model-computed and measured water-level changes at selected observation wells in the (a) northwestern, (b) eastern, and (c) western and southwestern parts of Salt Lake Valley, Utah, 1969–92. Numbers in parentheses represent row, column, and layer of model cell—Continued.

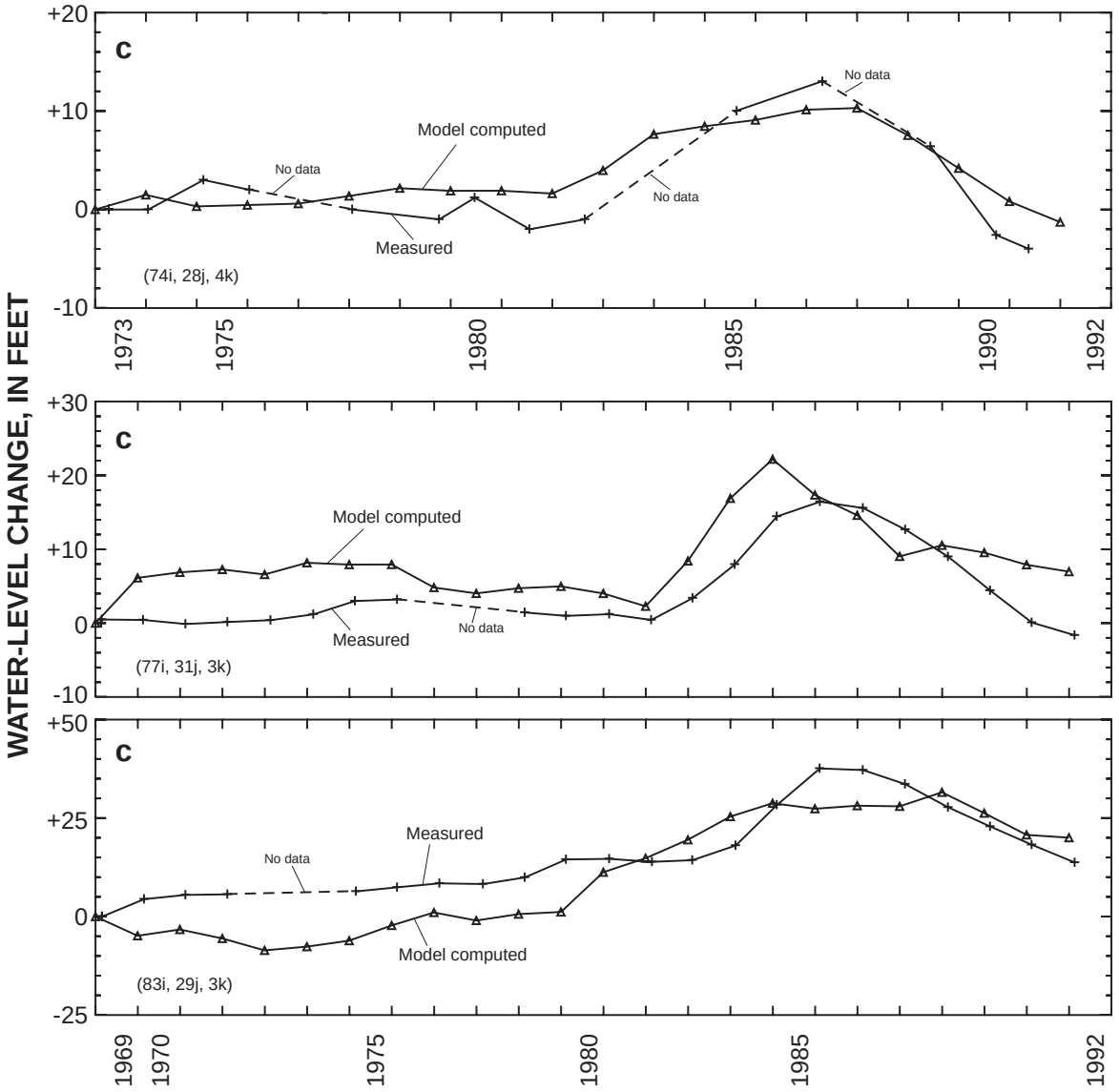

Figure 23. Model-computed and measured water-level changes at selected observation wells in the (a) northwestern, (b) eastern, and (c) western and southwestern parts of Salt Lake Valley, Utah, 1969–92. Numbers in parentheses represent row, column, and layer of model cell—Continued.

the northern end of the Oquirrh Mountains. A good match between model-computed and measured annual changes was generally achieved at these sites. The transient-state simulation generally reproduced measured water-level changes at wells in the eastern part of the valley (fig. 23b), where water levels are affected by fluctuations in recharge at the mountain front and increases in ground-water withdrawals in the southeastern part of the valley. Simulated and measured water-level changes at the well in cell 52i, 18j, 4k (i-row, j-column, k-layer) (fig. 23c) indicate the effects of fluctuations in recharge at the western mountain front. Observation wells at cells 74i, 28j, 4k and 77i, 31j, 3k are directly downgradient from evaporation ponds. The ponds were used to store excess runoff from Bingham Canyon during extreme wet periods, including 1983-84 (Kennecott Utah Copper, 1992a, p. 19). Model-computed and measured water-level rises during 1982-84 indicated in the hydrographs reflect recharge from seepage at these ponds during that period.

Model-computed water levels for stress period 23, which represents conditions at the end of 1991, were compared with water levels in 123 wells during 1991-92. Seventy-three of these measurements were made in wells in the southwestern part of the valley and were reported by Kennecott Utah Copper (1992c). Because of the large number of measurements made in the southwestern part of the valley, model-computed water levels were compared to this set of data separately. The model-computed potentiometric surface in model layer 3, which represents the upper zone of the principal aquifer, in the southwestern part of the valley and residuals for observation wells in the principal aquifer in that area are shown in figure 24. The mean of the residuals for observation wells in the southwestern part of the valley was 2.5 ft, the standard error (mean of absolute values of residuals) was 25.2 ft, and the standard deviation was 32 ft. Values for the standard error and standard deviation for residuals are substantially larger than those calculated for observation wells in the principal aquifer in the steady-state simulation (table 2). This is mainly because of the relatively large horizontal hydraulic gradient in the southwestern part of the valley, which in most areas, results in a change in water level across a given model cell of as much as 75 ft or greater. The model-computed potentiometric surface in model layer 3 and residuals for observation wells in the remainder of the valley are shown in figure 25. The mean for this set of 50 residuals was -3.0 ft, the standard error was 15.6 ft, and the standard deviation was 21.3 ft. Negative residuals in the northwestern part of the valley (fig. 25) indicate that model-computed water levels for the stress period representing 1991 are generally lower than actual water levels. The comparison of model-computed and measured water-level changes at observation wells in the northwestern part of the valley shown in figure 23a indicates that model-computed drawdowns in water levels from 1984 to 1991 exceed measured drawdowns and result in model-computed water levels that are too low. Estimates of ground-water withdrawals from wells for industrial use in the northwestern part of the valley during this period are based on few data. The simulation of water levels in this area that are consistently lower than measured water levels may indicate that the simulated pumpage from industrial wells in this area for 1984 to 1991 is too large.

The sum of model-computed flow at all river cells for the simulation period was compared with estimates of annual net gains from ground water in the Jordan River (fig. 26). Ground-water inflow to the Jordan River, including that from the downstream reaches of Little Cottonwood Creek, Big Cottonwood Creek, and Mill Creek was estimated from net gains in the river during winter months. Monthly gains in the Jordan River between Jordan Narrows and 2100 South Street for winter months (January, February, November, and December) were computed for each calender year and accounted for diversions from the river to canals and inflow to the river from tributaries and discharge from sewage plants. The smallest estimated monthly gain for January and February and the smallest estimated monthly gain for November and December in a calender year were averaged. The resulting average monthly rate was extrapolated for the year to obtain an estimate of annual discharge from ground water to the river from Jordan Narrows to 2100 South Street. An estimated gain of 1,000 acre-ft/yr (Hely and others, 1971, p.136) in the river upstream from 2100 South Street was assumed for the comparison. Estimated gains to the river for the winter months were used in order to minimize error in estimating gains from ground water caused by inflow to the river from surface irrigation return flow and runoff from local storms and snowmelt.

The comparison indicates a reasonable match between model-computed and estimated annual net gain in the Jordan River for most years of the simulation period. Model-computed gains, however, are substantially less than estimated values for 1983-86, a period of greater-than-normal annual precipitation on

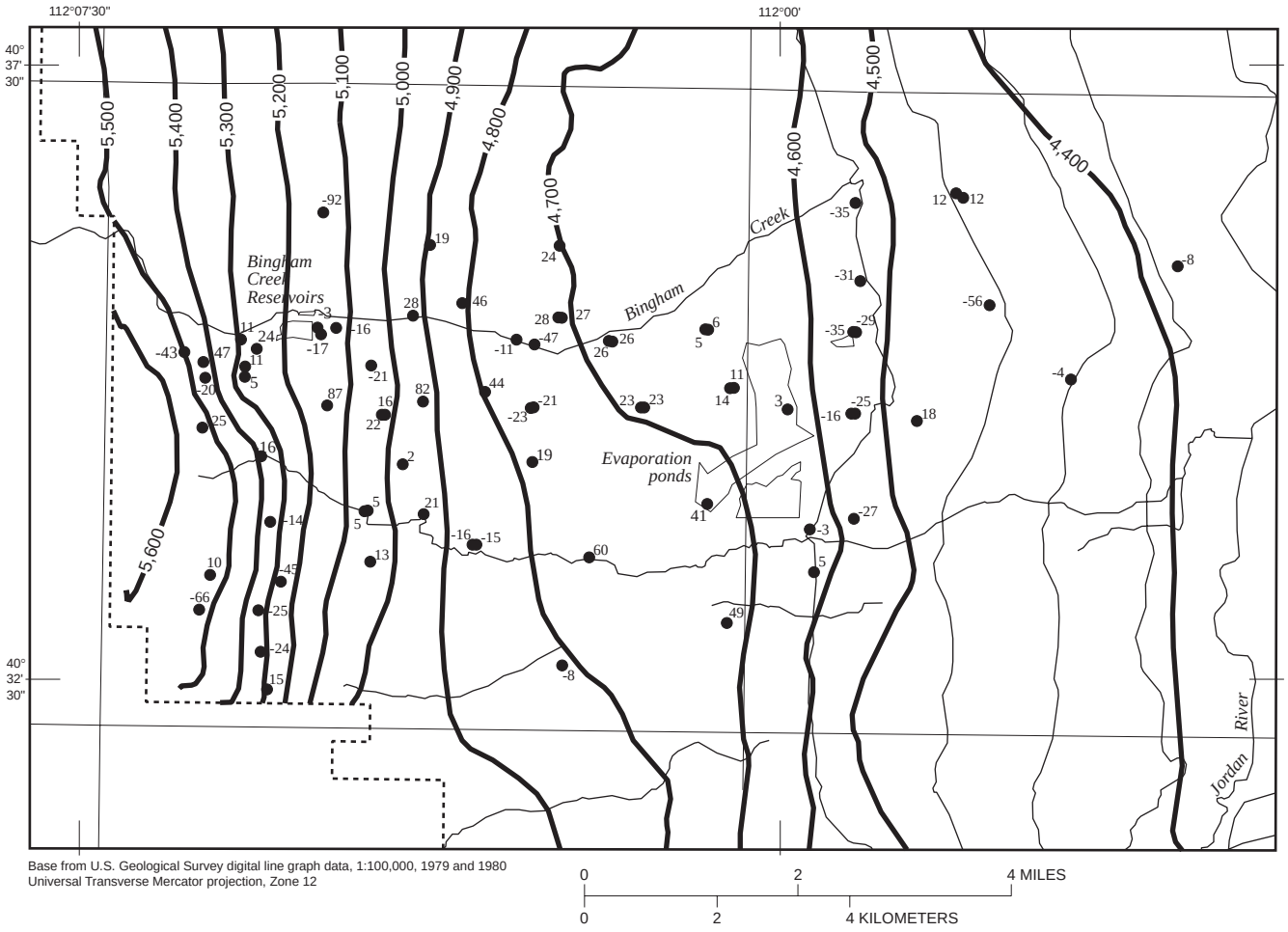

EXPLANATION

4,600 Potentiometric contour—Shows altitude of model-computed potentiometric surface. Contour interval is 100 feet. Datum is sea level

Boundary of active cells in model layer 3

-8 Observation well—Number is the difference between the model-computed water level and water level measured in 1991, in feet

Figure 24. Model-computed potentiometric surface of model layer 3 at the end of 1991 and the difference between model-computed and measured 1991 water levels at observation wells in the principal aquifer in the southwestern part of Salt Lake Valley, Utah.

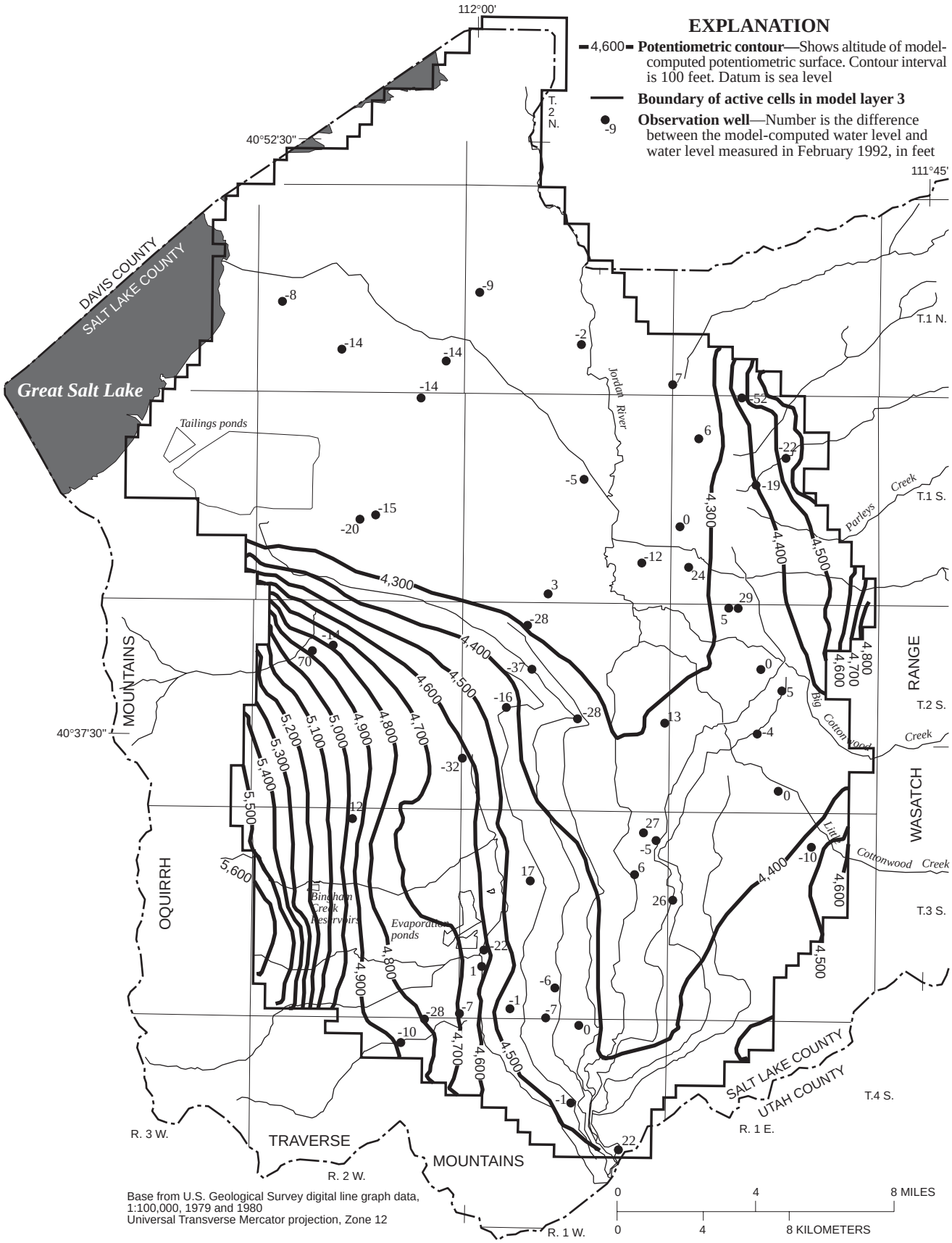

Figure 25. Model-computed potentiometric surface of model layer 3 at the end of 1991 and the difference between model-computed water levels and water levels measured in February 1992 at observation wells in the principal aquifer, Salt Lake Valley, Utah.

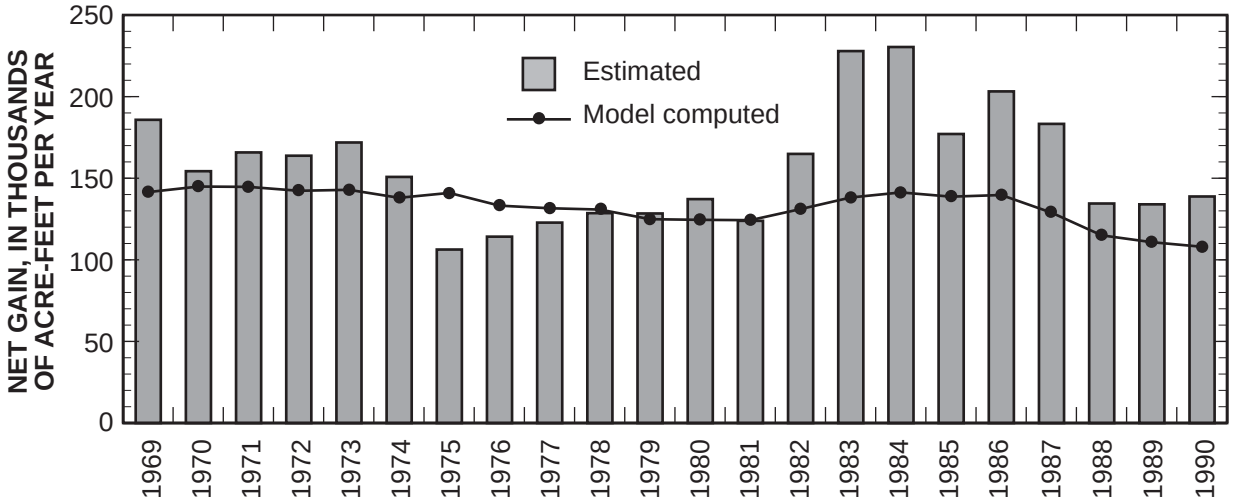

Figure 26. Model–computed and estimated annual net gain from ground water in the Jordan River, Utah, 1969–90.

the valley floor and in adjacent mountains (fig. 10). The results of the transient-state calibration indicate that the model simulated measured water levels and water-level changes near the Jordan River and throughout the modeled area with reasonable accuracy during this period. Attempts to improve the match between model-computed and estimated gains in the river for 1983-86 by adjusting model parameters that define aquifer properties or specified recharge resulted in an unsatisfactory match between model-computed and measured water-level changes. The apparent inability of the model to closely match estimated river losses and gains during some years may be, in part, the result of error in independent estimates of these quantities. Because of the large number of factors involved in estimating the amount of ground-water inflow from stream-flow records, the error associated with the computation could be large, particularly during years of greater-than-normal precipitation, when ungaged inflow may be substantial.

For each stress period, estimates for annual recharge to the ground-water flow system from consolidated rock, streams, and precipitation on the valley floor were calculated from steady-state values using equations 8, 9, and 10. During calibration, the simulated effects of annual fluctuations in precipitation throughout the valley and the surrounding mountains, and in flow in streams that enter the valley from the Wasatch Range, were adjusted by varying the coefficient *C* in equations 8, 9, and 10. Model-computed water-level changes in the principal aquifer near the margins of the valley were substantially affected by varying the coefficient *C*. The best match between model-computed and measured water-level changes was achieved using a value of 1 for the coefficient *C*, simulating a proportional change in recharge with the ratios defined in equations 8, 9, and 10. Annual rates of recharge simulated at specified-flux boundaries from consolidated rock, streams, and precipitation on the valley floor in the transient-state simulation are shown in figure 22.

The final distribution of storage-coefficient values for areas of the principal aquifer where confined conditions may be simulated, and specific-yield values for where unconfined conditions are simulated, are shown in figure 27. A specific-yield value of 0.15 was used in model layer 1. A storage-coefficient value of $1x10^{-3}$ was used in model layer 2. In areas where unconfined conditions were simulated in the principal aquifer below the active boundary of model layer 2, a specific-yield value of 0.15 was used. A storage-coefficient value of $1x10^{-3}$ was used in model layers 4 to 7 in areas where the shallow unconfined aquifer and the shallow confining layer were not simulated.

SENSITIVITY ANALYSIS

Sensitivity analysis is an evaluation of the effect of changes in individual model parameters on model results. The analysis provides an indication of the uncertainty with which model parameters have been estimated as a result of the calibration process and thus the uncertainty of the calibrated model. Observations of the sensitivity of the model to variations in model parameters were made throughout calibration of the

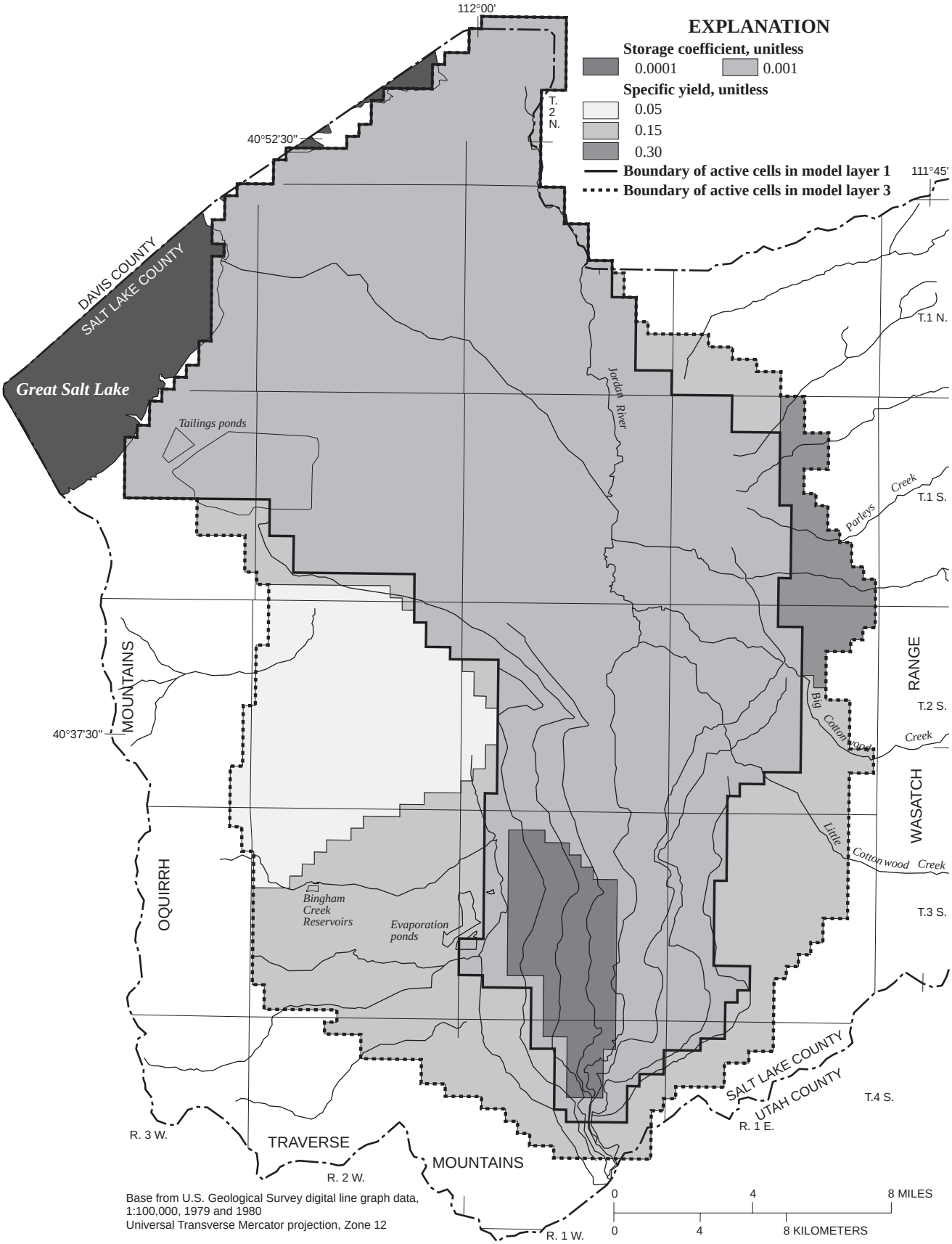

Figure 27. Final distribution of storage-coefficient values for confined zones of the principal aquifer and specific-yield values for unconfined zones in layer 3 of the ground-water flow model of Salt Lake Valley, Utah.

model. A more detailed analysis was done at the end of model calibration for selected model parameters with large defined ranges of possible values, or for which few data were available on which to base estimates. The sensitivity of the model to changes in model parameters that define aquifer and river-bed properties, including (1) hydraulic conductivity of the shallow unconfined aquifer represented by model layer 1, (2) vertical hydraulic conductivity of the shallow unconfined aquifer and the shallow confining layer incorporated in the model in the vertical leakance between model layers 1 and 2, and model layers 2 and 3, (3) vertical hydraulic conductivity of the principal aquifer incorporated in the model in the vertical leakance among model layers 3 to 7, and (4) hydraulic conductivity of the river bed incorporated in the model as riverbed conductance, was analyzed. The analysis was made by independently and uniformly varying each parameter, or the model input derived from the parameter, in the steady-state simulation. The effects of changes in storage coefficient and recharge from consolidated rock, streams, and precipitation on the valley floor on the model also were observed by varying these parameters in the transient-state simulation. All effects of changes discussed in the following paragraphs are presented with respect to final simulation results.

The selected parameters were decreased and increased independently in the steady-state simulation by a factor of 50 percent (an order of magnitude for the vertical hydraulic conductivity of model layers 3 to 7). After each simulation, model-computed water levels and flow rates were compared with those generated by the calibrated steady-state simulation to assess the effects resulting from the change in the model parameter. Model-computed water levels from each sensitivity-analysis simulation also were compared with the same set of measured water levels used during calibration of the model to steady-state conditions (figs. 16 and 17), and summary statistics for the difference between model-computed and measured water levels (residuals) were calculated (table 6). Comparisons of summary statistics for residuals resulting from the calibrated steady-state simulation and residuals resulting from subsequent sensitivity-analysis simulations indicate the effect of changes produced by the adjustments made to individual model parameters, and whether varying the parameter improved or worsened the match between simulated and measured conditions.

Decreasing the horizontal hydraulic conductivity in model layer 1 by 50 percent caused model-computed water levels to rise substantially throughout most of the model layer. Water-level rises were most prominent along the edges of the active section of the layer in the central and southern parts of the valley, where rises of up to 80 ft occurred. Water-level declines relative to calibrated values of less than 5 ft were simulated in the northern part of the valley in model layer 1. Decreasing horizontal conductivity in model layer 1 resulted in a large increase in the mean of residuals for observation sites in that layer (table 6), indicating a substantial bias toward positive residual values. Substantial increases in the standard error and standard deviation of residuals also resulted. Decreasing horizontal hydraulic conductivity in model layer 1 resulted in rises of as much as 10 ft in model-computed water levels throughout most of model layers 3 to 7. Rises of more than 30 ft in model layers 3 to 7 occurred locally below the southwestern border of the active section of model layer 1.

The model is less sensitive to increasing hydraulic conductivity than to decreasing hydraulic conductivity in model layer 1. Increasing hydraulic conductivity in model layer 1 by 50 percent produced declines in model-computed water levels of as much as 35 ft. The changes were most noticeable along the edges of the active section of the model layer. Water-level changes were less substantial in model layers 3 to 7, where model-computed water levels generally declined by 10 ft or less. Means of residuals for the shallow unconfined aquifer and the principal aquifer (table 6) are both negative for the simulation and indicate that model-computed water levels are generally lower than measured water levels.

Vertical leakance (VL) is used by the model to calculate vertical conductance between model layers and is a function of equivalent vertical hydraulic conductivity between the midplanes of model layers (K'_v) (equation 4). The sensitivity of the model to changes in vertical hydraulic conductivity (K_v) of sediments of the shallow unconfined aquifer and the shallow confining layer were examined by varying VL within the top three model layers by a factor of 50 percent. The results of the subsequent simulations indicate that the model is more sensitive to decreases in VL within model layers 1 to 3 than to increases in those values. Decreasing VL within the top three model layers by 50 percent caused water levels to rise by as much as 30 ft in model layer 1 in the central and southern parts of the valley where simulated ground-water flow through model layer 2 is downward, and caused water levels to decline slightly in model layer 1 in the northern part of the valley, where simulated ground-water flow through the shallow confining layer is upward. Water levels generally rose

Table 6. Statistics of differences between model-computed and measured water levels in the steady-state simulation and sensitivity-analysis simulations using the ground-water flow model of Salt Lake Valley, Utah

[Values calculated as model-computed minus measured water level, difference in feet; HC, hydraulic conductivity, VL, vertical leakance]

	Statistics of difference between model-computed and measured water levels in the steady-state simulation	Statistics of differences between model-computed and measured water levels in sensitivity-analysis simulations							
		Horizontal HC in model layer 1		VL between model layers 1 to 3		VL between model layers 3 to 7		Riverbed HC	
		x0.5	x1.5	x0.5	x1.5	x0.1	x10.0	x0.5	x1.5
Observation sites in the shallow unconfined aquifer (112 comparisons)									
Mean	1.1	10.9	-3.6	4.4	-0.9	1.7	1.1	2.8	0.6
Standard error (mean of absolute value of differences)	6.4	13.1	8.1	8.0	6.8	6.3	6.3	6.9	6.4
Standard deviation	8.2	18.7	10.8	10.5	8.6	8.4	8.1	8.8	8.1
Maximum difference lower than measured	-16.6	-13.3	-31.6	-13.5	-21.4	-16.4	-16.6	-14.3	-18.8
Maximum difference higher than measured	24.4	57.5	17.2	34.4	19.7	27.7	23.9	25.7	24.0
Observation sites in the principal aquifer (102 comparisons)									
Mean	1.0	6.4	-2.2	5.0	-1.2	3.6	.4	3.2	.1
Standard error (mean of absolute value of differences)	9.5	11.9	10.0	11.7	9.7	10.4	9.5	10.8	9.5
Standard deviation	13.1	15.4	13.7	15.2	13.0	13.9	13.2	14.4	13.0
Maximum difference lower than measured	-36.5	-34.4	-37.3	-32.5	-39	-29.5	-38.4	-35.7	-36.9
Maximum difference higher than measured	32.6	39.7	28.9	44.6	29.6	36.5	32.1	38.7	30.5

throughout model layers 3 to 7 by less than 10 ft. Increasing VL within the top three model layers by 50 percent did not substantially change model-computed water levels from calibrated values and did not substantially improve or worsen the overall match between model-computed and measured water levels (table 6).

The sensitivity of the model to vertical hydraulic conductivity (K_v) of sediments of the principal aquifer represented by model layers 3 to 7 was examined by decreasing and increasing vertical leakance (VL) within these layers by a factor of 10 from calibrated model values. Smaller variations of VL did not produce significant changes in model-computed water levels. Decreasing VL between model layers 3 to 7 by an order of magnitude caused water levels to decline in model layer 1 by as much as 5 ft in the northern end of the valley and along the Jordan River. Water-level rises in model layer 1 did not exceed 3 ft. Statistics of residuals (table 6) indicate that the adjustment did not have a substantial effect on the match between model-computed and measured water levels in model layer 1. Reducing VL in model layers 3 to 7 had a larger effect on water levels in those model layers. Water levels in the northern part of the valley rose as much as 15 ft, and statistics for residuals indicate the match between model-computed and measured water levels worsened slightly. Increasing VL within model layers 3 to 7 by an order of magnitude produced only a small amount of change from calibrated water levels.

The sensitivity of the model to the hydraulic conductivity of the river bed (K_{riv}) incorporated in the model input, termed river-bed conductance (*CRIV*), was analyzed by decreasing and increasing K_{riv}, and thus *CRIV*, by a factor of 50 percent. Decreasing *CRIV* by 50 percent caused model-computed water levels to generally rise throughout all model layers. Water levels

rose as much as 15 ft in model layer 1 and as much as 10 ft in model layers 3 to 7. Increasing *CRIV* by 50 percent produced less of an effect, causing declines in model-computed water levels as much as 8 ft in model layer 1. Model-computed water levels rose and declined in model layers 3 to 7 by less than 4 ft. Statistics for residuals (table 6) indicate that increasing *CRIV* by 50 percent did not substantially improve or worsen the match between model-computed and measured water levels.

Generally, model-computed flow rates were not substantially affected by independently decreasing or increasing selected model parameters as discussed above. Large changes in model-computed water levels in sensitivity-analysis simulations occurred mainly near the edges of model layers in the southern and central parts of the valley. Water-level changes near the Jordan River and in the northern part of the valley generally were smaller and thus did not substantially affect model-computed discharge or recharge at primary flow boundaries, including head-dependent river cells and evapotranspiration cells located in those areas. Model-computed discharge to head-dependent river cells and evapotranspiration cells in sensitivity-analysis simulations varied by less than 3 percent from calibrated values.

Storage coefficient of the principal aquifer and annual variations in recharge from consolidated rock, streams, and precipitation on the valley floor simulated at specified-flux boundaries were varied in the transient-state simulation during sensitivity analysis, and the effect of these changes on model-computed annual water-level changes was analyzed. An order-of-magnitude reduction of storage-coefficient values in confined zones of the principal aquifer affected the magnitude of water-level declines and rises in the aquifer only slightly. A more substantial effect on simulated water-level changes was noted when specific-yield values in model layer 3 were adjusted. An order-of-magnitude reduction in specific-yield values throughout the unconfined zone of the principal aquifer resulted in increasing simulated water-level rises and declines by more than 100 percent at most cells, including cells that represent the confined zone of the principal aquifer. Increasing specific-yield values in the unconfined zones of the principal aquifer produced values that exceeded the probable range of values defined during the development of the model; no simulations were made using these values. All uniform and independent changes in storage-coefficient values from calibrated values made during sensitivity analysis had adverse effects on the match between simulated and annual water-level changes at observation wells in the principal aquifer.

Estimating specified recharge from consolidated rock, streams, and precipitation on the valley floor using equations 8, 9, and 10 and different values of the coefficient C had a substantial effect on simulated water-level changes, particularly in primary recharge areas. For example, incorporating annual estimates of recharge from these sources that simulate no effect on recharge from annual fluctuations in precipitation or streamflow ($C = 0$) eliminated model-computed water-level rises in cell 32i, 51j, 3k (fig. 23b) in the transient-state simulation during 1980-86. Incorporating annual estimates of recharge using C equal to 2, which magnified the effects of annual fluctuations in precipitation and streamflow on recharge, increased simulated water-level rises in the same cell for the same period from 34 ft to 62 ft. In general, the match between simulated and measured water-level changes at observation wells worsened as a result of changes in the coefficient C from the calibrated value.

In summary, of the variations made in the steady-state simulation during the analysis, the calibrated model is most sensitive to decreasing horizontal hydraulic conductivity in model layer 1 and is generally more sensitive to decreases in the analyzed parameters than to increases in them. The model is relatively insensitive to (1) increasing vertical leakance within model layers 1 to 3 by 50 percent, (2) decreasing or increasing vertical leakance within model layers 3 to 7 by an order of magnitude, and (3) increasing the hydraulic conductivity of the river bed by 50 percent. Incorporation of parameter values within those ranges does not substantially worsen the match between model-computed and measured conditions. Generally, changes made to individual model parameters in the steady-state simulation did not substantially affect model-computed flow rates at constant-head and head-dependent flux boundaries. Changes made to storage-coefficient of the principal aquifer and simulated annual variations in recharge from consolidated rock, streams, and precipitation on the valley floor in the transient-state simulation produced substantial effects on simulated annual water-level changes and worsened the match between model-computed and measured annual water-level changes.

LIMITATIONS OF THE MODEL

The hydrologic system in Salt Lake Valley is complex and cannot be defined completely with available data. The model documented in this report is based on mathematical representations of ground-water flow and on a simplified set of assumptions about the hydrologic system. As a result, the calibrated model has limitations that need to be considered when evaluating simulation results.

Although the model was discretized into cells 0.35 mile on a side, many model parameters were derived from information available only on a smaller scale. Estimates for model parameters, including water-budget components and aquifer properties, were estimated for subregions of the modeled area. The simplifications of space and regional estimates of model parameters indicate that caution should be used in evaluating system responses for local areas. Limitations in time also should be considered when evaluating model results. The transient-state simulation period was discretized into yearly stress periods, and seasonal changes in water levels and flow at head-dependent boundaries were not simulated. Withdrawal from wells and flow in canals, which may change substantially during a given year, were averaged to obtain annual rates. If the model were used to simulate seasonal or monthly changes in recharge and discharge, it might be necessary to recalibrate the model.

Few field data were available with which to determine initial estimates and probable ranges of values for model parameters to define the vertical hydraulic conductivity of basin-fill material. A sensitivity analysis of the model indicates that increasing these parameters relative to calibrated estimates within reasonable limits does not substantially affect model results. Vertical gradients and flows simulated in the model are controlled, in part, by the vertical hydraulic conductivity incorporated in model input. The uncertainty of the final estimates of vertical hydraulic conductivity of the basin fill, and thus, vertical leakance between model layers, should be noted when evaluating future simulation results.

Water levels in the consolidated-rock aquifer and data needed to define the hydrologic connection between the basin-fill and consolidated-rock aquifer generally were not available. The simulation of recharge from consolidated rock into the basin-fill aquifer was therefore simplified in the model by using specified-flux boundaries in areas other than the northern end of the Oquirrh Mountains. Simulated recharge from consolidated rock at these boundaries does not change during problem solution in the steady-state simulation and is not affected by simulated events in the ground-water flow system in the transient-state simulation. The achieved match between simulated and measured hydrologic conditions indicates that this representation of recharge from consolidated rock probably is reasonable under the conditions simulated in the model. In the physical system, however, flow from the consolidated-rock aquifer to the basin-fill aquifer is head dependent, controlled by the difference in water level between the two aquifers and the hydrologic properties existing at the contact between the two aquifers. The head-dependent nature of flow between the two aquifers is not accounted for in the model other than at the northern end of the Oquirrh Mountains. Large declines in water level in the basin-fill aquifer locally near the margins of the valley may increase inflow from consolidated rock. Such effects on flow resulting from drawdowns at the margins of the valley are not simulated by the model.

Measured water levels, measured water-level changes, and estimated discharge to the Jordan River and its tributaries were not accurately reproduced in all areas and for all times during the simulation period. The overall accuracy of the simulations, however, is considered to be good on the basis of (1) the match between model-computed and measured water levels, (2) the match between model-computed and measured water-level changes, (3) the match between model-computed and measured ground-water discharge to the Jordan River, (4) the match between simulated and measured vertical hydraulic gradients between the principal aquifer and the shallow unconfined aquifer, and (5) the match between model-computed and estimated budget components.

The set of boundary conditions and parameters used in the model does not represent a unique solution. Different combinations of data entered into the model might yield similar results. Discrepancies between model-computed and measured or estimated water levels and flows may, in part, be the result of simplified assumptions used to develop and calibrate the model. A reasonable match between simulated and measured hydrologic conditions for the area was achieved, however, and it is believed that analyses of ground-water flow using this model and future simulations to determine the effects of regional changes in recharge and discharge to the ground-water flow system should yield reasonable results.

SUMMARY

In 1990, the U.S. Geological Survey, in cooperation with the Utah Department of Natural Resources, Division of Water Rights, and the Utah Department of Environmental Quality, Division of Water Quality, and local water users, began a study of ground-water flow and solute transport in Salt Lake Valley, Utah. The approach used in the study included the development of a three-dimensional, finite-difference, numerical model of the basin-fill ground-water flow system in Salt Lake Valley, Utah. The model described in this report can be used to evaluate the movement of ground water and can be used in combination with other computer models to evaluate the movement of solutes in ground water and the effects of water use on ground-water quality.

The model was calibrated to steady-state and transient-state conditions. The steady-state simulation was developed and calibrated using hydrologic data defining average conditions for 1968. The transient-state simulation was developed and calibrated using hydrologic data from 1969-91, using the results of the steady-state simulation as the initial condition.

Areally, the model grid is 94 rows by 62 columns, with each cell 0.35 mile on a side. Vertically, the aquifer system is divided into seven layers. The transient-state simulation period from January 1969 to December 1991 was divided into 23 stress periods of 1 year in length. The model incorporates specified-flux boundaries to simulate recharge to the ground-water flow system as (1) inflow from consolidated rock, (2) seepage from streams and canals, (3) infiltration of precipitation on the valley floor, (4) infiltration of unconsumed irrigation water from fields, lawns, and gardens, (5) seepage from reservoirs at the mouth of Bingham Canyon and evaporation ponds in the southwestern part of the valley, and (6) underflow at Jordan Narrows. Specified-flux boundaries also were used to simulate withdrawal from wells and discharge to springs, and discharge as seepage to canals. Head-dependent flux boundaries were used to simulate (1) ground-water flow to and seepage from the Jordan River and the lower reaches of its principal tributaries, (2) inflow from consolidated rock at the northern end of the Oquirrh Mountains, (3) discharge from the shallow unconfined aquifer to drains, and (4) discharge by evapotranspiration.

Available data were assembled and evaluated to develop and calibrate the model. Information defining spatial variations in subsurface lithology was evaluated and used to define system geometry and to distribute values that represent the hydrologic properties of the aquifer. The dimensions of the shallow confining layer and overlying shallow unconfined aquifer were determined on the basis of an analysis of well logs in the valley and simulated in the top two layers of the model. Active cells in model layers representing the principal aquifer (layers 3 to 7) were defined on the basis of the type of sediment they contained. Movement of ground water in the principal aquifer was simulated in basin-fill material of Quaternary age and, in areas, the upper zone of underlying basin-fill material of Tertiary age. Flow in the consolidated-rock floor of the valley was not simulated. Initial estimates and probable ranges of values for hydrologic properties of basin fill used during calibration of the model were defined from data collected during this study and previous studies.

In the transient-state simulation, specified recharge simulating inflow from consolidated rock, infiltration of unconsumed irrigation water from fields, lawns, and gardens, infiltration of precipitation on the valley floor, and seepage from streams was varied with time using the results of steady-state calibration as an initial condition. Recharge from consolidated rock was varied as a function of the ratio of annual precipitation in the adjacent mountains to annual average precipitation in the mountains. Recharge from irrigated fields, lawns, and gardens was varied in the transient-state simulation to represent the urbanization of agricultural and unused land during the simulation period. Recharge from precipitation on the valley floor was varied as a function of the ratio of annual precipitation on the valley floor to average annual precipitation on the valley floor. Recharge from streams was varied as a function of the ratio of total annual runoff in streams at the mouths of canyons to average annual runoff in streams at the mouths of canyons. Specified discharge simulating withdrawal from public-supply, industrial, and irrigation wells was varied temporally on the basis of values reported by water users and on unpublished records of the U.S. Geological Survey.

During steady-state calibration, model parameters defined as calibration variables were adjusted within probable ranges until a reasonable match between model-computed and observed conditions was achieved. The results of calibration indicate a reasonable match between model-computed and measured water levels. The match between model-computed and estimated total net discharge to the Jordan River is reasonably good. Comparison of model-computed and estimated gains in subreaches of the river, however, indicate substantial differences and may indicate that

the model is better able to reproduce measured gains in the river along long reaches than measured gains along short reaches. Generally, a satisfactory match between model-computed and measured vertical hydraulic gradient between the principal and shallow unconfined aquifer was achieved. The steady-state ground-water budget has a reasonable correspondence with independent estimates of budget components made during prior studies. Total flow into and out of the ground-water flow system computed in the steady-state simulation is less than independent estimates. Most of the decrease in recharge relative to independent estimates was the result of lower simulated rates of recharge from irrigated lawns and gardens.

The transient-state simulation was calibrated to historical annual water-level changes in the principal aquifer and estimated annual gains in the Jordan River and its tributaries. Transient-state calibration resulted in a reasonable match between model-computed and measured annual water-level changes in most of the modeled area and indicates that the model can approximate measured trends in water levels that result from fluctuations in recharge and ground-water withdrawals. The comparison of model-computed and estimated gains in the Jordan River indicates a reasonable match. Model-computed gains, however, are substantially smaller than estimated values from 1983-86, a period of greater-than-normal annual precipitation in the valley and nearby mountains. Measured water-level changes are reasonably approximated in the model for this period, however, and the apparent model inaccuracies may be, in part, the result of error in estimates of gain in the river.

At the end of model calibration, a sensitivity analysis was done to determine the response of the calibrated model to changes in selected model parameters. Calibration parameters with large defined ranges of possible values, or for which few data were available on which to base initial estimates, were independently varied relative to calibrated values; the effects of these adjustments on simulation results were noted. Generally, of the variations made in the steady-state simulation during the analysis, the calibrated model is most sensitive to decreasing horizontal hydraulic conductivity in model layer 1 and is more sensitive to decreases in the analyzed parameters than to increases in them. The model is relatively insensitive to (1) increasing vertical leakance within model layers 1 to 3 by 50 percent, (2) decreasing or increasing vertical leakance within model layers 3 to 7 by an order of magnitude, and (3) increasing the hydraulic conductivity of the river bed by 50 percent. Incorporation of parameter values within those ranges does not substantially worsen the match between model-computed and measured conditions used to determine the accuracy of the simulation. Changes made to individual model parameters in the steady-state simulation did not substantially affect model-computed fluxes at constant-head and head-dependent flux boundaries. Changes made to storage-coefficient values of the principal aquifer and simulated annual variations in recharge from consolidated rock, streams, and precipitation on the valley floor in the transient-state simulation produced substantial effects on model-computed annual water-level changes and worsened the match between model-computed and measured annual water-level changes.

The model described in this report can be used to evaluate ground-water flow under average conditions, or to evaluate the response of the ground-water flow system to changes in water use. The model simulates a complex system and is based on mathematical representation of ground-water flow and on a simplified set of assumptions about the system. The model is best suited for evaluating the ground-water flow system throughout a large area and for relatively long time periods (year or greater).

Measured water levels, historical water-level changes, and simulated discharge to the Jordan River were not accurately simulated in all areas and for all times. A reasonable match between simulated and measured hydrologic conditions for the area, however, was achieved, and it is believed that analyses of ground-water flow using this model and future simulations to determine the effects of regional changes in recharge and discharge to the ground-water flow system should yield reasonable results.

REFERENCES CITED

Arnow, Ted, Vanhorn, Richard, and LaPray, Reed, 1970, The pre-Quaternary surface in the Jordan Valley, Utah, *in* Geological Survey Research 1970: U.S. Geological Survey Professional Paper 700-D, p. D257-D261.

Arnow, Ted, and Stephens, D.W., 1990, Hydrologic characteristics of the Great Salt Lake, Utah: 1847-1986: U.S. Geological Survey Water-Supply Paper 2332, 32 p.

Batty, D.M., Allen, D.V., and others, 1993, Groundwater conditions in Utah, spring of 1993: Utah Division of Water Resources Cooperative Investigations Report No. 33, 106 p.

Bedinger, M.S., Langer, W.H., and Reed, J.E., 1986, Synthesis of hydraulic properties of rocks in the Basin and Range Province, southwestern United States: U.S. Geological Survey Water-Supply Paper 2310, p. 35-43.

Blaney, H.F., and Criddle, W.D., 1962, Determining consumptive use and irrigation requirements: U.S. Agricultural Research Service Technical Bulletin 1275, 59 p.

Cook, L.K., and Berg, W.J., Jr., 1961, Regional gravity survey along the central and southern Wasatch Front, Utah: U.S. Geological Survey Professional paper 316-E, p. 75-89.

Criddle, W.D., Harris, Karl, and Willardson, L.S., 1962, Consumptive use and water requirements for Utah: Utah State Engineer Technical Publication No. 8 (revised), 47 p.

Dames and Moore, 1988, Milestone report 1, data base synthesis mathematical model of ground water conditions, southwestern Salt Lake County, Utah: 64 p.

———1989, Ground water model, southwestern Salt Lake County, Utah: 36 p.

Engineering Technologies Associates, Inc., 1992, Groundwater assessment report of the Great Salt Lake area, Volume 1: p. VII-24 p.

Freeze, R.A., and Cherry, J.A., 1979, Groundwater: Englewood Cliffs, N.J., Prentice-Hall, 604 p.

Hely, A.G., Mower, R.W., and Harr, C.A., 1971, Water resources of Salt Lake County, Utah: Utah Department of Natural Resources Technical Publication No. 31, 244 p.

Herbert, L.R., Cruff, R.W., and Waddell, K.M., 1985, Seepage study of six canals in Salt Lake County, Utah, 1982-83: Utah Department of Natural Resources Technical Publication No. 82, 95 p.

Holdsworth, I.K., 1985, A preliminary groundwater flow and solute transport model along Bingham Creek in western Salt Lake County, Utah: Utah State University Masters of Science Thesis, 68 p.

Kennecott Utah Copper, 1992a, Groundwater assessment report of the southwestern Jordan Valley area, Volume 1, 131 p.

———1992b, Hydrogeological report for the Great Salt Lake area, Volume 1, 75 p.

———1992c, Groundwater assessment report of the southwestern Jordan Valley area, Volume 3.

Marine, I.W., and Price, Don, 1964, Geology and ground-water resources of the Jordan Valley, Utah: Utah Geological and Mineralogical Survey Bulletin 7, 68 p.

Mattick, E.R., 1970, Thickness of unconsolidated to semiconsolidated sediments in Jordan Valley, Utah: U.S. Geological Survey Professional Paper 700-C, p. C119-C124.

McDonald, M.G., and Harbaugh, A.W., 1988, A modular three-dimensional finite-difference groundwater flow model: U.S. Geological Survey Techniques of Water Resources Investigations, book 6, chap. A1.

Price, Don, 1988, Ground-water resources of the southern Wasatch Front area, Utah: Utah Geological and Mineral Survey Map 55-C, Wasatch Front Series, 1 plate.

Price, Don, and Conroy, L.S., 1988, Ground-water resources of the central Wasatch Front area, Utah: Utah Geological and Mineral Survey Map 54-C, Wasatch Front Series, 1 plate.

Rantz, S.E., 1968, A suggested method for estimating evapotranspiration by native phreatophytes, *in* Geological Survey Research 1968: U.S. Geological Survey Professional Paper 600-D, p. D10-D12.

ReMillard, M.D., and others, 1993, Water resources data for Utah, water year 1992: U.S. Geological Survey Water-Data Report UT-92-1.

———1994, Water resources data for Utah, water year 1993: U.S. Geological Survey Water-Data Report UT-93-1.

Robinson, T.W., 1958, Phreatophytes, U.S. Geological Survey Water-Supply Paper 1423, 84 p.

Salt Lake County Division of Water Quality & Water Pollution Control, 1981, Groundwater quality management: background report: 24 p.

Seiler, R.L., and Waddell, K.M., 1984, Reconnaissance of the shallow-unconfined aquifer in Salt Lake Valley, Utah: U.S. Geological Survey Water-Resources Investigations Report 83-4272, 34 p.

Taylor, G.H., and Leggette, R.M., 1949, Ground water in the Jordan Valley, Utah: U.S. Geological Survey Water-Supply Paper 1029, 356 p.

Thiros, S.A., 1992, Selected hydrologic data for Salt Lake Valley, Utah, 1990-92, with emphasis on data from the shallow unconfined aquifer and confining layers: U.S. Geological Survey Open-File Report 92-640, duplicated as Utah Hydrologic-Data Report No. 49, 44 p.

———1995, Chemical composition of ground water, hydrologic properties of basin-fill material, and ground-water movement in Salt Lake Valley, Utah: Utah Department of Natural Resources Technical Publication No. 110-A.

U.S. Department of Agriculture, 1969, Water budget analysis, Sevier River basin, Utah: Appendix IV, 92 p.

Waddell, K.M., Seiler, R.L., Santini, Melissa, and Solomon, D.K., 1987, Ground-water conditions in Salt Lake Valley, Utah, 1969-83, and predicted effects of increased withdrawals from wells: Utah Department of Natural Resources Technical Publication No. 87, 69 p.

500 10/95

Printed with vegetable oil ink.

Technical Publication No. 110-B, Utah Department of Natural Resources, 1995